Drillhole Spacing Determination with Value of Information

by

Benjamin E. Harding

A thesis submitted in partial fulfillment of the requirements for the degree of

Master of Science

in

Mining Engineering

Department of Civil and Environmental Engineering

University of Alberta

Abstract

Different quantities of information are available at various stages of the development of a mining project. Consequential decisions are made given the data available at the time. Geological uncertainty due to sparse data presents economic risks. The collection of additional information reduces geological uncertainty leading to a better technical decision and greater value. Subjectivity in the choice of data collection scheme may lead to sub-optimal outcomes. The value of information (VOI) allows a decision-maker to quantify the future value data could provide before collecting it. Evaluating many future configurations over a range of data spacings identifies the optimal given the value metric. The optimal data spacing represents the balance between the cost of uncertainty and the cost of information. A framework for establishing VOI in a mining context is proposed. The application of VOI is particularly useful for advanced mining projects with an established basis to calculate value. A geostatistical "resample" and "resimluate" approach is adopted. The resampling of simulated realizations provides access to virtually any future data configuration. Geological models are simulated conditional to future data and passed through an objective function to optimize a technical design and establish value. The difference in value generated with future information and the current information is the VOI. VOI is a non-linear response to the interaction of geologic scale, engineering scale and technical design parameters, decision-maker risk preferences and economic parameters. The relationship between these parameters and their influence on VOI and optimal sample spacing is addressed. The numerical VOI workflow and considerations for implementation are documented. Alternative methods for evaluating optimal data spacing based on geologic uncertainty measures

are addressed, establishing a link between uncertainty and value. A semi-automatic algorithm for partitioning future drillhole configurations into spatially reasonable groups based on data spacing is proposed. The methodology and techniques developed in this thesis are applied to synthetic examples and a case study. The case study encompasses VOI principles, data spacing, engineering design parameters, economic factors, and uncertainty in reserve calculation.

Dedication

To JER.

Acknowledgments

I would like to thank my supervisor Clayton Deutsch for his continued support throughout this process. Your ability to intrinsically motivate your students is unparalleled. I am grateful to the Centre for Computational Geostatistics for financial support over the last two years.

I would like to thank my new friends at the CCG for making this experience a memorable one.

Table of Contents

1 Introduction **1**

1.1 Problem Motivation 1

1.2 Literature Review 2

1.2.1 The Value of Information 2

1.2.2 Perfect versus Imperfect Information 3

1.2.3 Petroleum Applications 4

1.2.4 Hydrogeology and Environmental Applications 4

1.2.5 Mining Applications 5

1.2.6 Decision Analysis Framework 6

1.2.7 Decision Making in Spatially Correlated Problems 7

1.2.8 The Effect of Additional Information 8

1.2.9 Analytical Approaches to VOI 9

1.3 Data Spacing and Uncertainty 11

1.3.1 Measures of Data Availability 12

1.3.2 Measures of Uncertainty 13

1.3.3 The Learning Curve Concept 16

1.4 Utility and Value 17

1.4.1 Utility Functions 17

1.4.2 Transfer Functions 18

1.4.3 Time Value of Money 19

1.5 Thesis Outline 19

2 Numerical Value of Information Methodology **20**

2.1 Decision Framework 20

2.2 VOI Overview 21

2.3 Numerical Approach 22

2.4 Simulation Based Methodology 24

2.4.1 Simulate True Models 24

2.4.2 Simulate Data 25

2.4.3 Cost of Acquiring data 26
2.4.4 Simulate Realizations 26
2.4.5 Transfer and Value Functions 27
2.4.6 Value of Information 28
2.5 Considerations for the Simulation Based Methodology 29
2.5.1 Optimal Decision Alternatives 29
2.5.2 Confounding Factors 30
2.5.3 Geomodeling Details 30
2.6 VOI Plotting Conventions 31

3 Principals of the Value of Information - A 1D Example 33
3.1 Synthetic Data 34
3.2 Geologic Scale 35
3.2.1 Geologic Value 36
3.2.2 Variogram Range 36
3.2.3 Nugget Effect 37
3.3 Engineering Scale 37
3.3.1 Engineering Value 38
3.4 Interaction of Geologic and Engineering Scales 40
3.5 Cost Structure 43
3.5.1 Cost of Acquisition 43
3.5.2 Material Value 44
3.5.3 Relative Penalties 45
3.6 Decision Maker Preferences 47
3.7 Summary 47

4 Implementation Details of the Simulation Based Methodology 50
4.1 Data Collection 50
4.1.1 Generating Future Data Configurations 51
4.1.2 Resampling 54
4.1.3 Cost of Data 55
4.2 Transfer, Objective and Value Functions 55
4.3 Number of Realizations 58

4.4 Computational Considerations 60

5 Managing Uncertain Value **61**

5.1 Synthetic Data 61

5.1.1 VOI example 62

5.2 Geologic Uncertainty 63

5.2.1 Standard Deviation 64

5.2.2 Precision 64

5.2.3 Probability of Correct Classification 66

5.2.4 Link Between Geologic Uncertainty and Value 68

5.2.5 Optimal Data Spacing and Geologic Uncertainty 68

5.3 Economic Uncertainty 71

5.3.1 Commodity Prices 71

5.3.2 Operational Costs 72

5.4 Summary 72

6 Case Study **76**

6.1 Workflow Overview 76

6.2 Data Set 77

6.3 Normal Score Variograms 78

6.4 True Models 80

6.5 Future Data Configurations 81

6.6 Resample and Resimulate 82

6.6.1 Step One 82

6.6.2 Moving Window Average 84

6.6.3 Step Two 86

6.7 Stope Optimization 87

6.7.1 Value Function 88

6.7.2 Objective Function 90

6.7.3 Differential Evolution 91

6.8 Value of Information 92

6.9 Geologic Uncertainty 94

6.10 Reserve Uncertainty 95

6.11 Assumptions and Limitations 97
6.12 Summary 98

7 Conclusions and Future Work **103**
7.1 Topics Covered and Contributions 103
7.2 Limitations 105
7.3 Future Work 107

References **108**

List of Tables

5.1 Value function parameters. Costs are per tonne, values are in USD 63

6.1 Study Area Dimensions 78

6.2 Data configurations and with the number of drillholes, the number of drillhole groups and the average equivalent square drillhole spacing (DHS) within the domain. 85

6.3 Costs per meter of data acquisition 85

6.4 Declustered mean and standard deviation for resampled data configurations. . 86

6.5 Value function parameters. Costs are per tonne, values are in USD. 89

6.7 Differential evolution parameters. 91

6.6 Stope optimization technical constraints. 91

List of Figures

1.1 Uncertainty versus Data Spacing 9

1.2 Assessed (left) and inferred (right) probability trees. The posterior and pre-posterior probabilities are calculated with Bayes' Law. 11

1.3 Two dimensional drillhole density (left) expressed as the number of drillholes per hectare and drillhole spacing (right) expressed in meters. 13

1.4 Standard Deviation 14

1.5 Precision 15

1.6 Misclassification 15

1.7 Schematic expected uncertainty curve (left) and the learning curve, or rate of uncertainty reduction (right). Modified after Pinto (2015). 16

1.8 Utility Functions 18

2.1 Graphical representation of the numerical VOI work flow where T is the number of true models, C is the number of future data configurations, L is the number of realizations, and TF represents the transfer function. The expected VOI is taken for each of the C data configurations. 25

2.2 Schematic value of information curve highlighting the maximum net VOI which is the optimal sample spacing. 29

2.3 Schematic cumulative VOI plot identifying the optimal data spacing and maximum net VOI. 31

3.1 Five unconditional realizations which are resampled to generate future data configurations. 34

3.2 As additional information is collected (black dots), the resulting conditional realizations approach the reference model (pink grid nodes). 35

3.3 Distributions (n=1000) of value for various sample spacings and 64, 32, 16 and 1 unit range variogram models. The red bars are ± standard deviation. 38

3.4 Distributions (n=1000) of value relative to the reference model for various sample spacings and 0.10, 0.25, 0.5 and 0.99 nugget effect variogram models. All variogram models are single structure spherical models with 16 unit range. The red bars are ± standard deviation. 39

3.5 Four technical designs with different scales of engineering selectivity. As the degree of selectivity increases, ore loss and dilution decreases. The pink nodes are "inside" the design. 40

3.6 Distributions of value (n=10) for technical designs against the respective reference model. The black line is the expected value of the distribution. All variogram models are single structure spherical models with 32 unit range. The red bars are ± standard deviation. 41

3.7 Optimal sample spacing relative to domain size (left) and percent of maximum expected net VOI (right) for a range of engineering and geologic scales. The y-axis in both plots is variogram range. 42

3.8 Four cumulative VOI curves for different costs of data acquisition. The optimal sample spacing is shown near the vertical dashed line and the corresponding net VOI is shown along the horizontal dashed line. Note the blue gross VOI curve is the same for all scenarios. 44

3.9 Four cumulative VOI curves for different ratios of ore value to waste value. The optimal sample spacing is shown near the vertical dashed line and the corresponding net VOI is shown along the horizontal dashed line. Note the green cost curve is the same for all scenarios. 45

3.10 Four cumulative VOI curves for different ratios of dilution to ore loss penalties. The optimal sample spacing is shown near the vertical dashed line and the corresponding net VOI is shown along the horizontal dashed line. Note the green cost curve is the same for all scenarios. 46

3.11 Cumulative VOI curves for risk neutral ($a = 0$), risk averse ($a = 0.25$) and opportunity seeking ($a = -0.25$) exponential utility functions. (d) shows three technical designs optimized considering expected utility (5 of 100 realizations are shown). 48

4.1 Number of iterations versus objective function value generated when optimizing three technical designs using the one-dimensional example in Chapter 3. The example uses a single structure spherical variogram model with a 32 unit range, a design selectivity of 4 units and fixed ore and waste values of 10 and -1 units, respectively. 57
4.2 Root mean squared error (RMSE) for various combinations of T and L 59

5.1 An example of one true model of gold grams per tonne (left) and rock type (right). The black line is the boundary realization. 62
5.2 An example of a single realization of gold grams per tonne (left) and rock type (right) conditional to a 32 unit future data configuration resampled from the true model in Figure 5.1. The black line is the boundary realization. 62
5.3 Cumulative VOI curves for the parameters in Table 5.1. The vertical dashed line highlights the optimal data spacing while the horizontal highlights the maximum net VOI. 63
5.4 Expected standard deviation versus data spacing. The optimal sample spacing which corresponds to the maximum net VOI is highlighted by the vertical dashed line while the horizontal highlights the corresponding measure of uncertainty. Each coloured line represents one of the $T = 10$ true models and the black line is the average of all true models. 65
5.5 Expected probability to be $\pm$ 15% of the mean versus data spacing. The optimal sample spacing which corresponds to the maximum net VOI is highlighted by the vertical dashed line while the horizontal highlights the corresponding measure of uncertainty. Each coloured line represents one of the $T = 10$ true models and the black line is the average of all true models. 66
5.6 Expected probability of correct classification versus data spacing. The optimal sample spacing which corresponds to the maximum net VOI is highlighted by the vertical dashed line while the horizontal highlights the corresponding measure of uncertainty. Each coloured line represents one of the $T = 10$ true models and the black line is the average of all true models. 67

5.7 Expected gross VOI versus (a) expected standard deviation, (b) probability to be ± 15% of the mean and (c) expected probability of correct classification. Each coloured line represents one of the $T = 10$ true models and the black line is the average of all true models. 69
5.8 Expected standard deviation versus number of drillholes. The horizontal dashed line is the target uncertainty and represents a reasonable point of diminishing returns. Each coloured line represents one of the $T = 10$ true models and the black line is the average of all true models. 70
5.9 Average monthly gold price in USD from 2000-01-31 to 2020-07-31. Retrieved from the World Gold Council (2020). 72
5.10 Cumulative VOI curves and distributions of gold prices for (a, b) $T = 10$, (c, d) $T = 25$ and (e, f) $T = 50$. The vertical dashed line highlights the optimal data spacing while the horizontal highlights the maximum net VOI. 74
5.11 Cumulative VOI curves with variable operational costs for (a) $T = 10$, (b) $T = 25$ and (c) $T = 50$. The vertical dashed line highlights the optimal data spacing while the horizontal highlights the maximum net VOI. 75

6.1 3 meter capped Au composites within the study area looking east. Coordinate labels are in UTM meters, elevation is meters above sea level and the scale bar is meters. 78
6.2 Empirical cumulative distribution functions of capped gold values and summary statistics for all, low grade and high grade composites based on GSR deterministic grade shells. All composites encompass HG, LG and data outside either grade shell. 79
6.3 Directional variograms of the normal scores of Au for all composites 80
6.4 Directional variograms of the normal scores of Au for low grade composites . . 80
6.5 Directional variograms of the normal scores of Au for high grade composites . . 81
6.6 Plan view section of the first true model with drillhole composites. 82
6.7 East-west section of the first true model with drillhole composites. 83
6.8 North-south section of the first true model with drillhole composites. 83
6.9 Variogram and histogram reproduction for $T = 10$ true models. 84

6.10 Configuration $c = 1$ which corresponds to an average equivalent square drillhole spacing of 30.51 m. Drillhole fans are collared on the 670 m and 700 m sublevels. View is looking east and the scale bar is meters. 85
6.11 Cumulative declustered histograms of resampled datasets for the first true model. The dashed black line (and stat block) is the distribution of real drillhole composites. 86
6.12 Au histogram reproduction for configuration $c = 10$ drawn from true model $t = 1$. 87
6.13 Plan view section though a grade shell model. Category 0 is outside, 1 is LG and 2 is HG. 88
6.14 LG (left) and HG (right) grade shell volumes for each data configuration for true model $t = 1$. The dashed gray and black lines overlap for category 2. 89
6.15 Objective function value versus iterations. The sign of the value is negative the algorithm converges towards a minimum value. Each line represents the objective function value for a single stope geometry. 92
6.16 Optimized stope geometries for the 670 m sublevel for data configurations $c = 1$ (top left), $c = 4$ (top right), $c = 8$ (bottom left) and $c = 12$ (bottom right) plotted over the true model $t = 1$. 93
6.17 Cumulative expected VOI curves. The optimal drillhole spacing of 12.4 m is highlighted by the vertical dashed line. Thin blue and orange lines represent the gross and net VOI curves for each of the $T = 10$ true models. 95
6.18 Average expected standard deviation of Au against (a) equivalent square drillhole spacing and (b) number of additional drillholes. The optimal drillhole spacing of 12.4 m corresponds to 165 additional drillholes. Each coloured line represents one of the $T = 10$ true models and the black line is the average of all true models. 96
6.19 Uncertainty in panel tonnes by drillhole spacing. The dashed lines are the expected values of the respective distributions. All plots share both x and y axes. UPI = undiluted perfect information, NAD = no additional data. 99
6.20 Uncertainty in panel Au grade by drillhole spacing. The dashed lines are the expected values of the respective distributions. All plots share both x and y axes. UPI = undiluted perfect information, NAD = no additional data. 100

6.21 Uncertainty in panel recovered Au ounces by drillhole spacing. The dashed lines are the expected values of the respective distributions. All plots share both x and y axes. UPI = undiluted perfect information, NAD = no additional data. . 101

6.22 Incomplete information factor for tonnes (top), Au grade (middle) and recovered Au ounces (bottom) by drillhole spacing. The orange line is the average of the realizations. 102

List of Symbols

Symbol	Description
$A(\mathbf{u})$	Search area
C	Number of future data configurations
cf	Conversion factor
$c_{ga}(\mathbf{u})$	General and administrative cost at location $\mathbf{u}$
$c_m(\mathbf{u})$	Cost of mining at location $\mathbf{u}$
$c_p(\mathbf{u})$	Cost of processing at location $\mathbf{u}$
c	Future data configuration index
DHD($\mathbf{u}$)	Drillhole density at location $\mathbf{u}$
DHS($\mathbf{u}$)	Drillhole spacing at location $\mathbf{u}$
$D(scale,\ G(c,\ L))$	Technical design of *scale*, optimized across L realizations
dc_i	Average distance to centroid for remaining drillholes i
$dd_{i,j}$	Average distance between remaining drillholes i and j
dhs_i	Drillhole spacing for i drillholes
$E\{\}$	Expected Value
$F(z;\mathbf{u}\|(n))$	Conditional cumulative distribution function at $\mathbf{u}$
$G(c,\ L)$	Geologic model conditioned to data c, defined by L realizations
g_i	Goodness of remaining drillholes
$\mathbf{h}$	Lag vector
ix, iy, iz	Block model indices
L	Number of realizations
l	Realization index
max	Maximum
m	Meter
N	Number of blocks
$n_V(\mathbf{u})$	Number of samples within search volume $V(\mathbf{u})$
$n_A(\mathbf{u})$	Number of samples within search area $A(\mathbf{u})$

Symbol	Description
ndh	Number of drillholes
n_{rem}	Number of remaining drillholes
ns	Number of samples in remaining drillholes
$O(D(scale,\ G(c,\ L)))$	Objective function value for a technical design and geologic model
P^{II}	Probability of type II errors
P^{I}	Probability of type I errors
$P_{corr.}$	Probability of correct classification
P_{econ}	Economic parameters for value calculation
$P_{mis.}$	Probability of misclassification
$PoV(y)$	Posterior value given future data y
$P(y\|z)$	Probability of y given z
P_{dil}	Penalty for dilution
P_{loss}	Penalty for ore loss
p	Selling price
$r(\mathbf{u})$	Recovery at location $\mathbf{u}$
SG	Specific gravity
$Prec(ti)$	Precision given the tolerance interval ti
σ_Z	Standard deviation of random variable Z
ti	Tolerance interval
T	Number of true models
$U(V_{econ})$	Utility of an economic value
$\mathbf{u}$	Location in space
$V^t(0)$	Value given current data configuration $c = 0$ and true model t
$VOI^t(c)$	Value of information given future data c and true model t
$V^{cost}(c)$	Cost of future data configuration c
$V^t(c)$	Value given future data configuration c and true model t
$V_{econ}(D,\ G,\ P_{econ})$	Value of design D, geologic model G and parameters P_{econ}
γ	Variogram value

Symbol	Description
$V(\mathbf{u})$	Search volume
Z	Random Variable
$\mathrm{z}(\mathbf{u})$	Random variable outcome at location $\mathbf{u}$

List of Abbreviations

Abbreviation	Description
2D	Two-dimensional
3D	Three-dimensional
CDF	Cumulative Distribution Function
DE	Differential Evolution
DH	Drillhole
DHD	Drillhole Density
DHS	Drillhole Spacing
GSB	GSLIB-like Binary
GSLIB	Geostatistics Software Library
GSR	Golden Star Resources
GVOI	Gross Value of Information
HG	High Grade
IIF	Incomplete Information Factor
LG	Low Grade
NAD	No Additional Data
NN	Nearest Neighbour
NPV	Net Present Value
NVOI	Net Value of Information
PoV	Posterior Value
PV	Prior Value
QA/QC	Quality Assurance / Quality Control
RMSE	Root Mean Squared Error
SGS	Sequential Gaussian Simulation
SSO	Stochastic Shape Optimizer
TF	Transfer Function
UDE	Uniform Drillhole Elimination

Abbreviation	**Description**
UPI	Undiluted Perfect Information
USD	United States Dollar
VOI	Value of Information
VOIP	Value of Perfect Information

Chapter 1

Introduction

The Value of Information (VOI) is a multidisciplinary concept encompassing probability theory, decision and risk theory, economics and psychology. The fundamental question is, does the value derived from a decision exceed the cost of implementing the decided upon action? VOI is the difference in value generated by a decision with and without additional information and defines the maximum value one should be willing to pay to acquire the information (Howard, 1966a):

$$VOI = [Value\ with\ future\ information] - [Value\ with\ current\ information] \quad (1.1)$$

We can apply this framework to spatially correlated problems in the earth sciences. Our knowledge of an orebody or petroleum reservoir is inherently uncertain at all stages of development. Data collection resolves this uncertainty; however, at a point, this becomes cost-prohibitive. Few data may only provide small contributions, and many data may have diminishing returns. VOI in spatially correlated scenarios is intimately related to the modelled variable's spatial continuity and the scale relevant to the engineering decision.

1.1 Problem Motivation

Geologic uncertainty is related to data availability. Data collection reduces uncertainty, allowing a decision-maker to make a better technical decision. In many earth science scenarios, data is expensive to collect; this is particularly true for mining and petroleum resource exploration and delineation. Therefore, if deciding to collect data, one would like the outcome to generate the maximum possible value. The significant costs associated with these types of decisions warrant a detailed review of the alternatives. The data configuration that generates the most significant value for the least cost should be selected. It is also beneficial to understand the maximum value one should be willing to pay for information.

VOI is a metric that quantifies the additional value information could provide before collecting it—comparing the decision outcome with future information to the decision outcome

with current information. The information acquired may be in the form of drill core, surface geochemical samples, geophysics, or any information that can influence the decision outcome. These decisions are often capital intensive and are irreversible once implemented. Howard (1968) and Eidsvik, Mukerji, and Bhattacharjya (2015) describe the action of making a decision as an irreversible or irrevocable allocation of resources. Decisions may be a simple binary choice such as drill or do not drill. Decisions may involve a set of alternatives, or sequential data gathering and multiple decision scenarios. The information collected may be of different types, and collection may occur at one time or sequentially. The question then posed is how much and what type of data should one collect? VOI analysis allows the practitioner to answer (1) is the reduction in uncertainty worth the cost?; (2) if there are multiple possible sources of information, which is best?; and (3) which configuration or sequence of information is optimal (Scheidt, Li, & Caers, 2018)?

The application of VOI is particularly useful for advanced mining projects with established transfer and value functions. For example, in the context of drilling for stope planning and development, additional information in the form of diamond drillholes reduces geologic uncertainty leading to improved stope placement. The improved technical design generates greater value though the information comes at a cost. VOI allows the practitioner to balance the cost of the geologic uncertainty and the cost of information. This balance is the optimal amount of information for their given transfer function.

1.2 Literature Review

The theory of information value relates to probability theory, decision analysis theory, risk and utility theory and economics. Overlap commonly present in the literature. VOI considers a probabilistic decision analysis framework.

1.2.1 The Value of Information

The explicit use of VOI originates with applications in business economics. Schlaifer (1959) is the first to define “the value of additional information” in managerial economics. He introduces the concept of terminal or final decisions and the choice to collect information before making one. He poses the question of not deciding to make a decision in the presence of new information but was collecting the information in the first place the right action to

take. Many of the examples are framed in the context of determining the optimal information collection scheme, which minimizes the expected loss of a set of decision alternatives. Raiffa and Schlaifer (1961) then define the value of information as the expected increase in value one would receive from learning a particular outcome and the expected net gain as that value less the expected cost of acquiring it. Howard (1966b) introduces the concept of information value in a probabilistic sense, and those uncertain outcomes must consider economic consequences, not just probabilities of occurrence, for the decision-maker to truly appreciate the uncertainty. Laxminarayan and Macauley (2012) ask the question "what is value?" and discuss its dependence on problem context and available data. They outline numerous scenarios where information does and does not have value and approaches to calculating VOI. Kochenderfer (2015) defines VOI as the increase in expected utility that one receives with an observation of new information and states that the expected utility can only increase if the information leads to a different optimal decision. Ultimately, the VOI for a particular information collection strategy depends on the decision framework, the quality of the information, and the decision-makers risk preferences (Eidsvik et al., 2015).

1.2.2 Perfect versus Imperfect Information

Many authors distinguish between perfect and imperfect information (Eidsvik et al., 2015; Howard & Abbas, 2015) or alternatively the "reliability content" of the information (Caers, 2011; Scheidt et al., 2018; Trainor-Guitton, Caers, & Mukerji, 2011). Earlier literature refers to the value of perfect information (VOPI) as the value of "clairvoyance" or the value achieved by removing all prior uncertainty. The VOPI is the upper bound for the cost of information collection. There is no need to consider alternatives with a cost that exceeds this threshold (Eidsvik et al., 2015).

Information quality forms a spectrum between perfect and complete sampling and noisy, incomplete sampling. In practice, perfect and complete information is never possible. If information is perfect, such as a diamond drill core sample, it is incomplete or sparse. If information is exhaustive or complete, such as a geophysical survey, it is imperfect where the information represents a noisy measurement of the variable of interest (Eidsvik et al., 2015). Caers (2011) refers to imperfect information as the reliability content or the probability of what the information says given the actual state of nature. Inverse modelling problems in

petroleum applications often account for information quality, while resample and resimulate applications (Barnett, 2014; Rojas & Cáceres, 2011) assume perfect, incomplete information.

1.2.3 Petroleum Applications

Grayson (1960) first mentions VOI concerning earth science problems with application to petroleum exploration. He states that at many points during the development or exploration of a petroleum resource, one is faced with the decision to purchase additional information before making a final decision. In the 2000s, numerous papers with an explicit focus on the VOI were published, primarily focused on the value of acquiring seismic information to improve exploration or production well placement (Bickel, Gibson, McVay, Pickering, & Waggoner, 2006; Coopersmith, Burkholder, & Schulze, 2006; Eidsvik, Bhattacharjya, & Mukerji, 2008; Eidsvik, Dutta, Mukerji, & Bhattacharjya, 2017; Stegall et al., 2005; Waggoner, 2002). Bratvold, Bickel, and Lohne (2009) provides a thorough literature review and commentary on the implementation of VOI analysis in the oil and gas industry from 1960 to 2006. More recently, books by Bratvold and Begg (2009), Caers (2011), Eidsvik et al. (2015) and Scheidt et al. (2018) provide in-depth documentation of VOI theory, application and implementation in case studies primarily concerning the value of seismic data or value of optimal well placement. Applications often involve decision trees and Bayesian statistics to update a prior distribution from the marginal and likelihood to determine the optimal course of action. Barnett, Lyster, Pinto, MacCormack, and Deutsch (2018) demonstrates a numerical "resample and resimulate" approach for optimal well spacing in a northern Alberta shale oil case-study. VOI is estimated numerically for numerous well spacings, and the configuration which maximizes net VOI is selected.

1.2.4 Hydrogeology and Environmental Applications

Though there is no direct mention of VOI, Englund and Heravi (1993) presents an early application of the resample and resimulate methodology. The design of sampling programs for contaminated soil sites is optimized using conditional simulation. They utilize an economic objective function to determine the sample configuration that generates the maximum value for minimum cost. Polasky and Solow (2001) considers the value of additional information in selecting sites for the establishment of ecological reserves. Lu, Ye, Neuman, and Xue (2012) present a case study for designing the collection of aquifer moni-

toring information by optimizing the balance between "data-worth" and cost. Caers (2011), Trainor-Guitton, Mukerji, and Knight (2013) and Trainor-Guitton, Ramirez, et al. (2013) apply VOI analysis to aquifer recharge and aquifer contamination problems, respectively. Witter, Trainor-Guitton, and Siler (2019) discuss the application of decision analysis and VOI to geothermal systems. Athens and Caers (2019) apply VOI analysis for the decision of optimal geothermal well placement.

1.2.5 Mining Applications

In contrast to the oil and gas industry, VOI application to mining problems is less well documented. Rojas and Cáceres (2011) evaluate different data configurations in infill drillhole campaigns for a copper porphyry using a resample and resimulate workflow and economic metrics though there is no direct mention of VOI. Barnes (1986) explicitly mentions VOI and ties deterministic geologic uncertainty in the form of kriging variance to economic risk with application to a coal mining scenario. He views data collection and uncertainty reduction as an economic commodity that is inherently valuable. Phillips, Newman, and Walls (2009) presents a VOI case study regarding the value of integrating ore grade scanners for blending purposes at an operating iron ore mine. Minimizing the cost of ore misclassification is the mode of value generation. Eidsvik and Ellefmo (2013) and Eidsvik et al. (2015) discuss VOI for exploration drillhole placement and the following sampling methods at an oxide ore-deposit. The reduction in uncertainty with planned drillholes is quantified. VOI is the difference in the resource value with and without additional information. Froyland, Menabde, Stone, and Hodson (2018) present a study on the value of additional infill drilling in an open-pit scenario. They compare the net present value (NPV) of the mine schedule with future information to the NPV with current information. Yüksel, Minnecker, Shishvan, Benndorf, and Buxton (2019) and Benndorf (2020) investigate the VOI of integrating on-belt radiometric sensors for live measurements of local coal impurities in an operating lignite mine. Real-time updating of the resource model and subsequent optimization of the mine plan to minimize blending penalties generate value. VOI is the difference in value between Scenarios with and without sensor information.

1.2.6 Decision Analysis Framework

The origins of decision analysis date back to the 18th-century work of Daniel Bernoulli. The analysis includes breaking down an uncertain, potentially problematic decision into the available information, possible alternatives, and the preferences of the decision-maker (Bernoulli, 1954; Howard, 1980). Bernoulli (1954) states the optimal decision is the one that maximizes the decision maker's expected utility. Though the concept of a utility function to capture decision-maker preferences was introduced in 1738, it was not formalized until the 20th century (Von Neumann & Morgenstern, 1944). The decision analysis theory has developed over time, though the decision analysis framework's principles remain based on applying simple logic to decision-making scenarios (Howard & Matheson, 1983). Howard and Abbas (2015) describes the six elements of a good decision as having the right frame, the right alternatives, the right values, the right information, the right reasoning and a decision-maker committed to taking action.

Howard (1966a) first introduced the term "decision analysis" and defines a decision as an "irrevocable allocation of resources". Modern decision analysis requires a probabilistic model that one can make inferences from. Howard (1966a) breaks down the decision analysis framework into (1) framing the decision, identifying the alternatives and assigning values to outcomes in a deterministic phase; (2) quantifying uncertainty, determining a position on risk and selecting the best alternative in a probabilistic phase; (3) deriving the value of uncertainty reduction and developing an economic information gathering scheme in a "post-mortem" phase. Howard (1968) further refines his rationale of the decision analysis framework with a detailed discussion of decision structure, risk preferences, utility and the concept of certain equivalents. He discusses how the monetary value derived from a decision outcome does not necessarily correspond to the utility the decision-maker receives. Howard and Matheson (1983) present a thorough review of the decision analysis framework in two volumes of papers on the application of decision analysis to investment planning, research and development, social policy and health and safety. Keeney and Raiffa (1993) presents an in-depth discussion of the decision analysis paradigm with particular focus on decision scenarios with multiple, often conflicting objectives. They stress that the maximization of several objectives simultaneously will lead to trade-offs in the real world. Howard and Abbas (2015) presents a complete and modern review of decision analysis, information collection

and VOI. Applying the principals of information collection to any scenario involves: (1) the information must be relevant to the decision problem; (2) the information must have the possibility of changing the decision; (3) collecting the information must be economical given the scenario. Bratvold and Begg (2009), Parnell, Bresnick, Tani, and Johnson (2013), Eidsvik et al. (2015) and Kochenderfer (2015) further discuss the application of probability and utility theory to rational decision making.

1.2.7 Decision Making in Spatially Correlated Problems

Random variables in earth science problems commonly exhibit spatial correlation related to the underlying phenomena of deposition. Our knowledge of the random variables is uncertain. Uncertainty is related to geologic heterogeneity and incomplete sampling. Uncertain inputs lead to decisions with uncertain outcomes; this commonly encountered scenario with prior spatial uncertainty warrants the application of rational decision analysis (Trainor-Guitton, Mukerji, & Knight, 2013). Bhattacharjya, Eidsvik, and Mukerji (2010) refers to spatial decision problems as those where there is a choice of alternatives over space, and the variable of interest is spatially correlated. Many decision analysis framework fundamentals remain the same; a rational decision-maker must have clearly defined objectives, logical alternatives based on the objective, a preference on risk, and a metric for utility (Scheidt et al., 2018). However, spatially correlated problems present unique complexities in that the information collected is spatially dependent, and the collection of information is rarely a discrete event (Eidsvik et al., 2015). In practice, a decision alternative may be a combination of multiple alternatives consisting of various data types. The decision-maker is not only faced with the question of how much information but what type of information. Bratvold and Begg (2009), Caers (2011) and Eidsvik et al. (2015) present the most thorough and modern documentation of decision making in spatially correlated scenarios with the latter providing in-depth discussion of the unique complexities faced by earth science decision-makers. Eidsvik et al. (2015) states that many possible decision alternatives provide an advantage to decision-makers as it becomes possible to tune the spatial coverage or accuracy of the information given the objective. Given the presence of spatial correlation, few data could potentially inform the entire domain.

Consistent with the decision analysis framework, a probabilistic model characterizing the

distribution of the variable must be constructed to facilitate the decision making and information collecting process. The distribution of prior uncertainty is typically accessed though a stochastic algorithm such as sequential Gaussian simulation (C. V. Deutsch & Journel, 1998) or multiple-point statistics (Strebelle, 2002). Additional spatial information updates the prior distribution of uncertainty. Integration of new information may be performed numerically as in Englund and Heravi (1993), Wilde (2010), Rojas and Cáceres (2011), Pinto (2015) and Barnett et al. (2018) or through an analytical, inverse modeling approach as in Bratvold and Begg (2009), Bhattacharjya et al. (2010), Caers (2011), Trainor-Guitton et al. (2011), Trainor-Guitton, Mukerji, and Knight (2013) and Eidsvik et al. (2015).

1.2.8 The Effect of Additional Information

The true inherent state of nature is not uncertain. Only one true distribution of the variable of interest exists. Our incomplete knowledge leads to uncertainty as few data relative to the volume of interest are available. The underlying geologic processes are too complex to be fully characterized by sparse data (Pinto, 2015). This uncertainty is often reduced when additional information is collected (Barnett et al., 2018; Rossi & Deutsch, 2013; Wilde, 2010). To understand the effect of additional information, one must understand the factors which control the prior uncertainty at a scale relevant to the technical decision. Common uncertainty measures are standard deviation or the probability to be within a particular threshold about the mean. C. V. Deutsch and Beardow (1999), Wilde (2010) and Pinto (2015) show that measures of uncertainty decrease asymptotically as the level of information increases (Figure 1.1). In spatially correlated scenarios, there is often unresolvable intrinsic uncertainty, regardless the amount of additional information.

Information is collected to reduce uncertainty to an acceptable level and, in turn, minimize or maximize a metric of interest. Information, however, comes at a cost. An optimal amount of information would balance the cost of uncertainty and the cost of information. The choice of metric to determine optimality is subjective. The cost of uncertainty is model and project-specific. C. V. Deutsch and Beardow (1999) describes the cost of uncertainty in an oil sands project as uncertain strip ratios, sub-optimal road placement or increased cost due to uncertainty in bitumen to fines ratio. Barnett et al. (2018) describes the cost of uncertainty in the development of an oil shale play as lost net present value due to

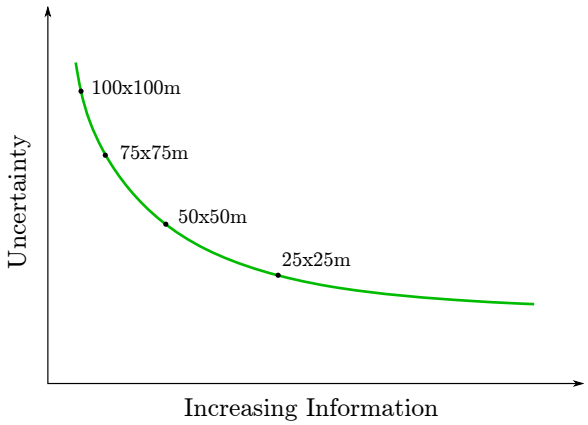

Figure 1.1: Schematic figure of a measure of uncertainty versus available information. Uncertainty often decreases asymptotically beyond a certain threshold. The black dots represent hypothetical data spacings.

developing poor drainage areas or final placement of a producing well at a sub-optimal elevation.

1.2.9 Analytical Approaches to VOI

The value with current information is referred to as the prior value (PV), while the value with future information is the posterior value (PoV). Analytical VOI paradigms directly evaluate the prior and posterior values using their respective probability distributions. Analytical approaches are generally limited to scenarios where prior and likelihood probability distributions are discrete or in more complex scenarios rely on the assumption that the distributions are parametric. In simple cases, prior and likelihood probability distributions could be from some degree of belief, past production or previous knowledge (Bratvold & Begg, 2009). Parametric approaches typically rely on strong Gaussian assumptions, and parameterization of those posterior distributions by linear combinations of the variables (Bhattacharjya et al., 2010; Eidsvik & Ellefmo, 2013). Without making a Gaussian assumption, there may be no analytical solution, and a numerical approach must be adopted.

A simple application of the analytical paradigm is common in petroleum problems. The posterior probability distribution is evaluated analytically from prior and likelihood distributions. The prior distribution represents the uncertainty about the variable of interest and the likelihood distribution represents the relevance of the future information for predicting the variable of interest. Consider the collection of information y which provides imperfect in-

formation about a discrete variable z, such as lithology within a binary decision framework. The expected value of z for a decision alternative A is $E\{V(z;A)\}$.

$$PV = max\left[\sum_{z} E\{V(z;A)\} \cdot P(z)\right] \tag{1.2}$$

$$PoV(y) = \sum_{y} max\left[E\{V(z;A)\}\,|\,y\right] \cdot P(y) \tag{1.3}$$

Where $P(z)$ and $P(y)$ represent the prior and pre-posterior distributions, respectively. The posterior probability density function is used to determine the posterior value, that is the value of the decision conditional to the future data observations (Ulrych, Sacchi, & Woodbury, 2001). Establishing the pre-posterior distribution $P(y)$, requires knowledge of the prior, $P(z)$, and likelihood, $P(y|z)$, distributions. The prior and pre-posterior distributions can be evaluated analytically by "flipping" the probabilities from assessed to inferred form with Bayes' Law (Bratvold & Begg, 2009):

$$P(z|y) = \frac{P(y|z)P(z)}{P(y)} = \frac{P(y|z)P(z)}{\sum_z P(y|z)P(z)} \tag{1.4}$$

$$P(y) = \frac{P(y|z)P(z)}{P(z|y)} \tag{1.5}$$

Consider a simplified application. The hypothetical binary decision scenario is to drill an exploration well to determine the presence of rock type 1, or not. Geophysical data is proposed to improve the well placement. Based on conditioning data the prior probability of rock type 1, $P(RT = 1)$, is 0.40. Based on historical data the likelihood of the geophysical data correctly identifying rock type 1, $P(y|RT = 1)$, is 0.90. If the value of successfully drilling rock type 1 is 10 units and the value of an unsuccessful well is -1 unit, how much should one be willing to pay for the geophysical data? Figure 1.2 shows the inferred probabilities calculated with Bayes' Law.

The posterior probability for rock type 1 given a positive geophysical response is:

$$\begin{aligned} P(RT = 1|y) &= \frac{P(RT = 1)P(y|RT = 1)}{P(RT = 1)P(y|RT = 1) + P(RT = 0)P(y|RT = 0)} \\ &= \frac{(0.4)(0.9)}{(0.4)(0.9) + (0.6)(0.1)} = 0.86 \end{aligned} \tag{1.6}$$

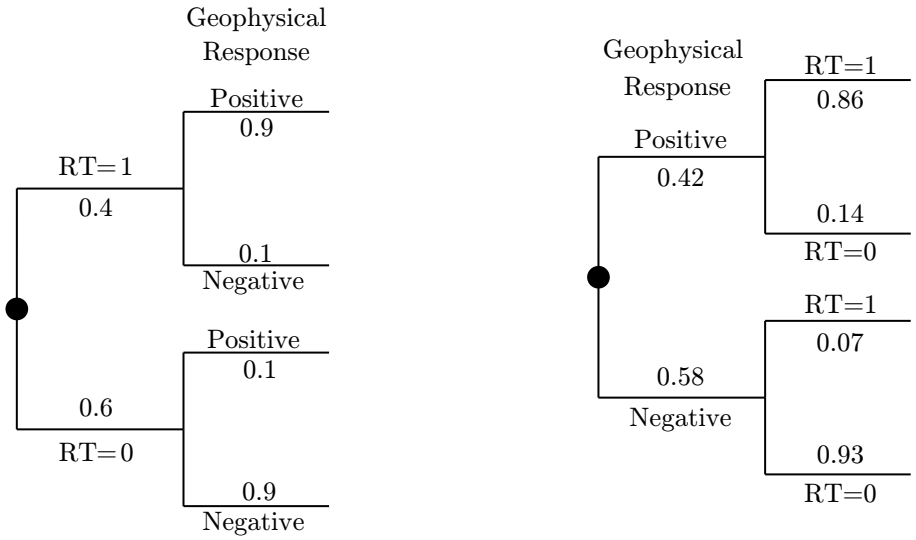

Figure 1.2: Assessed (left) and inferred (right) probability trees. The posterior and pre-posterior probabilities are calculated with Bayes' Law.

The pre-posterior probability is:

$$P(y) = \frac{P(RT=1)P(y|RT=1)}{P(RT=1|y)} = \frac{(0.4)(0.9)}{0.86} = 0.42 \tag{1.7}$$

The prior and posterior values for the decision framework are:

$$PV = max[0,\ (10 \times 0.4) + (-1 \times 0.6)] = 3.40 \tag{1.8}$$

$$\begin{aligned} PoV(y) &= 0.42 \cdot max[0,\ (10 \times 0.86) + (-1 \times 0.14)] + 0.58 \cdot max[0,\ (10 \times 0.07) + (-1 \times 0.93)] \\ &= 0.42 \cdot max[0,\ 8.46] + 0.58 \cdot max[0,\ -0.23] \\ &= 3.54 \end{aligned} \tag{1.9}$$

The value of zero comes from the decision alternative to take no action. The value of information is the difference between the posterior and prior values:

$$VOI(y) = 3.54 - 3.40 = 0.14 \tag{1.10}$$

The maximum value one should be willing to pay for geophysical data in this scenario is 0.14 units. These simple analytical examples are interesting and useful to understand principles, but may not apply in more complex realistic situations.

1.3 Data Spacing and Uncertainty

Wilde (2010) and Pinto (2015) present in detail the interaction of data spacing and uncer-

tainty measures. The concepts are presented here in summary, as they are fundamental to VOI analysis.

1.3.1 Measures of Data Availability

Standard measures of data availability include drillhole density (DHD) and drillhole spacing (DHS). DHD and DHS can be measured in both two and three dimensions. Calculating one metric from the other is possible, so the choice of metric is not critical.

Drillhole density is simply the number of drillholes per unit area or volume. A densely sampled area will have a high data density and sparsely sampled area will have low data density (Figure 1.3 (left)). The density in two dimensions at a location $\mathbf{u}$ is the number of samples within a given area A centered on $\mathbf{u}$, divided by the area:

$$DHD(\mathbf{u}) = \frac{n_A(\mathbf{u})}{A(\mathbf{u})} \tag{1.11}$$

Reporting density as drillholes per hectare ($10000m^2$) is typical. As data density directly relates to the physical volume of information present, it permits a simple calculation of the collection cost.

Drillhole spacing is the distance between neighbouring drillholes within an area. A densely sampled area will have a low data spacing and sparsely sampled area will have high data spacing (Figure 1.3 (right)). In two dimensions with regularly gridded data the spacing is equal to:

$$DHS(\mathbf{u}) = \sqrt{\frac{A(\mathbf{u})}{n_A(\mathbf{u})}} \tag{1.12}$$

Where $A(\mathbf{u})$ is the area of interest defined by dimensions d_x and d_y and $n_A(\mathbf{u})$ is the number of samples within the area. In three dimensions, if the drillholes are vertical the problem reduces to two dimensions. For irregularly spaced and non-vertical drillholes, the equivalent regular data spacing is calculated as the number of regularly spaced vertical drillholes which would contain the same number of samples as the real drilling within the volume $V(\mathbf{u})$ (Machuca-Mory & Deutsch, 2006; Wilde, 2010):

$$DHS(\mathbf{u}) = \sqrt{\frac{V(\mathbf{u})}{c \cdot n_V(\mathbf{u})}} \tag{1.13}$$

Where c is the down hole composite length. Equation 1.13 requires either a fixed number of samples or a fixed volume in three dimensions. If the volume is fixed, $n_V(\mathbf{u})$ is calculated as

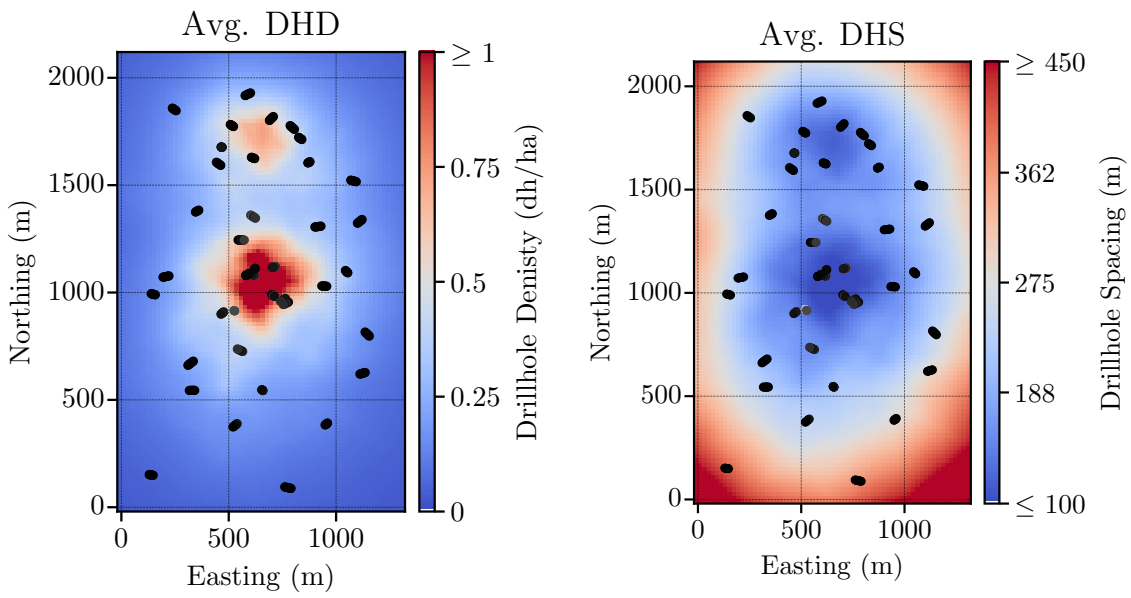

Figure 1.3: Two dimensional drillhole density (left) expressed as the number of drillholes per hectare and drillhole spacing (right) expressed in meters.

the number of samples within the volume $V(\mathbf{u})$. If $n_V(\mathbf{u})$ is fixed, $V(\mathbf{u})$ is calculated such that n_V samples fall within it. In practice $n_V(\mathbf{u})$ is often fixed. There is no theoretically correct value for $n_V(\mathbf{u})$ however 10 to 20 typically gives stable results (Barnett et al., 2018).

1.3.2 Measures of Uncertainty

The state of incomplete knowledge of a continuous random variable is characterized by the cumulative distribution function (CDF). In a simulation context, local uncertainty at a location $\mathbf{u}$ is characterized by the conditional CDF or probability distribution of L possible values, where L is the number of simulated realizations conditional to (n) data.

$$F(z;\mathbf{u}|(n)) = Prob\{Z(\mathbf{u}) \leq z|(n)\} \ \in [0,1] \tag{1.14}$$

Common measures of local uncertainty used in geostatistics are standard deviation, precision and the probability of misclassification. Standard deviation is the square root of the expected squared difference from the mean and provides a measure of dispersion about the mean value in the same units as the variable (Figure 1.4).

$$\sigma_Z = \sqrt{E\{[Z - m_z]^2\}} \tag{1.15}$$

Precision is a measure of the narrowness of a distribution and characterized by the propor-

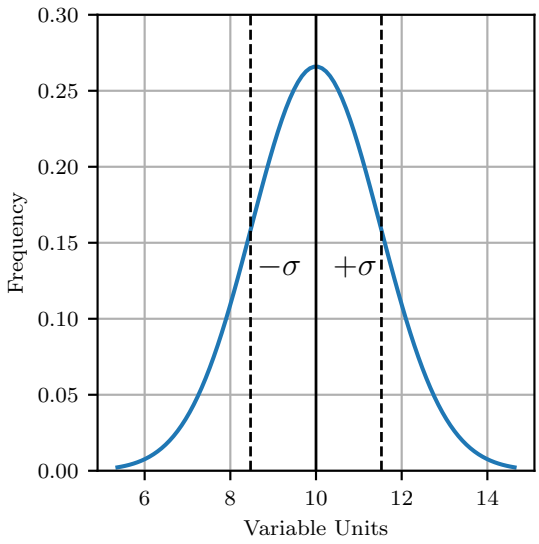

Figure 1.4: Standard deviation about the mean of the distribution.

tion of values that fall within a certain distance from the mean (Wilde, 2010). The narrower the distribution, the more values fall within the interval. A measure of precision requires a specified tolerance interval, ti, about the mean; a common tolerance value, t, in mining is $\pm$ 15% (Dohm, 2005) shown in Figure 1.5.

$$ti = E\{Z\} \cdot t \tag{1.16}$$

Precision is then the probability to be within the specified tolerance interval:

$$Prec(t) = Prob\{E\{Z\} - ti \leq Z \leq E\{Z\} + ti\} \tag{1.17}$$

Consider a threshold, z_c, which discretizes both a true and an estimated distribution into two categories. Plotting the true distribution against the estimate with the threshold z_c generates four discrete quadrants shown in Figure 1.6.

The lower right and upper left quadrants represent Type I and Type II errors, respectively. Type I errors or false positives occur when the estimated value is greater than z_c while the true value is less. Type II errors or false negatives occur when the estimated value is less than z_c while the true value is greater. The probability of misclassification is the probability of Type I (P_I) and Type II (P_{II}) errors occurring. Conversely, the probability of correct classification could be calculated as 1 minus the probability of misclassification.

$$P_{mis.} = P^I + P^{II} \tag{1.18}$$

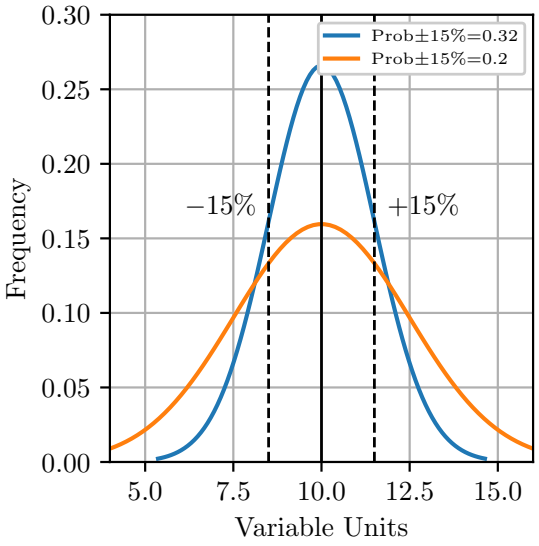

Figure 1.5: Two distributions with the same mean and different variances. The blue distribution is narrower and therefore a greater proportion of values fall within the ±15% tolerance interval. The probability to be within 15% of the mean is 0.32 and 0.20 for the blue and orange distributions, respectively.

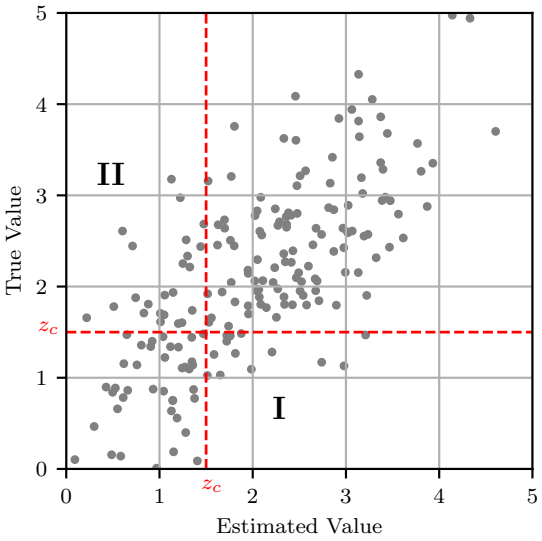

Figure 1.6: Schematic diagram of Type I and Type II errors given the cutoff z_c (red dashed lines).

$$P_{corr.} = 1 - P_{mis.} \tag{1.19}$$

There are many different ways to summarize a distribution of uncertainty. It is important that we be able to predict uncertainty at the scale of relevance for the available data. The uncertainty may decrease in a non-linear way with additional data.

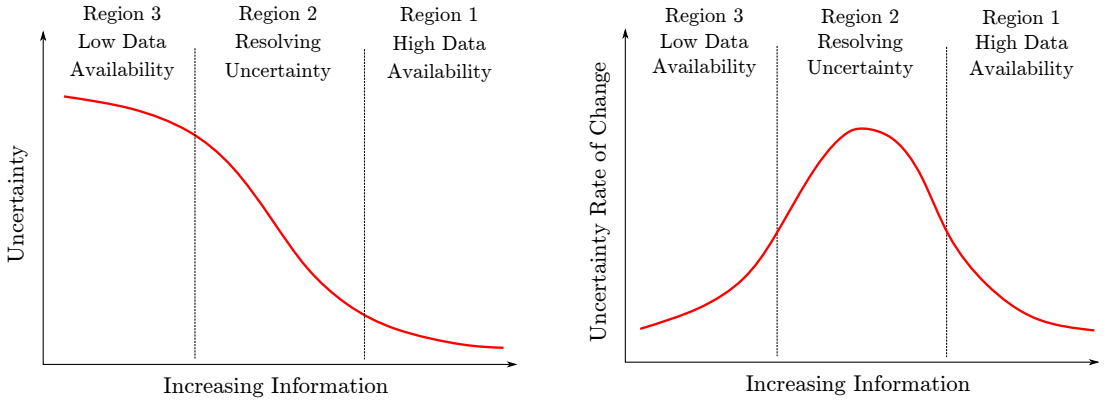

Figure 1.7: Schematic expected uncertainty curve (left) and the learning curve, or rate of uncertainty reduction (right). Modified after Pinto (2015).

1.3.3 The Learning Curve Concept

The concept of the learning curve is summarized from Pinto (2015). The rate of uncertainty resolution is a function of data availability and the variogram model. The learning curve can help a decision-maker determine the minimum amount of data required to achieve an acceptable level of uncertainty.

The learning curve (Figure 1.7 (right)) is the first derivative of the expected uncertainty curve (Figure 1.7 (left)). The expected uncertainty curve is the conditional mean of the uncertainty measure versus the measure of data availability. Dividing the expected uncertainty curve into three regions identifies (1) a low uncertainty region related to high data availability, (2) a region of uncertainty reduction and (3) a high uncertainty region related to low data availability. The learning curve or the rate of uncertainty reduction can be subdivided into three corresponding regions: (1) diminishing returns due to high data availability, (2) region of uncertainty reduction and (3) small contributions due to low data availability.

The learning curve concept is directly applicable to VOI analysis as the economically optimal decision alternative likely lies near the boundary between region 1 and 2 (Barnett et al., 2018). Much of the uncertainty relative to the scale of the decision has been resolved at this boundary. Understanding the rate of uncertainty resolution is essential for decision-makers to design information collection schemes and choose appropriate information types.

1.4 Utility and Value

Quantifying value in monetary units in natural resource industries is common. Quantifying value involves passing a geostatistical model through an appropriate transfer function. The utility or the usefulness of a particular value depends on the decision-makers' risk preferences and is a function of the value, $U(Value)$. Utility is an important concept in the decision-making framework.

1.4.1 Utility Functions

Incorporating the decision-makers' risk preferences can be done with a utility function (Von Neumann & Morgenstern, 1944). The utility function is a mathematical construct which takes units of value as an input and returns units of utility (Eidsvik et al., 2015). There are three positions a decision-maker can take on risk: (1) risk-averse with a convex utility function, (2) risk-neutral with a linear utility function and (3) opportunity-seeking with a concave utility function. There is a continuous spectrum between these positions. A neural risk position always generates the greatest expected value, as there is no penalization of low values or preference for high values.

Common utility functions are exponential (Equation 1.20) and power law (Equation 1.21) where $V(z)$ is the metric of value for the given outcome, z.

$$U_{exp}(V(z)) = \begin{cases} 1 - e^{-V(z)a}/a, & \text{if } a \neq 0 \\ V(z), & \text{if } a = 0 \end{cases} \tag{1.20}$$

$a > 0$ indicates risk aversion, $a = 0$ indicates risk neutrality and $a < 0$ indicates opportunity seeking preferences (Figure 3.11 (left)). a is practically within $[-1, 1]$.

$$U_{pow}(V(z)) = \left(\frac{V(z) - V_{min}}{V_{max} - V_{min}} \right)^{\omega}, \quad \omega > 0 \tag{1.21}$$

$0 < \omega < 1$ indicates risk aversion, $\omega = 1$ indicates risk neutrality and $\omega > 1$ indicates opportunity seeking preferences (Figure 3.11 (right)). ω is practically within $[0.1, 5]$. Equation 1.21 requires limiting minimum and maximum values V_{min} and V_{max}, respectively. Choice of V_{min} and V_{max} is subjective and influences the calculated utility.

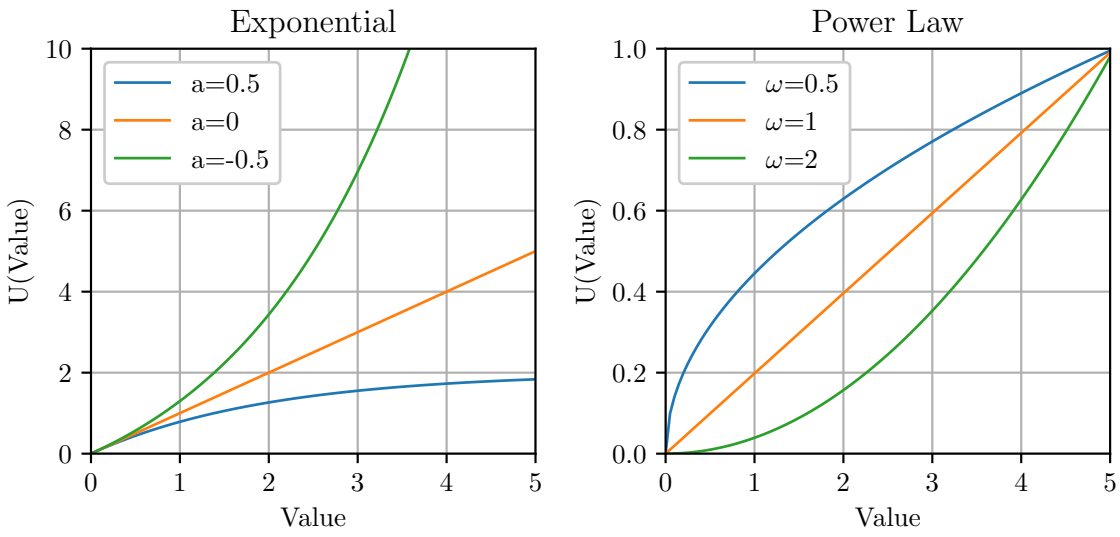

Figure 1.8: Exponential (left) and power law (right) utility functions.

Most decision-makers are naturally risk-averse. Risk aversion is an appropriate position when the consequences of underperformance are critical such as a medium-term decision like a 5-year mine plan. A risk-neutral position is appropriate for repeated short-scale decisions such as grade control, where generating maximum value is optimal. Risk neutrality is also appropriate for long-range decisions related to the life of a project; plans will likely change, and maximum value should be the goal. An opportunity-seeking approach is appropriate for decision scenarios where a few outliers generate significant value, such as mineral exploration or project acquisition decision scenarios.

1.4.2 Transfer Functions

A transfer function is any function that calculates an output from a geostatistical model. Transfer function input is a complete model of relevant characteristics, and the output is the desired response in units of utility. For decision scenarios with large solution spaces, the transfer function may be optimized stochastically through the formulation of an objective function considering the expected value across all $l = 1, ..., L$ realizations:

$$O(z) = \frac{1}{L}\sum_{l=1}^{L} U^l(V^l(z)) \tag{1.22}$$

A transfer function in a mining context could be generating an engineering design to calculate contained pounds of copper or ounces of gold for each simulated realization. The

transfer function converts quantities of metal to monetary units, and uncertainty in the expected response's expected value can be directly observed. Uncertainty in the predicted responses should initiate iteration within the decision analysis framework. Is the level of uncertainty acceptable given the decision goal? Should more information be collected to reduce the response uncertainty? Should a final decision be made?

1.4.3 Time Value of Money

The time value of money states that a given sum of money is worth more now than that same sum in the future. A mining project's value is measured in net present value (NPV) due to the generally long-lived operational nature. It is common practice to discount expected future cash flow to account for interest and potential risk (Hustrulid, Kuchta, & Martin, 2013). The sum of the discounted cash flows expected for a series of mining periods is the NPV. The collection of information, such as an infill drill program, is considered to be a capital expense (Cuba-Espinoza, 2014). The collection of information in any given period alters the projected cash flow and, subsequently, the project NPV. The total amount of information and the timing of information collected over the mining project's life are essential concepts when establishing value. For simplicity of implementation, the time value of money is not directly accounted for in this thesis.

1.5 Thesis Outline

Chapter 2 presents an overview of the numerical VOI paradigm and introduces the general concepts and approach of the simulation-based workflow. Chapter 3 introduces the principals of VOI illustrated with a 1D synthetic example. Details that influence VOI, such as geologic continuity, engineering scale, material value and decision making preferences, are investigated. Chapter 4 presents the implementation details of the simulation methodology using sequential Gaussian simulation. Practical considerations, such as the required number of true models and simulated realizations, are discussed. Chapter 5 addresses the management of uncertain value and the link between geologic uncertainty and value. Chapter 6 is a case study applying the numerical VOI paradigm to a greenstone-hosted gold deposit in West Africa.

Chapter 2

Numerical Value of Information Methodology

Assessing the VOI requires knowledge of future information or a numerical model of possible future information. Quantifying the effect of this information on a technical decision is achieved through a numerical approach. A discussion of analytical or model-driven approaches is not present in this thesis. It is not evident how analytical methods extend to complex decision scenarios with continuous or large solution spaces. Numerical VOI methods involve simulating future information to directly observe its influence on the prior distribution and decision outcomes. This chapter introduces the VOI decision framework and the concepts and general approach to calculating VOI with a numerical, simulation-based approach.

2.1 Decision Framework

Any VOI study begins with a decision framework where the problem is structured by identifying possible decision alternatives. Decisions in a mining context are often two-fold. The first decision may be to put an operation into production or not, follow a particular mine plan, or mine a particular underground stope geometry. The second part of the decision is whether or not to collect more information before performing the first part. Additional information likely influences the first part of the decision and is inherently valuable if the decision-maker can remain flexible and adapt to the new information. In this thesis the first part of the decision framework is to determine the optimal technical design to mine a particular volume. The second part of the decision framework is whether or not to drill more to improve that design. Additional information typically improves the technical design placement and generates greater value though there are scenarios where uncertainty is so high that additional information is no help. If additional information is valuable, the optimal amount must be quantified.

Some decision alternatives are not binary or easily enumerated; there may be many possible alternatives. The range of feasible mine plans or stope geometries is virtually infinite. The best decision alternative is optimized considering the expected value across a set of simulated realizations. The decision-maker must provide a reasonable initial framework given technical and economic parameters, existing infrastructure and other project-specific considerations. The decision-maker must then decide whether collecting additional information could improve the decision alternative. The decision-maker should also consider the type, quality and amount of additional information. Information collection should consider topography, existing infrastructure, and the mine plan. A range of information should be considered to give the decision-maker insight into how uncertainty reduction generates value. The optimal decision alternative is then determined for each additional data configuration. Considering additional or future information provides access to the VOI. Of all the evaluated decision alternatives, the one which maximizes the net VOI is selected.

2.2 VOI Overview

VOI paradigms establish how the value of a decision alternative changes with additional information. As decision making in earth science problems involves spatially correlated variables, the decision alternatives are spatially dependent. The decision of stope geometry depends on the spatial distribution of mineralization. Each decision alternative has a corresponding value as a function of the decision outcome, the variable's spatial distribution, the scale of the technical design, economic parameters, and the cost of acting. Framing the result of a decision alternative in terms of value provides additional information to the decision-maker beyond reducing uncertainty. Units of value also permit multiple alternatives to be directly compared, even if different information types are collected. Generally, monetary units are straightforward to conceptualize and will be the unit of value in this work.

The collection of information resolves uncertainty around the variable of interest, updating a prior distribution of uncertainty to a posterior distribution. In general terms, VOI is the difference in value between the decision alternative with posterior uncertainty and prior uncertainty. Consider $c = 1, ..., C$ future data configurations where the current configuration is $c = 0$. The value generated by a particular data configuration is $V(c)$. The value of

information for a particular data configuration is then:

$$VOI(c) = V(c) - V(0) \tag{2.1}$$

The value $V(c)$ is a function of a technical design D of a particular scale optimized on a geologic model G conditioned to a data configuration c, characterized by L realizations, economic parameters P_{econ} and a true geologic model conditioned to data configuration $c = 0$. Notation for the geologic model, technical design and economic value are presented below:

$$Geolgic\ Model = G(c,\ L) \tag{2.2}$$

$$Design = D(scale,\ G(c,\ L)) \tag{2.3}$$

$$Enonomic\ Value = V_{econ}(D(scale,\ G(c,\ L)),\ G(c,\ L),\ P_{econ}) \tag{2.4}$$

The value conditional to future data configuration c is then:

$$V(c) = V_{econ}(D(scale,\ G(c,\ L)),\ G(0,\ L),\ P_{econ}) \tag{2.5}$$

The value with current information is constant for a particular design and scale and represents the current state of knowledge:

$$V(0) = V_{econ}(D(scale,\ G(0,\ L)),\ G(0,\ L),\ P_{econ}) \tag{2.6}$$

The L realizations related to the design need not be the same L related to the value function's geologic model. Equation 2.5 is evaluated for all future data configurations and VOI is calculated with Equation 2.1. For a particular data configuration, if $VOI(c)$ is greater than the cost of acquiring c, the decision-maker should consider purchasing the information.

2.3 Numerical Approach

Decision scenarios in earth science are commonly flexible because the decision-maker may choose from many alternatives. The value generated from a particular decision alternative is often a complex, non-linear function of spatially dependent model properties. Increased decision flexibility may lead to a large solution space to optimize over and a subsequent

increase in computational requirements. It may be impossible to evaluate future value parametrically in these complex scenarios, and a numerical approach must be adopted.

Numerical methods utilize a "resample and resimulate" methodology and is the approach adopted in this thesis. A stochastic simulation algorithm generates point scale, equiprobable realizations of the variable of interest's spatial distribution. Sequential Gaussian simulation (SGS) (C. V. Deutsch & Journel, 1998) is a commonly implemented algorithm. These realizations both characterize the prior uncertainty and provide access to future information. As the realizations are simulated at the data scale and honour the input histogram and variogram, they can be sampled in such a way to simulate the collection of future information (Journel & Kyriakidis, 2004). Samples are drawn from the realizations to mimic data collection schemes. The subsequent realizations conditional to these samples characterize the posterior distribution updated by the given data configuration. Passing the realizations through a transfer and value function leads to a technical decision and a corresponding value. The VOI calculation is given in Equation 2.1.

The general simulation based work flow is as follows:

1. Generate a true model with the existing data configuration, $c = 0$.

2. Sample a true model with $c = 1, ..., C$ data configurations generating C datasets of the variable of interest

3. Calculate the cost to acquire each data configuration, $V^{cost}(c)$

4. For each $c = 0, ..., C$ data configurations:

    a. Generate L realizations conditional to c

    b. Pass L realizations through an objective function to generate a technical design

    c. Calculate the value of the technical design against the true model as $V(c)$

    d. Calculate gross VOI as $VOI(c) = V(c) - V(0)$

    e. Calculate net VOI as $NVOI(c) = VOI(c) - V^{cost}(c)$

5. Repeat all steps for T true models

6. Calculate expected net VOI as $E\{NVOI(c)\} = \frac{1}{T}\sum_{t=1}^{T} NVOI^t(c), \quad t = 1, ..., T \quad c = 1, ..., C$

7. Select the data configuration that maximizes $E\{NVOI\}$

The first step characterizes the prior uncertainty. Steps 2 and 4a characterize the posterior uncertainty for C future data configurations. Steps 4b-4c determine the prior value when $c = 0$ and the posterior value when $c > 0$. The expected VOI is the average across all true models. The workflow is presented graphically in Figure 2.1.

The numerical approach to VOI is conceptually straightforward. Resampling provides access to future information with realistic variability, and resimulation updates the prior distribution of uncertainty. The direct observation of the economic impact of uncertainty reduction is possible, as is VOI calculation. The following sections present the details of each step in the numerical resample and resimulate methodology.

2.4 Simulation Based Methodology

2.4.1 Simulate True Models

The first step in the simulation-based workflow is to generate a set of reference models for resampling. These reference models are considered the truth and define the geologic model $G(0,\ T)$. Consider the random variable Z as the variable of interest. In practice there may be a combination of continuous and categorical variables. The realizations are defined by $G(0,\ T) = \{z^t(\mathbf{u}),\ \forall\ \mathbf{u} \in A,\ t = 1, ..., T\}$ where A is the domain of interest, and T is the number of true models. These realizations reproduce the input histogram and variogram with statistical fluctuations. The true models are conditional to the data, representing the current state of knowledge if they are available. However, they may be unconditional given knowledge of the underlying histogram and variogram.

The number of true models has practical implications for the stability of the results. Considering a set of true models is required, so an unusually high or low realization does not bias results. Discussion regarding the choice of T is presented in Chapter 4.

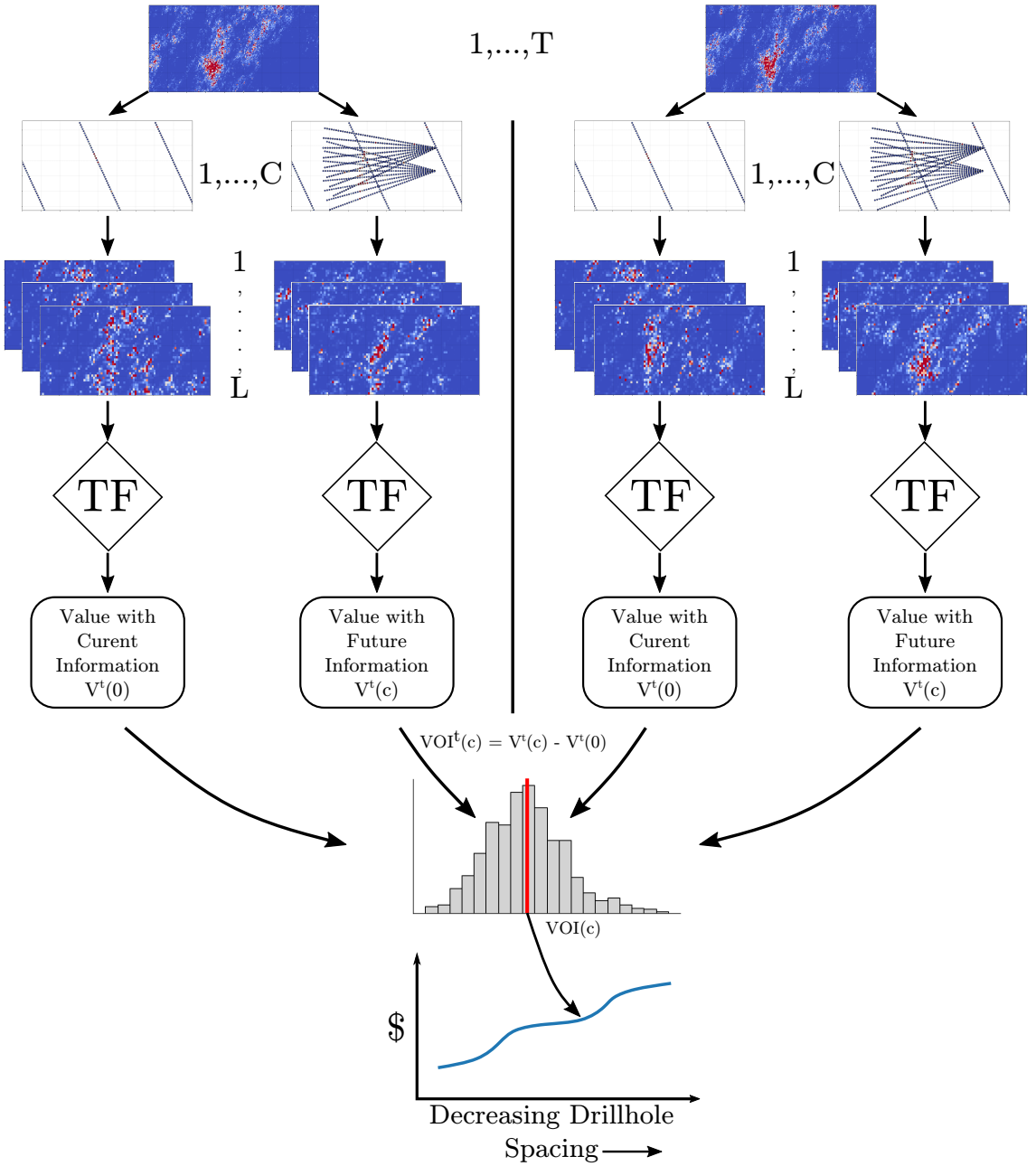

Figure 2.1: Graphical representation of the numerical VOI work flow where T is the number of true models, C is the number of future data configurations, L is the number of realizations, and TF represents the transfer function. The expected VOI is taken for each of the C data configurations.

2.4.2 Simulate Data

The next step is to sample the true models with $c = 1, ..., C$ future data configurations generating C new data sets $\{z_c^t(\mathbf{u}_i),\ i = 1, ..., n_{dh};\ c = 1, ..., C\}$ for each true model. The number of data for each configuration, n_{dh}, depends on the deposit and the decision-making framework. Random error could be added to the samples through a Monte-Carlo approach

to replicate imperfect sampling or to simulate different data qualities (Wilde, 2010).

2.4.3 Cost of Acquiring data

The cost of acquiring data depends on a large number of external factors. These costs are scenario, project and site-specific and also depend on the type of data collected. The total cost includes any additional costs associated with data collection and processing. Typically the cost of data is well understood by project operators. Calculating the cost to acquire each of the C future data configurations, $\{V^{cost}(c),\ c = 1, ..., C\}$, is performed before passing realizations through transfer and value functions. The cost of the current data configuration is zero, $V^{cost}(0) = 0$.

2.4.4 Simulate Realizations

Once the future data has been generated, the next step is to simulate L realizations of z conditional to each $c = 1, ..., C$ data set to characterize the geologic model $G(c,\ L)$. For a particular data configuration c, the set of realizations are defined as $G(c,\ L) = \{z_c^l(\mathbf{u}),\ \forall\, \mathbf{u} \in A,\ l = 1, ..., L\}$. This process generates $C * L$ total realizations for each true model.

High resolution, simulated realizations are at the same support as the conditioning data; however, calculation of uncertainty measures and the application of transfer functions must occur at an SMU scale relevant to the technical decision. Journel and Kyriakidis (2004) suggest simulating on a dense grid and arithmetically averaging the simulated nodes within a relevant SMU volume $V(\mathbf{u})$ to achieve a block support distribution of $z_c^l(\mathbf{u})$.

$$z_{V,c}^l(\mathbf{u}) = \frac{1}{|V|}\int_{V(\mathbf{u})} z_c^l(\mathbf{u})d\mathbf{u} \simeq \frac{1}{n_V}\sum_{i=1}^{n_V} z_c^l(\mathbf{u}_i) \tag{2.7}$$

Where n_V is the number of simulated nodes within the volume V. The transfer and value functions utilize the upscaled realizations. Like the number of true models, the number of realizations has practical implications for numerical stability. Discussion regarding the choice of L is presented in Chapter 4.

2.4.5 Transfer and Value Functions

The realizations conditional to future data configurations are passed through transfer and value functions converting the spatial distribution of Z to monetary units. The transfer, objective, and value functions are necessarily scenario, project and site-specific. The complexity of the objective function and choice of algorithm depends on the stage of project development. Late exploration or pre-feasibility stage projects may have uncertainties regarding operational costs, metallurgical parameters or economic parameters. This scenario may warrant a simple objective function until more detailed knowledge of relevant parameters is obtained. Some values, such as the cost of removing waste, may be fixed. Later stage projects in production have a better understanding of operational costs, penalties, recoveries, royalties and other relevant parameters. These scenarios warrant a more complex objective function that incorporates additional variables.

Transfer functions in this work consider the optimal placement of an engineering design such as a dig limit or stope boundary. The placement of the design is optimized through the application of an objective function. The objective function value is a function of the chosen utility function, the geologic model, economic parameters and the geometric configuration of the of the design:

$$O(D(scale,\ G(c,\ L))) = \frac{1}{L}\sum_{l=1}^{L} U^l(V^l_{econ}(D(scale,\ G(c,\ L)),\ G(c,\ l),\ P_{econ})) \qquad (2.8)$$

The value generated by the engineering design is a function of the design itself, the distribution of Z, and the operation's cost structure. Penalization of any factor relevant to the operation such as dilution or lost ore is possible. The synthetic examples presented in subsequent chapters utilize a simple greedy objective function with random perturbations. The case study in Chapter 6 utilizes a Stochastic Shape Optimizer (SSO) for stope geometry optimization. SSO is an application of Differential Evolution (DE) for the purpose of stope shape optimization across a set of simulated realizations realizations. This algorithm is deemed more appropriate for a realistic three dimensional study.

DE is a heuristic direct search algorithm, a practical algorithm for non-linear and non-differentiable objective functions (Rainer & Price, 1997). An initial population of size

$NP \times D$ is generated by randomly sampling the objective function space within the defined constraints. NP is the number of individuals in the population, and D is the number of the problem's dimensions. Each row vector in the initial population is an instance of the objective function parameters. Each vector from the initial population is passed through the objective function to calculate its economic value or evaluate its evolutionary "fitness". A mutant vector is then generated from the population by adding the scaled difference between two randomly selected vectors to a third randomly selected vector (Price, Storn, & Lampinen, 2006). A user-defined mutation factor scales this difference. A trial vector is generated by recombining the mutant vector with the initial population's current row vector considering a user-defined crossover probability. The trial vector's fitness is compared to the current population vector's fitness in an evolutionary sense. If the trial vector's fitness exceeds the current population vector's, it replaces the current population vector. Each iteration of the algorithm compares all population vectors to a randomly generated trial vector and accepts the trial vector if its fitness is greater than the current vector. The "surviving" vectors from each algorithm iteration become the parent vectors or the next iteration population.

2.4.6 Value of Information

Once the technical design has been optimized considering the space of uncertainty, the value of the design is calculated against the true model. For T true models, C values are calculated $\{V^t(0),\ V^t(c),\ c = 1, ..., C;\ t = 1, ..., T\}$.

$$V^t(0) = V^t_{econ}(D(scale,\ G(0,\ L)),\ G(0,\ t),\ P_{econ}) \tag{2.9}$$

$$V^t(c) = V^t_{econ}(D(scale,\ G(c,\ L)),\ G(0,\ t),\ P_{econ}) \tag{2.10}$$

Gross VOI is calculated as the difference in value between the technical decision made with the current data configuration and C future data configurations. For T true models, C gross VOI values are calculated as:

$$VOI^t(c) = V^t(c) - V^t(0),\ c = 1, ..., C;\ t = 1, ..., T \tag{2.11}$$

Net VOI is calculated as the difference between gross VOI and the cost of acquisition for

the particular data configuration:

$$NVOI^t(c) = VOI^t(c) - V^{cost}(c),\ c = 1, ..., C;\ t = 1, ..., T \tag{2.12}$$

The expected NVOI is then taken as the average NVOI value across all T true models:

$$E\{NVOI(c)\} = \frac{1}{T}\sum_{t=1}^{T} NVOI^t(c),\ c = 1, ..., C;\ t = 1, ..., T \tag{2.13}$$

Plotting the expected $NVOI$ for all data configurations identifies the maximum value and corresponding optimal data configuration.

2.5 Considerations for the Simulation Based Methodology

2.5.1 Optimal Decision Alternatives

VOI is commonly non-linear due to varying scales of geologic variability. As data spacing reaches a threshold, resolution of a particular scale of geologic heterogeneity occurs, leading to increased VOI values (Barnett et al., 2018). Various scales of heterogeneity may lead to multiple local VOI maximums, as shown schematically in Figure 2.2. Between these maximums, the generation of significant value does not occur.

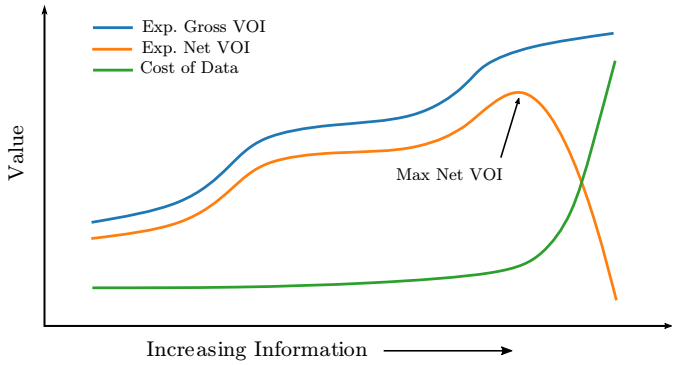

Figure 2.2: Schematic value of information curve highlighting the maximum net VOI which is the optimal sample spacing.

The optimal decision alternative is the data configuration that maximizes NVOI. This data configuration represents the optimal balance between the cost of uncertainty and the cost of data acquisition. The cost of uncertainty does not sufficiently reduce by collecting fewer data than the optimal configuration. Beyond this point, additional information has diminishing

returns, and the value generated does not justify its cost.

2.5.2 Confounding Factors

An essential concept is that data is not the only factor contributing to uncertainty. Though data availability is a principal driver of uncertainty, multiple confounding factors contribute to the total uncertainty.

Common confounding factors are the decision of first and second-order stationarity, adoption of a multivariate Gaussian assumption, the proportional effect, parameter uncertainty and the scale of modelling of the variable of interest. The conceptual geologic model, interpretation and inference of parameters, and the choice of modelling algorithms may also all affect the relationship between data spacing and uncertainty. These factors ultimately affect the relationship between data spacing and value generated from a technical decision. Though not discussed in detail here, Wilde (2010) and Pinto (2015) present each in detail. Chapter 4 discusses less common factors, such as the number of simulated realizations and the number of true models.

2.5.3 Geomodeling Details

A consideration of the simulation-based approach is that knowledge of the histogram and variogram of the variable required before implementing the methodology. A certain amount of data must already be collected to describe the variable's spatial distribution reliably. Therefore a certain amount of data is required to understand the relationship between data spacing and uncertainty; there must be enough data to understand how much data is required.

Another consideration of the simulation-based approach is the assumptions involved in generating a spatial model of uncertainty with SGS. An implementation of SGS means only continuous variables are considered. The assumption of first and second-order stationarity and Multivariate Gaussianity after the normal score transform is implicit. An assumption is that the variogram model characterizes the variable's spatial continuity, the quality of which may be affected by the amount of information available. Barnett et al. (2018) note the accuracy of a simulation-based VOI study depends on appropriate hierarchical geomodeling and incorporating as many "known unknowns" into the uncertainty model. Failing to do so

may result in a model of uncertainty where no meaningful relationship between information availability, geologic uncertainty and value can be determined.

2.6 VOI Plotting Conventions

Within this work, all plots that consider data spacing will show increasing information to the right as in Figure 2.2 and Figure 2.3. As the amount of information increases, the data spacing decreases—values on the x-axis decrease to the right. In three dimensions with irregular data configurations, the nominal data spacing is the equivalent square data spacing calculated with Equation 1.13 using a fixed volume. The equivalent square data spacing is the data spacing that would be achieved if the deposit was drilled with a regular square pattern. It is equivalent to the data spacing of regularly spaced drillholes perpendicular to the plane of greatest continuity that would contain the same number of samples as actually observed within the fixed volume (Pinto, 2015).

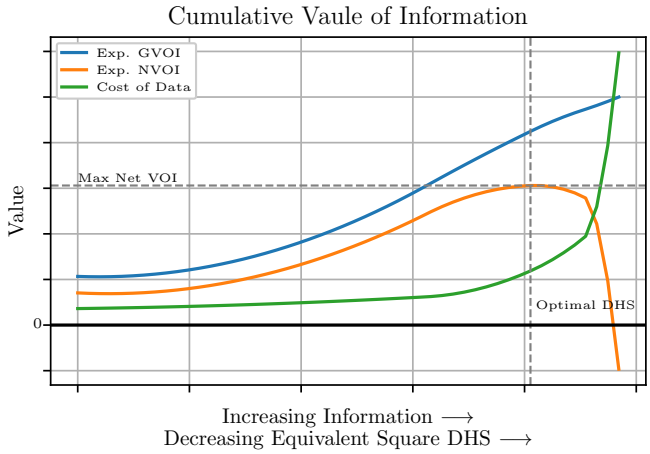

Figure 2.3: Schematic cumulative VOI plot identifying the optimal data spacing and maximum net VOI.

Figure 2.3 shows a schematic cumulative VOI plot with decreasing data spacing to the right. Gross (blue) and net (orange) VOI curves are relative to the true model $V(0)$ and not the previous configuration c. As the x-axis is the equivalent square data spacing, the cost of data (green curve) increases non-linearly. Cost is directly related to the number of samples collected. The number of samples, for example, per hectare ($100m^2$) increases at a rate of $\left(\frac{100}{DHS}\right)^2$. The dashed vertical line identifies the optimal data spacing based on the

maximum net VOI, identified by the horizontal dashed line.

Chapter 3

Principals of the Value of Information - A 1D Example

VOI is typically a complex response to the interaction of geologic scale, engineering scale, decision-maker risk preferences and economic parameters. The geologic scale in this work refers to a measure of spatial continuity, such as a variogram or correlogram. Engineering scale refers to the degree of selectivity in a technical design permitted by the mining method, geotechnical characteristics, available mining equipment or other considerations. A utility function captures risk preferences, which are non-linear for risk-averse or opportunity-seeking preferences. Economic parameters are predominantly project-specific; however, uncertainty may exist around market selling prices and exchange rates.

The geologic scale is straightforward to conceptualize. Additional data provide little information with very short variogram ranges as the data inform a very short distance away from the new data. At very long variogram ranges, additional data provide little information as the data become redundant. The engineering scale is also straightforward to conceptualize. Additional data provide little information if a technical design cannot capture newly resolved geologic detail. As the selectivity increases, the design can capture more geologic detail. Additional parameters may introduce non-linearity. A non-linear utility function may reject a decision alternative that generates greater expected value. Economic parameters may introduce additional non-linearity through asymmetric operational penalties such as different costs for dilution and lost ore.

The interaction of these parameters is not straightforward to conceptualize. Understanding these interactions is essential for quantifying VOI and selecting the optimal decision alternative. This chapter will introduce and illustrate each concept with a synthetic one-dimensional data set.

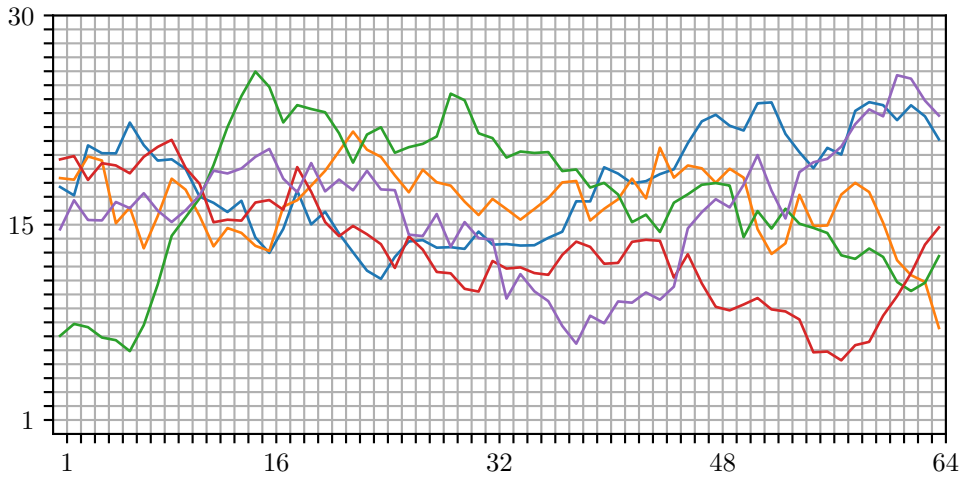

Figure 3.1: Five unconditional realizations which are resampled to generate future data configurations.

3.1 Synthetic Data

The synthetic data set comprises a 64 by 30 unit domain. The unconditional simulation of Gaussian deviates generates a one-dimensional array of point scale values. The distribution has a mean of 15 units and a standard deviation of 5 units. The spherical variogram model is a single structure. Simulated values are calculated as $z(\mathbf{u}) = y(\mathbf{u}) \cdot 5 + 15$. Figure 3.1 shows an example of five realizations. The simulated values could be considered a boundary realization. Grid nodes below the boundary are considered "inside" and tagged as 1; nodes above are considered "outside" and tagged as 0. The unconditional realizations characterize the true geologic model and are considered current knowledge for VOI calculations.

Future information is collected by sampling the array of Gaussian deviates at decreasing sample spacing (black dots in Figure 3.2). $c = 1, ..., 6$ future data configurations are considers with sample spacings of $[64, 32, 16, 8, 4, 2]$ units. Realizations are then resimulated conditional to future information. Comparing a set of realizations or a technical design against a true model determines correct classification, ore loss and dilution. Technical designs are optimized through a simple greedy objective function using the design geometry and fixed costs. The design's geometry is randomly perturbed, and the expected value is calculated as the average across all realizations. The new geometry is retained if the value is greater than the previous iteration, else it is rejected. A heuristic approach is deemed appropriate, given the simplicity of the scenario. The value of the design is the sum of the

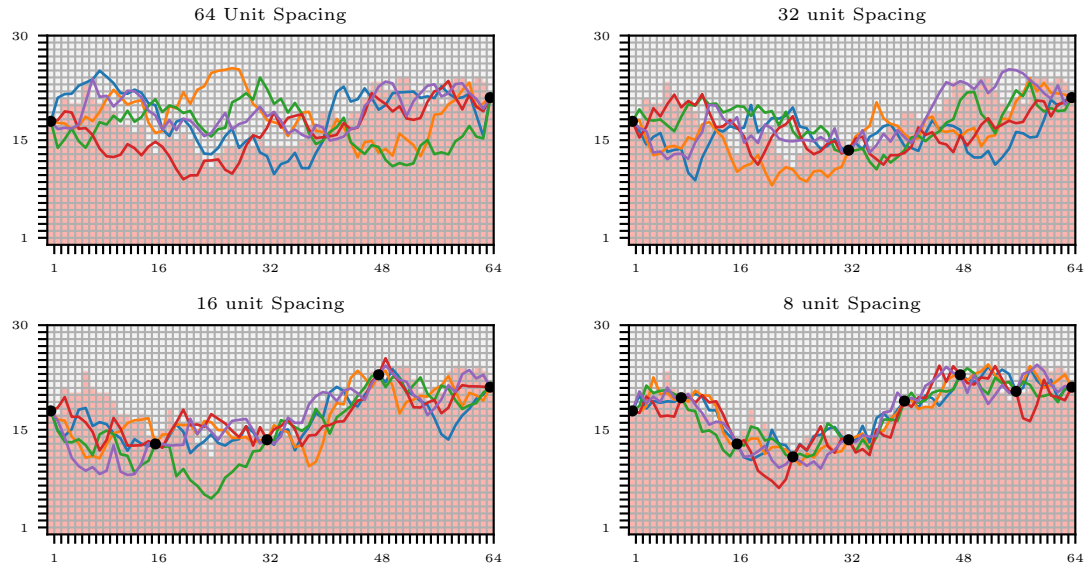

Figure 3.2: As additional information is collected (black dots), the resulting conditional realizations approach the reference model (pink grid nodes).

value of the blocks that fall within it. Throughout the chapter, the value of correct classification, misclassification, operational costs and operational penalties will change. Unless stated otherwise, the following examples consider a base case of $T = 10$ true models and $L = 100$ realizations.

3.2 Geologic Scale

Geologic variability is inherently present at all scales and is quantified statistically through a measure of variability versus distance, such as the variogram. As spatial continuity increases, the variability between two data separated by some fixed distance $\mathbf{h}$ decreases. The interaction of the geologic scale concerning the decision optimal of sample spacing is nonlinear. Consider a pure nugget variogram model where adjacent samples are uncorrelated. The uncertainty is so high and present at a scale less than the data, no amount of additional information may resolve it. The value of dense sampling may be the same as collecting few, widely spaced samples, or no information. Now consider a long-range, continuous variogram model where adjacent samples are highly correlated. Additional information resolves little uncertainty and quickly becomes redundant. Again, the value of dense sampling may be similar to sparse sampling, and little additional information may be the correct decision. Scenarios with short geologic scales require less information to make an optimal decision.

More information is required as spatial continuity increases though it reaches a threshold, and less is required due to redundancy. The geologic scale directly influences the optimal sample spacing.

3.2.1 Geologic Value

The geologic value of information is equivalent to the scenario of perfect selectivity and does not consider an engineering design. As additional data is collected, the resulting realizations approach the true model (Figure 3.2). Comparing each realization to the true model generates an expected geologic value. As geologic value assumes perfect selectivity, additional information always produces value.

The following example investigates the impact of the variogram model on geologic value—one scenario with constant nugget effect and variable range and one scenario with variable nugget effect and constant range. One true model is generated for each variogram model through unconditional simulation, as described above. The true model is sampled at 64, 32, 16, 8, 4 and 2 unit spacings, generating six new data sets. Sampling is nested. That is, the 2 unit sample spacing is inclusive of all previous sampling. $L = 1000$ unconditional realizations are generated to represent the current state of knowledge, $G(0,\ L = 1000)$. $L = 1000$ realizations are then generated conditional to each of the new data sets. These conditional realizations represent the state of knowledge with future data and characterize the geologic models $\{G(c,\ L = 1000),\ \forall\ C\}$. Scenarios use a fixed value of 10 units for correct classification and -5 units for misclassification. Assuming perfect selectivity, the value of the true model is the maximum attainable value.

3.2.2 Variogram Range

The following example considers four variogram models with ranges of 64, 32, 16 and 1 units. The models are a single spherical structure with no nugget. Figure 3.3 shows the results of varying the variogram range. “Uncond.” on the x-axis stands for unconditional realizations and represents the current state of knowledge. The y-axis shows the proportion of the maximum attainable value achieved by a particular data configuration. The variogram range has an impact on how additional information resolves uncertainty and generates value. The unconditional realizations generate roughly the same proportion of value; however, due

to ergodic fluctuations and a finite domain, the uncertainty (red error bars) is larger with a longer range variogram model. In general, as the variogram range decreases, a smaller proportion of value is generated, resolving less uncertainty for a given data configuration. Figure 3.3 highlights the non-linear influence of the variogram range. With a longer range variogram, as in panel (a), the relative change in value from large to small sample spacings is small due to data redundancy. As the variogram range decrease as in panels (b) and (c), the black curve becomes steeper and the relative change in value from large to small sample spacings increases. If the variogram range is short as in panel (d), the relative change in value from large to small sample spacings becomes small again as new samples are essentially uncorrelated, resolving little uncertainty.

3.2.3 Nugget Effect

Four variogram models are considered with nugget effects of 0.10, 0.25, 0.5 and 0.99. Each model is a single structure spherical model with the range held constant at 16 units. This section utilizes the same methodology as Section 3.2.2. Figure 3.4 shows the results of varying the nugget effect. As the nugget effect increases, the maximum attainable value for all sample spacings decreases, resolving less uncertainty. The increase in short-scale variability leads to smaller relative changes in value from large to small sample spacings. The non-linearity observed when changing the variogram range is not seen when changing the nugget effect. Though the proportion of overall value realized decreases as the nugget effect increases, dense sampling can still generate value even with a nugget effect variogram model, as seen in panel (d).

3.3 Engineering Scale

Perfect selectivity is never possible in practice. Mining must progress at a scale much larger than the data due to equipment and available data to support correct selection. An engineering design of a particular scale must be overlaid onto a geologic interpretation to establish economics, whether this is a pit shell, a stope design or a grade control boundary. Ore loss and dilution are always present. As more information is collected, the geologic interpretation approaches the real underlying geology. The engineering scale determines the design's ability to conform to the geology as shown in Figure 3.5.

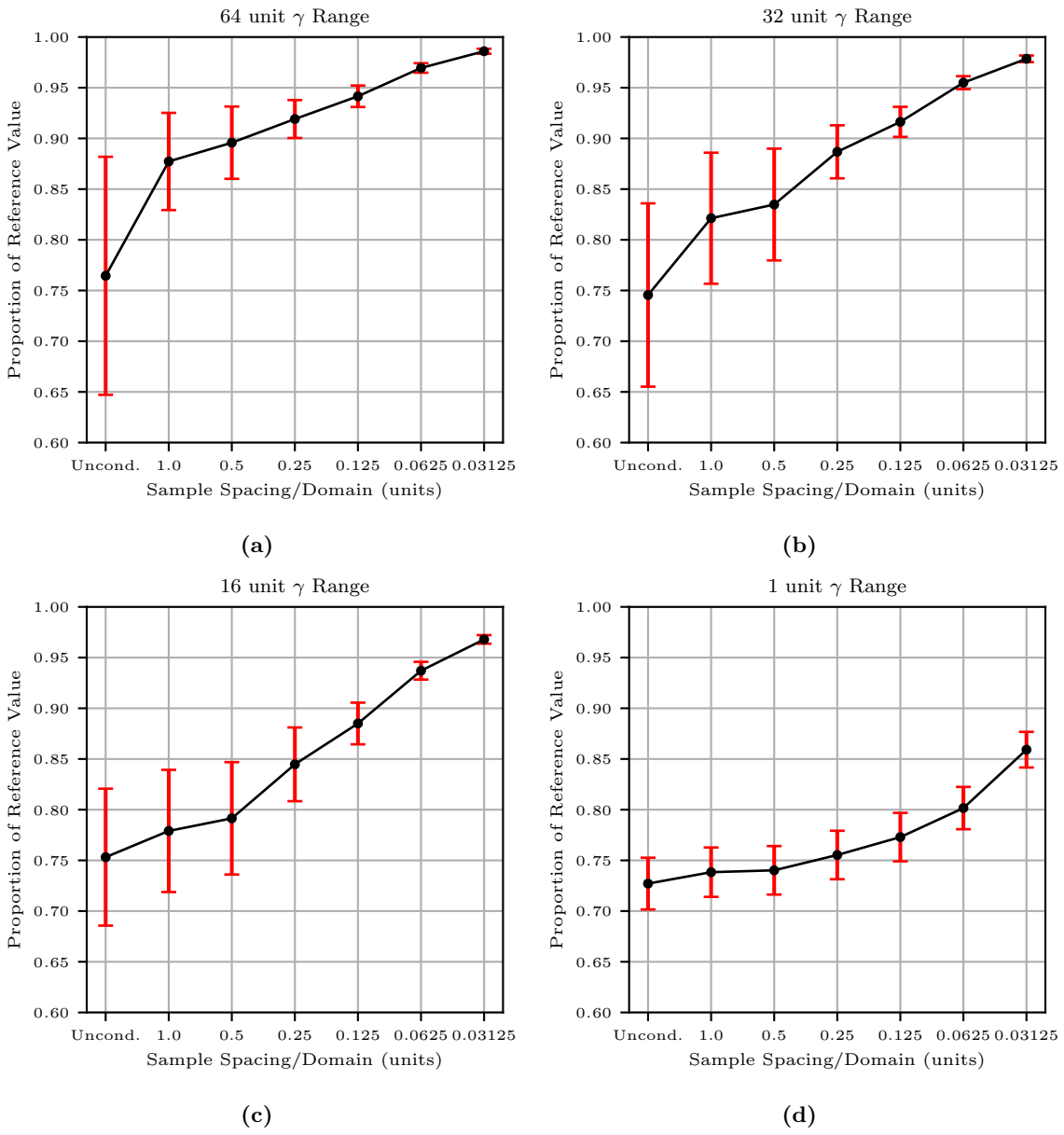

Figure 3.3: Distributions (n=1000) of value for various sample spacings and 64, 32, 16 and 1 unit range variogram models. The red bars are ± standard deviation.

3.3.1 Engineering Value

An engineering design could capture all resolved geologic detail with perfect selectivity. The optimal sample spacing in this situation is infinitely small (provided data has no cost) as any geologic feature resolved by additional information will generate value. The value of additional information increases consistently. Now, consider an engineering design with coarse selectivity or few degrees of freedom. Additional information is collected resolving

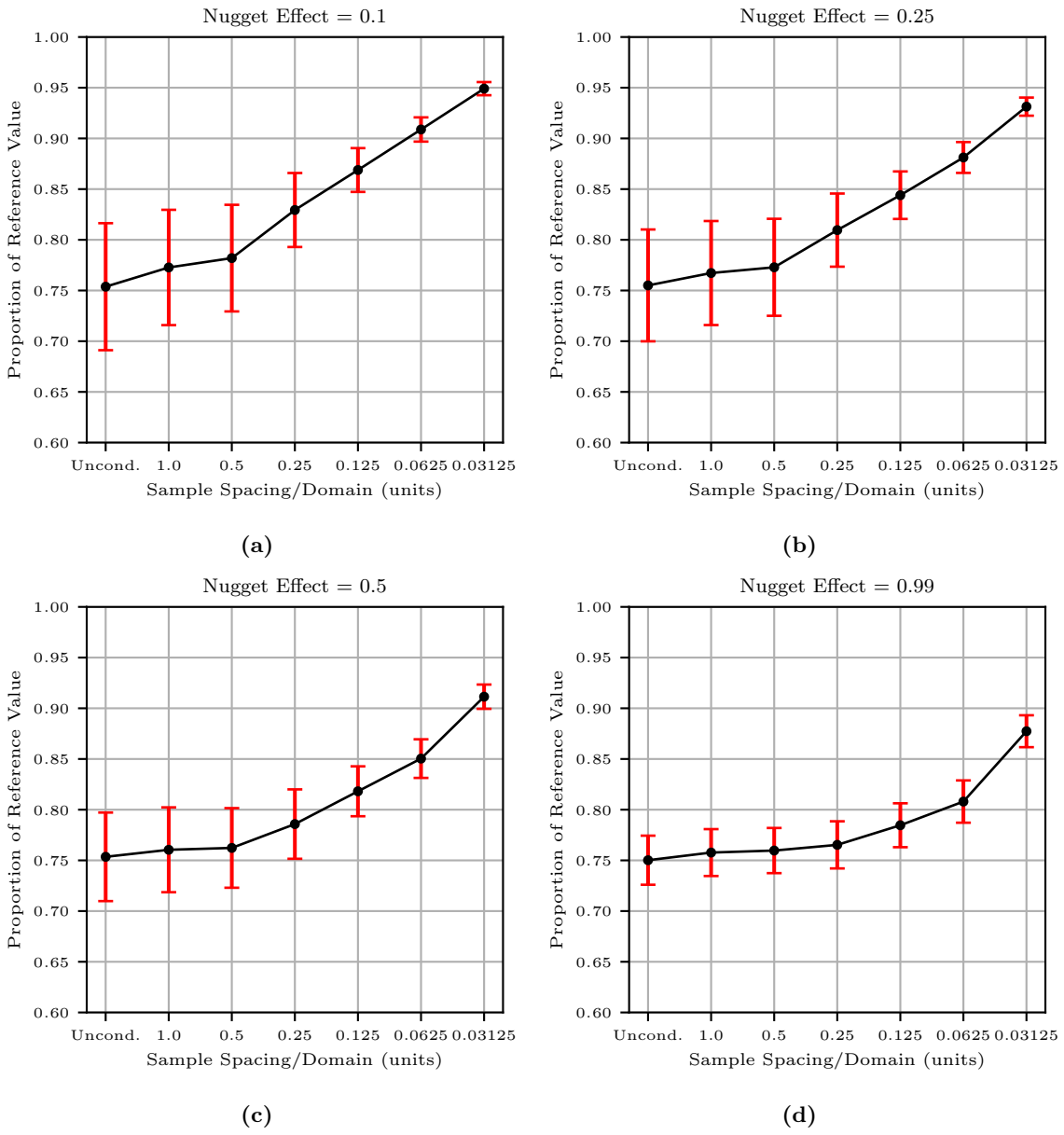

Figure 3.4: Distributions (n=1000) of value relative to the reference model for various sample spacings and 0.10, 0.25, 0.5 and 0.99 nugget effect variogram models. All variogram models are single structure spherical models with 16 unit range. The red bars are ± standard deviation.

geologic uncertainty; however, the design's limited flexibility may prevent taking advantage of the new detail. The coarse scale of the design prevents additional information from generating value. The optimal sample spacing may be few widely spaced samples or no additional information at all. The engineering scale directly influences the decision of optimal sample spacing.

Comparing an engineering design optimized on a geologic model, $D(scale,\ G(c,\ L))$ against

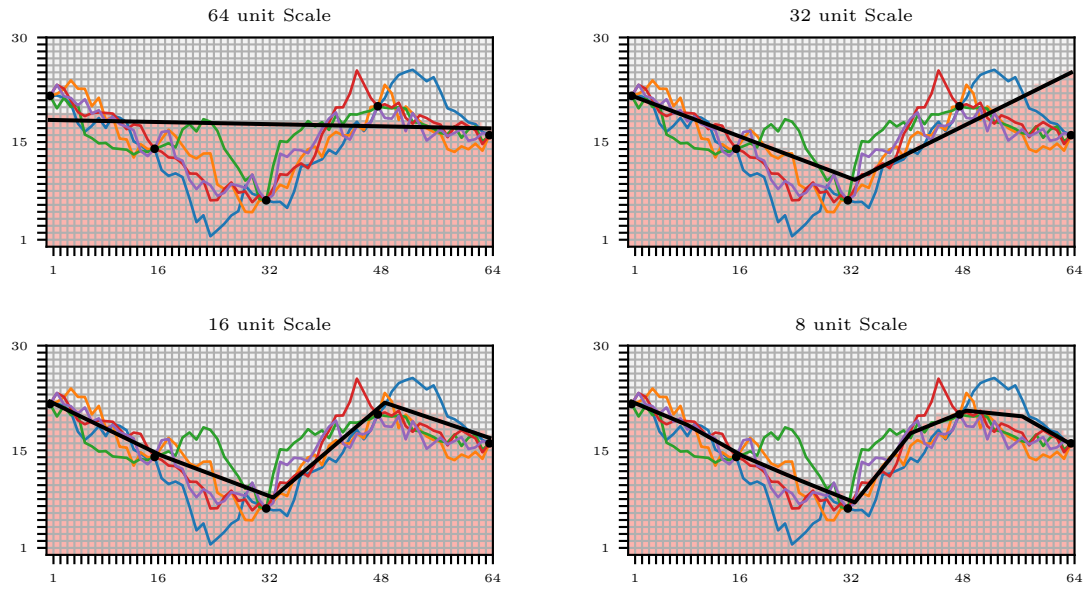

Figure 3.5: Four technical designs with different scales of engineering selectivity. As the degree of selectivity increases, ore loss and dilution decreases. The pink nodes are "inside" the design.

the true model $G(0,\ T)$ generates value. The following example considers design scales of 64, 32, 16 and 8 units with a fixed value of correct classification of 10 unit and misclassification of -5 units. Unlike geologic value, the value derived from an engineering design must consider dilution within the design (and potential ore loss penalties). As the degree of selectivity increases, ore loss and dilution decreases. Figure 3.6 shows the relationship between the engineering scale and the maximum attainable value. Reaching the maximum attainable value is not possible due to the selectivity of the design. A more selective design generates a greater proportion of maximum value; however, information has diminishing returns beyond a certain threshold. In panels (a), (b) and (c), sampling at spacing smaller than $\frac{1}{4}$ of the domain size generates relatively little additional value. In panel (d) with a finer 8 unit design scale, diminishing returns occur beyond sample spacing of $\frac{1}{8}$ of the domain size.

3.4 Interaction of Geologic and Engineering Scales

The relationship between the scale of the design and the spatial continuity of the variable is non-linear. Understanding this interaction for a particular spatially correlated scenario may enable the practitioner to infer the optimal decision outcome for a different set of

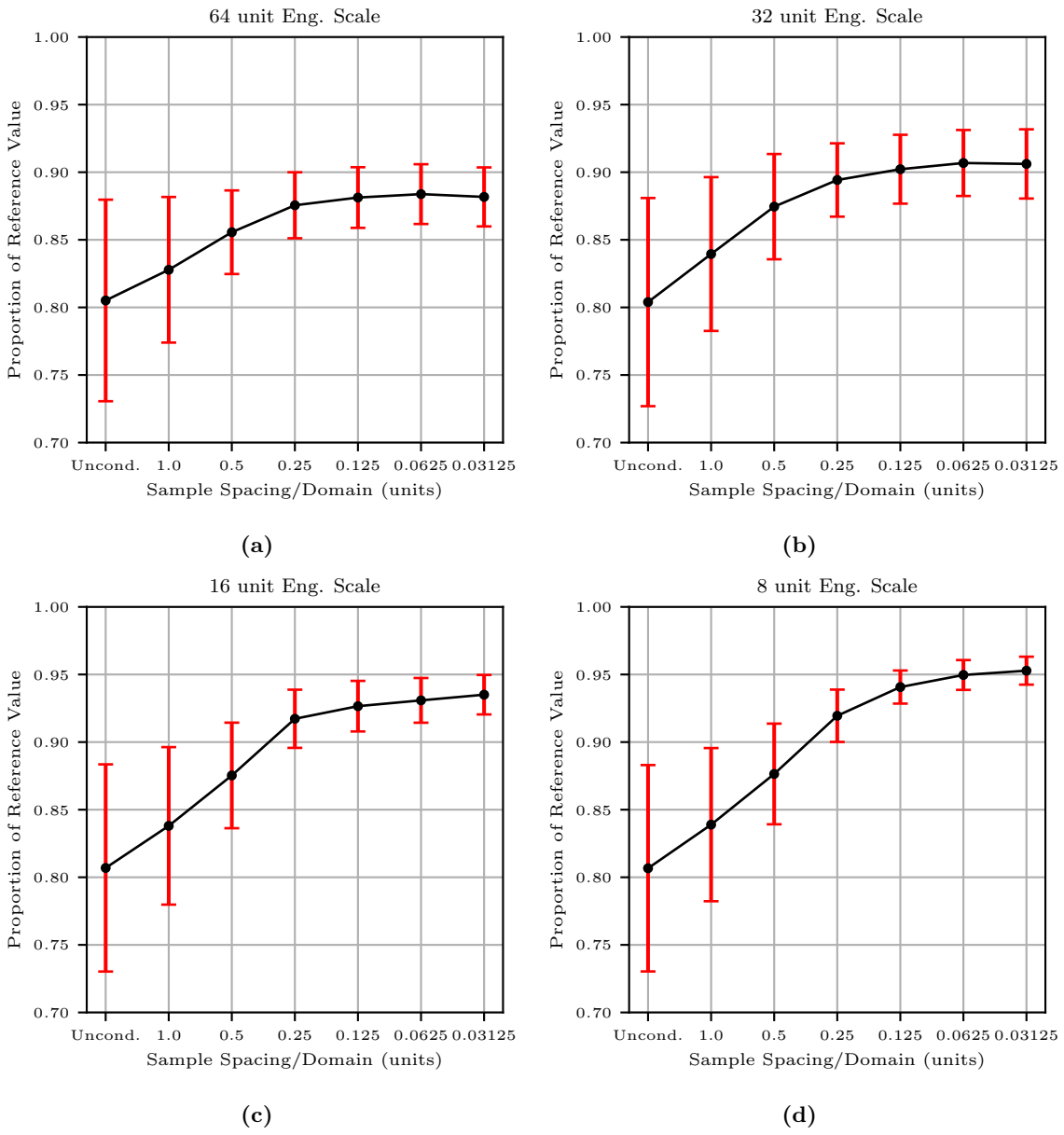

Figure 3.6: Distributions of value (n=10) for technical designs against the respective reference model. The black line is the expected value of the distribution. All variogram models are single structure spherical models with 32 unit range. The red bars are ± standard deviation.

alternatives without repeating the full numerical VOI workflow. Figure 3.7 shows the results of the numerical VOI workflow using the synthetic data set for a range of engineering design scales and variogram ranges to generate an optimal sample spacing surface. The optimal sample spacing is the one that maximizes the expected net VOI. The example considers fixed values of 10 and -5 units for ore and waste values, and a fixed cost of 50 units per additional sample. The previous examples considered the gross value and did not include

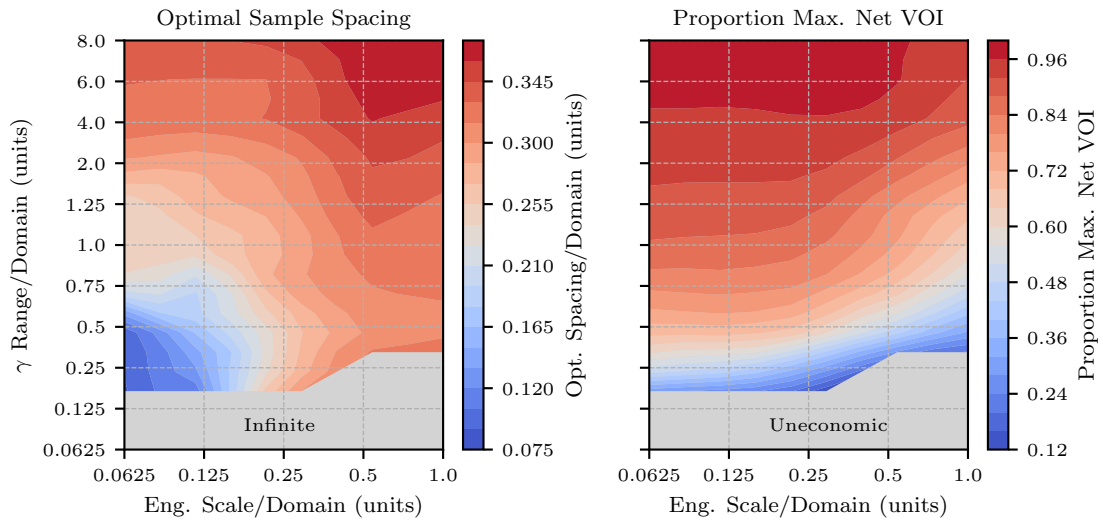

Figure 3.7: Optimal sample spacing relative to domain size (left) and percent of maximum expected net VOI (right) for a range of engineering and geologic scales. The y-axis in both plots is variogram range.

the cost of data acquisition.

Intuitively, additional information has the most significant contribution when geologic continuity is high, and the engineering design scale is small. There is less geologic uncertainty, and the design can capture finer geologic details. Conversely, when the geologic continuity is short, and the design scale is coarse, additional information may be uneconomic. The left plot in Figure 3.7 shows optimal sample spacing. The gray area at the bottom of the plot is a region of infinitely small data spacing. That is, for all design selectivities, no amount of information can resolve the uncertainty to generate positive net VOI. The right plot shows the maximum expected net VOI. The gray area at the bottom of the plot indicates the corresponding uneconomic region where any combination of geologic and engineering scales always generates negative net VOI. The correct course of action is to collect no additional information.

As the engineering scale increases, the optimal sample spacing increases while the maximum net VOI decreases. As the design capture less detail, additional information about the actual underlying geology is less useful as the decision-maker cannot adapt to it. As the variogram range increases, the optimal sample spacing increases, and the maximum net VOI increases as geologic features are more continuous. As continuity increases, additional information about real underlying geology becomes redundant and fewer or more widely spaced samples

are required to make an optimal decision.

3.5 Cost Structure

The net value of additional information is dependent not only on the cost to acquire it but also on operational and project-specific costs captured within the transfer and value functions. Transfer and value functions lead to a technical design. The unique geological, technical and economic characteristics of a mining project typically determine the cost structure. A particular deposit may be sensitive to dilution due to metallurgy or marginal ore grades. Geotechnical characteristics may necessitate a particular mining method that has a higher cost per tonne. The cost of mining and processing and operational penalties for ore loss and dilution may influence a technical design, impacting VOI. Penalties for dilution are often implicitly included in value functions as low-grade material generates negative revenue. Establishing lost opportunity or lost ore cost is not straightforward and would likely be a management policy decision. Changes in VOI may be relative where the optimal sample spacing is the same, but the VOI is different, or absolute, where the optimal sample spacing and VOI change.

3.5.1 Cost of Acquisition

Consider the limit cases for the cost of information collection. If there were no cost to acquire information, the optimal sample spacing would infinitely small. If the cost to acquire information is prohibitively expensive, the optimal sample spacing would be widely spaced or no data at all. Figure 3.8 shows how the net VOI changes as the cost of acquiring information increases. The following example explores the ratio of information cost to ore value using 2.5, 5, 7.5 and 10 and fixed values of 10 and -5 for ore and waste values. As the cost of information increases, the optimal sample spacing becomes wider, and the maximum net VOI decreases. The point of diminishing returns is approached quicker as the cost of data increases. Beyond this point, the value derived from the information no longer justifies its cost. Varying the cost of acquiring information has an absolute change in the optimal sample spacing.

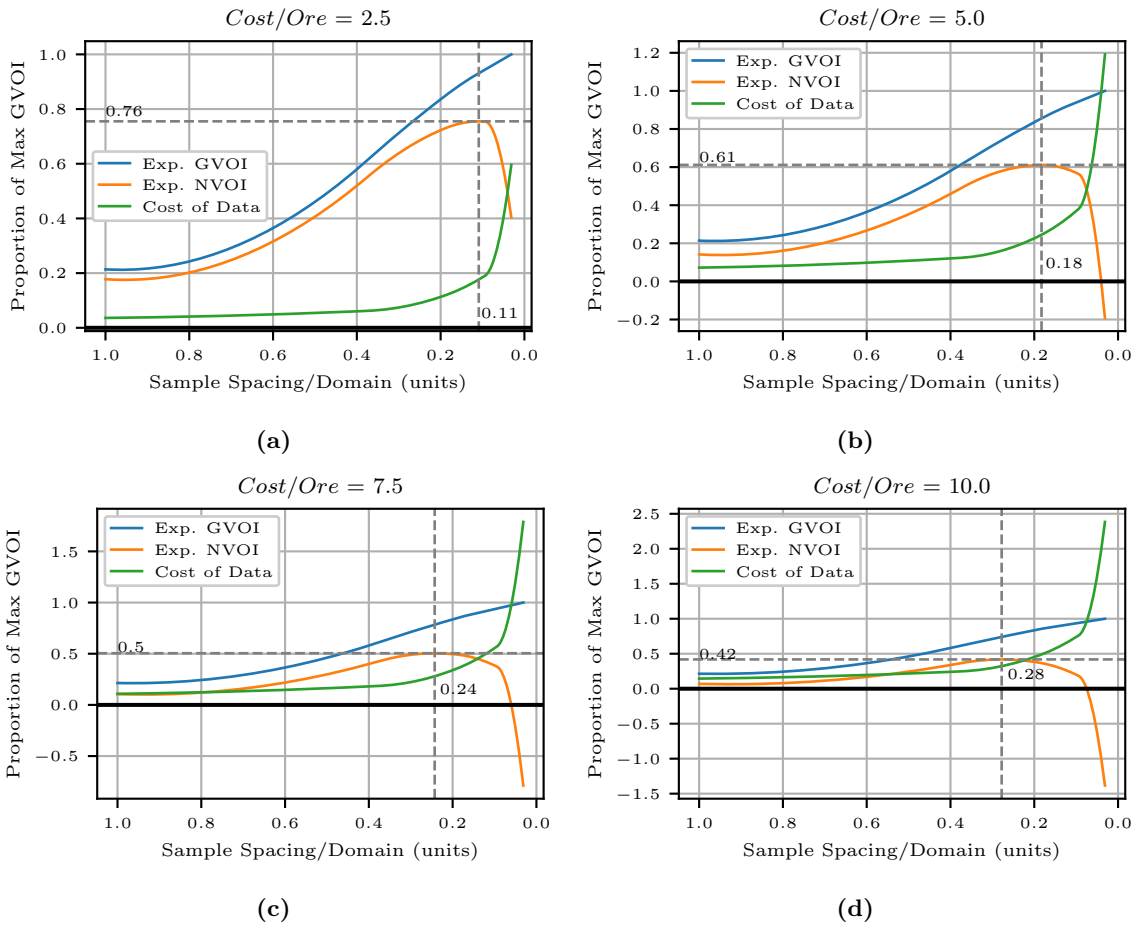

Figure 3.8: Four cumulative VOI curves for different costs of data acquisition. The optimal sample spacing is shown near the vertical dashed line and the corresponding net VOI is shown along the horizontal dashed line. Note the blue gross VOI curve is the same for all scenarios.

3.5.2 Material Value

The selling price of the modelled variable is a primary driver of the value of the technical design. High-value commodities like precious metals may justify the collection of greater amounts or more expensive information. The opposite holds for lower value commodities like base metals. Interestingly, greater uncertainty often exists about distributions of precious metals and more information is naturally required. The ratio of ore to waste values impacts the choice of optimal sample spacing. The following example considers ratios of 1, 2, 3 and 10 with a fixed cost of misclassification of -5 units and data acquisition of 50 units. Figure 3.9 shows the results. As the correct classification value increases, the optimal sample spacing decreases as the reduction in uncertainty provided by future information justifies the additional cost. Panels (a) and (b) show relative changes in VOI while (c) and

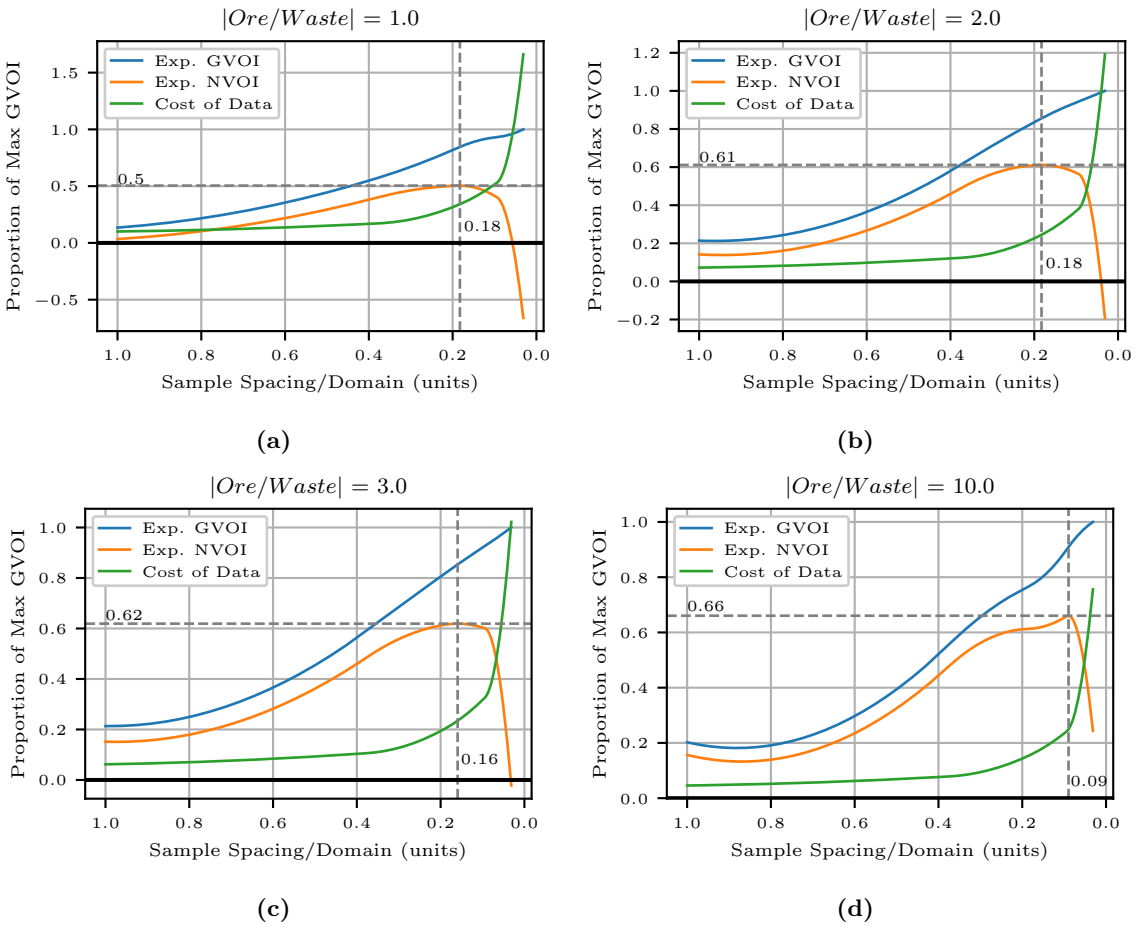

Figure 3.9: Four cumulative VOI curves for different ratios of ore value to waste value. The optimal sample spacing is shown near the vertical dashed line and the corresponding net VOI is shown along the horizontal dashed line. Note the green cost curve is the same for all scenarios.

(d) show absolute changes.

3.5.3 Relative Penalties

Penalties for dilution and ore loss directly impact the geometric configuration of the engineering design. Depending on the value function, dilution is often implicitly accounted for; however, some scenarios may warrant additional penalties. If the penalty for dilution is high, the resulting engineering design will erode causing ore loss. If the penalty for lost ore is high, the design will dilate and "chase" ore blocks leading to increased dilution. As operational penalties increase relative to the value of correct classification, optimal design placement requires more significant uncertainty reduction. This uncertainty reduction requires additional information and a closer sample spacing is optimal.

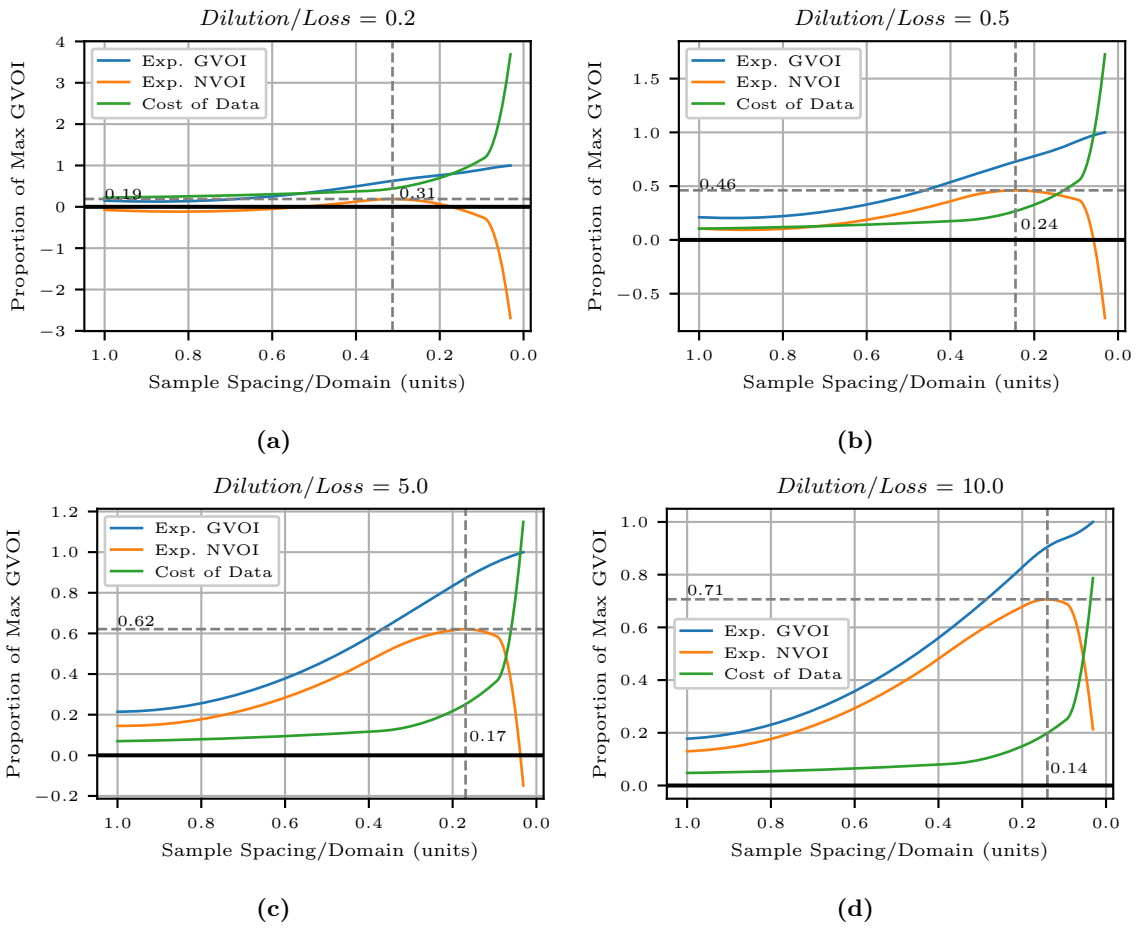

Figure 3.10: Four cumulative VOI curves for different ratios of dilution to ore loss penalties. The optimal sample spacing is shown near the vertical dashed line and the corresponding net VOI is shown along the horizontal dashed line. Note the green cost curve is the same for all scenarios.

The ratio of dilution to ore loss penalties impacts the optimal choice of sample spacing. The following example considers ratios of 0.2, 0.5, 5 and 10 with a constant ore value of 10 units. Figure 3.10 shows the results. As the penalty for lost ore increases, the optimal sample spacing becomes wider. If the penalty is sufficiently high, no additional information may be optimal, as shown in panel (a). There is no practical sense in collecting additional information for marginal gains. As the penalty for ore loss decreases, the optimal sample spacing decreases with a greater net VOI. The ratio of dilution to ore loss penalties has an absolute impact on the optimal sample spacing.

3.6 Decision Maker Preferences

A utility function captures a decision maker's preference towards risk. The utility function maps units of value from an uncertain outcome to units of utility. A particular value may have different utilities to different decision-makers given their utility functions. In general, most decision-makers are risk-averse and have a concave utility function. Aversion to risk means underperformance is consequential, penalizing values in the lower tail more heavily. Opportunity seeking preferences have a convex utility function, rewarding high values in the upper tail. The utility function is linear when risk-neutral, and the expected value is equal to the expected utility.

Risk preferences could be captured with a exponential utility function (Equation 1.20) where $a = [-0.25, 0, 0.25]$ for opportunity seeking, risk-neutral, and risk-averse preferences. The following example uses constant values for correct classification and dilution of 10 and -5 units, respectively, with a fixed cost of 50 units for additional samples.

Figure 3.11 shows cumulative VOI curves for three positions on risk as well as an example of an optimized engineering design for each position (panel (d)). In this example, the use of a non-linear utility function leads to a relative change in VOI. The choice of optimal sample spacing remains the same for each scenario though a relative change in the proportion of the max gross VOI generated occurs. With risk-averse preferences and uncertain geology, the technical design is conservative to limit downside exposure - this leads to larger cumulative VOI values as the value of the current data configuration is smaller. The same is valid with opportunity-seeking preferences. The convex utility function favours high values, and a single high realization could lead to an "aggressive" design that experiences significant dilution when compared against the true model. This scenario also leads to greater cumulative VOI values as the current data configuration's value is smaller. In general, if a preference other than risk-neutrality is adopted, future information is more valuable as the decision-maker can learn more about the downside risk or upside potential.

3.7 Summary

The variogram range and nugget effect both affect the proportion of maximum attainable value. As the variogram range decreases, additional information resolves less uncertainty

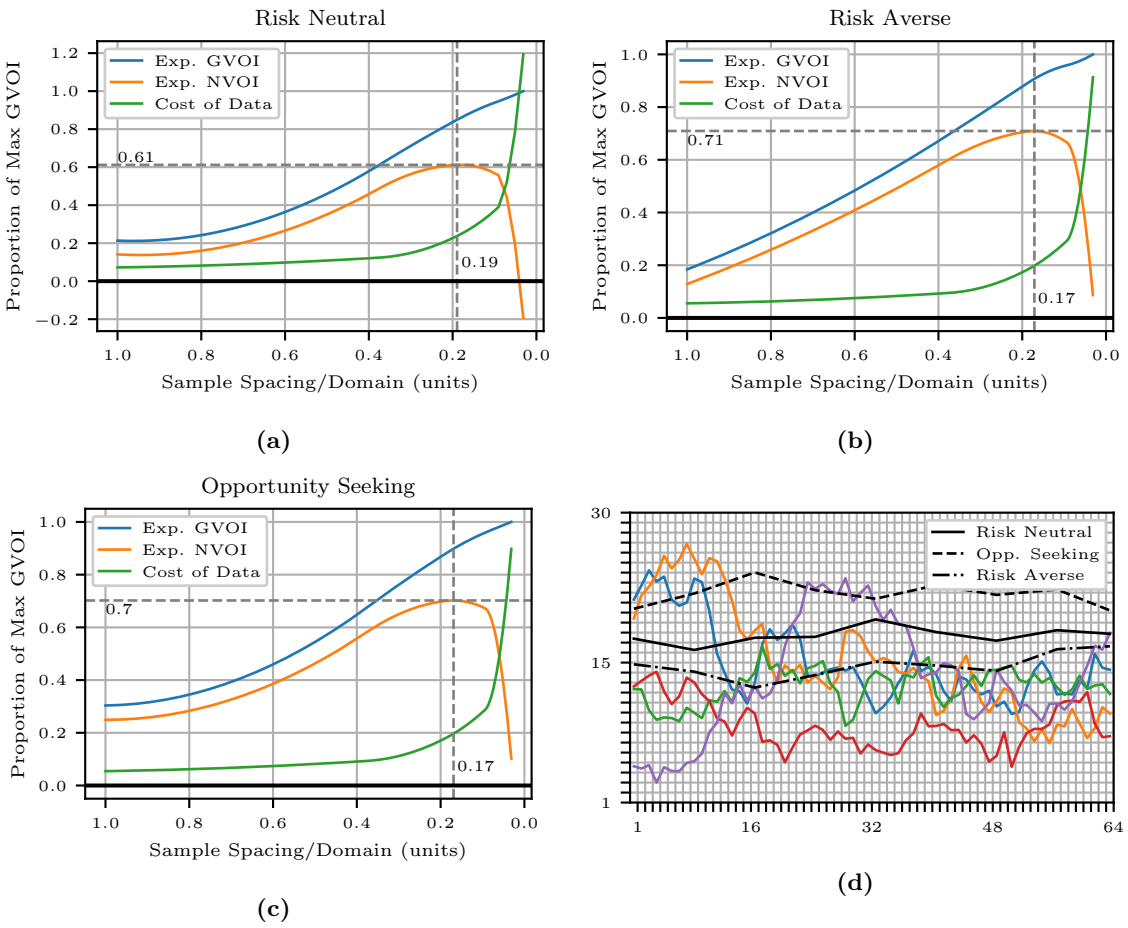

Figure 3.11: Cumulative VOI curves for risk neutral ($a = 0$), risk averse ($a = 0.25$) and opportunity seeking ($a = -0.25$) exponential utility functions. (d) shows three technical designs optimized considering expected utility (5 of 100 realizations are shown).

and generates a smaller proportion of value. The same is true as the nugget effect increases. As the engineering design becomes more selective, it generates a more significant proportion of the maximum attainable value. As selectivity increases, the design can capture new detail, reaching the point of diminishing returns later. The interaction between geologic and engineering scales is non-linear. With very short variogram ranges, no amount of information can resolve the geologic uncertainty and the optimal sample spacing is infinite. When economic, more information is required when the variogram range is short, and the engineering design is selective. With a coarse engineering scale and short-range variogram, wider data spacing is optimal. The optimum becomes narrower as the variogram range increases and becomes wider again at long variogram ranges due to data redundancy. A highly selective design with a long variogram range generates the greatest proportion of value.

As the cost of information increases, the optimal sample spacing becomes wider, and the maximum net VOI decreases. As the correct classification value increases, the optimal sample spacing decreases as the reduction in uncertainty provided by future information justifies the additional cost. As the penalty for lost ore increases, the optimal sample spacing becomes wider, and as the penalty for ore loss decreases, the optimal sample spacing decreases with a greater net VOI. Introducing a non-linear utility function calls for more information as the decision-maker has the opportunity to learn about the downside risk or upside potential

Chapter 4

Implementation Details of the Simulation Based Methodology

The simulation-based VOI methodology is conceptually straightforward, though, in practice, the implementation may be challenging. Simulating future data configurations must consider technical and operational constraints. An objective and value function must be determined that are representative of the operation. Optimization could consider a stochastic algorithm using an objective function to maximize expected utility across all realizations.

Additionally, the resample and resimulate approach may be computationally expensive. The number of realizations required expands significantly when multiple true models and future data configurations are considered. This chapter discusses some practical implementation details of the simulation-based VOI methodology.

4.1 Data Collection

Future information must be simulated to access VOI. A resampling approach is used to simulate future information. This requires the generation of a true geologic model $G(0,\ t = 1, ..., T)$, characterized by T realizations conditional to the current $c = 0$ data configuration. These realizations are generated at the data scale and honour the input histogram and variogram. C future data configurations are defined and each $t = 1, ..., T$ true models is sampled by $c = 1, ..., C$ data configurations. Resampled data represents drillhole data characterized by a collar location, azimuth, dip, hole length and sample length. Data configurations are collected cumulatively such that all samples in configuration c are present in configuration $c + 1$. Data collection in this work is assumed to be static. That is, data is collected once at a single point in time. Sequential data collection schemes may be more realistic but are more difficult to implement in practice. This could be an interesting avenue for future research.

4.1.1 Generating Future Data Configurations

"Future" data configurations may or may not be sampled. In cases with limited data, simulation of future data configurations considers hypothetical data locations. If many data are available, one may be interested in decimating the existing data to "roll-back" to a particular data spacing. The calculation of VOI then considers subsets of existing data. This process could potentially highlight over or under drilling by the project operator. The development stage of the operation determines the data availability.

Consider a scenario with limited data. As future data configurations do not physically exist, hypothetical data locations must be generated. Data locations will depend on the type of data, operational considerations of the project and physical constraints such as topography or existing infrastructure. Ideally, the mine plan should also be considered such that the placement of the hypothetical diamond drill rig does not interfere with mining operations. Future information in this work considers data collection at the same support as the existing conditioning data. A range of data configurations with decreasing data spacing is considered such that the solution will be reasonably bounded. That is, data configuration C should contain more data than the practical maximum.

Data configurations at some regular data spacing intervals such as 20m, 15m or 10m are the most straightforward to conceptualize; however, the decision of where and how many additional drillholes to achieve a particular data spacing is challenging. Manually generating drillhole locations is tedious and impractical. One approach could be to assemble hypothetical drillholes in the densest configuration reasonably possible and sequentially eliminate holes until one achieves a desired average data spacing. If repeated for all drillholes, all possible average data spacings given the initial configuration can be calculated as $dhs_i,\ i = 1, ..., ndh$. Provided the elimination process occurs so that data configurations nest together naturally, simulating a hypothetical infill drill campaign in reverse is possible.

This section presents the Uniform Drillhole Elimination (UDE) algorithm for the generation of practical nested drillhole configurations. UDE sequentially eliminates drillholes while maintaining uniformity within the remaining holes. After the removal of each drillhole, calculation of the data spacing of the remaining holes occurs. The elimination process must consider the spatial configuration of the remaining drillholes. The algorithm consid-

ers the distances between all drillholes and the standard deviation of those distances to generate a natural or uniform elimination sequence with minimal clustering. When considering a drillhole for removal, the average distance between all remaining drillholes should be high, and the standard deviation of the distances should be low to enforce an element of uniformity. A small random component is included to avoid artifacts and more closely replicate irregular drillhole configurations. The random component is small as purely random drillhole selection may lead to unnatural or clustered drillhole configurations.

UDE aims to eliminate drillholes in a way that would mimic a natural infill drill campaign. The location of the initial drillholes is typically near the center of the domain. Additional drillholes are then sequentially added, working outwards towards the edge of the domain. Starting at the densest configuration, UDE favours drillholes away from the domain center. When considering a drillhole for removal, the average distance between all remaining drillholes and the standard deviation of those distances are considered to impose an element of uniformity. On each iteration of UDE, the measure of goodness for each drillhole is calculated as:

$$g_i = w_{cent} \cdot dc_i + w_{rem} \cdot dd_i + w_{rand} \cdot rn_i - w_\sigma \cdot \sigma_{dd_i},\ i = 1, ..., n_{rem} \tag{4.1}$$

Where dc_i is the distance between the drillhole and the centroid of the data - drillholes near the domain's edges are preferred. dd_i is the average distance between the drillhole and all other remaining drillholes - larger spacing between remaining holes is preferred. rn_i is a uniform random number $\in [0, 1]$. σ_{dd_i} is the standard deviation of the distances between all remaining drillholes - penalizing higher standard deviations. w_{cent}, w_{rem}, w_{rand} and w_σ are user-defined weights applied to each measure. Setting the weight to zero will ignore a particular measure. The drillhole with the highest measure of goodness, g_i, is removed. The number of remaining drillholes, n_{rem}, is updated, and the algorithm continues.

Distances are calculated as the average distance between all samples (ns) in the remaining drillholes:

$$dc_i = \frac{1}{ns_i} \sum_{j}^{ns_i} \sqrt{(x_{i,j} - xc_{i,j})^2 + (y_{i,j} - yc_{i,j})^2 + (z_{i,j} - zc_{i,j})^2},\quad i = 1, ..., n_{rem} \tag{4.2}$$

$$dd_{i,j} = \frac{1}{ns_i}\frac{1}{ns_j}\sum_{k}^{ns_i}\sum_{l}^{ns_j}\sqrt{(x_{i,k}-xc_{i,l})^2+(y_{i,k}-yc_{i,l})^2+(z_{i,k}-zc_{i,l})^2}, \quad i,j=1,...,n_{rem} \tag{4.3}$$

The resulting elimination sequence contains the sequence of drillhole IDs to eliminate and the corresponding average data spacing in a cumulative fashion. After the drillhole elimination sequence is determined, the calculation of each possible configuration's data spacing occurs. The algorithm implementation includes a fixed volume approach considering anisotropy (J. L. Deutsch, Barnett, & Deutsch, 2015) for three dimensions or a two-dimensional search for a fixed number of samples or within a fixed area (Silva, D. S. F. & Boisvert, J. B., 2014). Methods for calculating data spacing are not the focus of this thesis. The elimination sequence and corresponding average data spacing measurements provide access to all possible data spacing and drillhole configurations, given the final data configuration C and the chosen parameters.

As the placement of drillholes is somewhat subjective, it may not be straightforward to codify a solution for all drilling scenarios. The UDE algorithm described above aims to enforce the uniformity of the remaining drillholes, which may not work well for data with mixed drilling campaigns. If real drillhole data is to be reduced or rolled back, combinations of different drill campaigns such as early exploration surface drillholes mixed with dense underground drill fans may require some form of drillhole grouping and careful tuning of parameters. Gridded data mixed with irregular configurations may also require some form of grouping.

The practitioner should review and tune the method used to calculate data spacing and reporting of values. Data spacing calculations are straightforward for regularly spaced configurations. If the drilling is predominantly vertical or regularly gridded, a two-dimensional approach searching for either a fixed area or fixed number of samples could be adopted. Adopting a fixed volume approach is appropriate for irregular or highly deviated drilling in three-dimensions. Subjective parameter choices such as the fixed volume, search anisotropy or the fixed number of samples to search for influence the resulting data spacing. The volume should be sufficiently large to include sparsely sampled areas (J. L. Deutsch et al., 2015), and the number to search should be large enough such that the results are not noisy

(Silva, D. S. F. & Boisvert, J. B., 2014). It is common to report data spacing as a single number taken as the average data spacing in some finite domain. This nominal data spacing within the domain is sensitive to clipping limits at the edges of the study volume. Reasonable clipping limits should consider the type of deposit and the data configuration.

4.1.2 Resampling

After the synthetic data locations are generated, the data values are sampled from the true geologic model $G(0,\ T)$. The true model should be simulated at sufficiently fine resolution given the scale of the geology and proposed resampling methodology. The grid node resolution should be fine enough it can be resampled by the proposed composite length in a reasonable way. For example simulating a true model at a 1x1x1 meter resolution to be sampled by 3 meter composites is appropriate. Grid node dimensions greater than the composite length will lead to non-unique data indicies and the same node being sampled more than once. Down hole data locations are calculated from the x, y, z location of the collar, the azimuth and dip of the hole and the simulated composite length. Sample locations are considered to be the mid point of the composite interval. Using GSLIB (C. V. Deutsch & Journel, 1998) grid conventions the data x, y, z locations are converted to model indices ix, iy, iz:

$$ix_i = ceil((x_i - x_{min})/x_{size} + 0.5), \quad i = 1, ..., nd \tag{4.4}$$

$$iy_i = ceil((y_i - y_{min})/y_{size} + 0.5), \quad i = 1, ..., nd \tag{4.5}$$

$$iz_i = ceil((z_i - z_{min})/z_{size} + 0.5), \quad i = 1, ..., nd \tag{4.6}$$

The one dimensional model index or data location is then calculated as:

$$\mathbf{u}_i = idx_i = ix_i + iy_i * nx + iz_i * nx * ny, \quad i = 1, ..., nd \tag{4.7}$$

The simulated drillhole value is then extracted from the true model as $\{z_c^t(\mathbf{u}_i),\ i = 1, ..., nd;\ c = 1, ..., C;\ t = 1, ..., T\}$. The same data locations are used for each true model. The resampling process generates $C * T$ new data sets; each is used to condition a subsequent geologic model $\{G(c,\ L)\ \forall\ T\}$.

Consideration of data quality during the resampling process is possible, though not accounted for in this work. Mineral resource estimates are commonly made using composited

diamond drill core or reverse circulation assays. These two data types are of different quality and thus have different sampling error. Assayed values are subject to sampling errors related to sample extraction, preparation and instrument errors (Abzalov, 2016). Fundamental sampling error (Pitard, 1993) is related to the constitutional heterogeneity of the sampled material and does not introduce bias. Extraction errors are related to the type of drilling and would introduce bias into the samples. Understanding error distributions with non-zero means are beyond the scope of this thesis. Neufeld (2005) suggests from experience that the fundamental sampling error, which can be calculated based on material properties or estimated from QA/QC data (Silva & Deutsch, 2019), accounts for only half the total sample error and doubling this value is a more realistic estimate of the total sample error. Wilde (2010) shows that adding a sampling error drawn from an error distribution with a mean of zero does not significantly change the expected measure of uncertainty; however, the variability in the distribution of uncertainty increases.

4.1.3 Cost of Data

All relevant costs should be included when determining the cost of future data. Drilling, assaying, logging and consumable costs should be accounted for as well as any other relevant costs. Consider a drilling cost $C_{drill} = \$105/m$, a lab cost $C_{lab} = \$12/m$, a geologic logging cost $C_{geo} = \$10/m$ and a consumable cost $C_{aux} = \$0.25/m$ for a future infill diamond drill program (personal communication, GSR). The future drill program will contain 6000 meters of drilling and assume a composite length of 3 meters generating 2000 new samples. The cost of the data configuration is calculated as:

$$V^{cost}(c) = n_{samp} * len_{comp} * (C_{drill} + C_{lab} + C_{geo} + C_{aux}) = 2000 * 3 * 127.25 = \$763,500 \quad (4.8)$$

Time costs associated with the interruption of mining or discounts for drilling multiple holes from a single location could be included, though not accounted for in this work.

4.2 Transfer, Objective and Value Functions

A transfer function is required to convert a geologic model to a response in units of value. As introduced in Chapter 2 the optimal decision alternative may exist within a continuous or combinatorially large solution space. The geometry of the technical design is the basis

of the transfer function and is formulated through the application of an objective function. The objective function in turn is a function of the value and utility functions. The objective function considers all L realizations in the geologic model $G(c,\ L)$. Recall Equation 2.8:

$$O(D(scale,\ G(c,\ L))) = \frac{1}{L}\sum_{l=1}^{L} U^l(V^l_{econ}(D(scale,\ G(c,\ L)),\ G(c,\ l),\ P_{econ})) \tag{4.9}$$

The general economic value function V^l_{econ} is defined as:

$$V^l_{econ} = \left[\sum_{i=1}^{N} \frac{z^l_c(\mathbf{u}_i)\cdot r(\mathbf{u}_i)}{cf}\cdot p_z - (c_m(\mathbf{u}_i) + c_p(\mathbf{u}_i)) + c_{ga}(\mathbf{u}_i))\right] - P_{dil.} - P_{loss} \tag{4.10}$$

N is the number of blocks to be mined by design $D(scale,\ G(c,\ L))$, $r(\mathbf{u}_i)$ is recovery of z at location $\mathbf{u}_i$, cf is a conversion factor, p_z is the selling price of z, $c_m(\mathbf{u}_i)$, $c_p(\mathbf{u}_i)$ and $c_{ga}(\mathbf{u}_i)$ are the costs of mining, processing and general and administrative costs at location $\mathbf{u}_i$, respectively, and $P_{dil.}$ and P_{loss} are penalties for dilution and ore loss, respectively. Any number of additional factors could modify the value function depending on project specifics. A dilution factor could be added based on expected over breakage in an underground scenario or a mine call factor for open-pit operations. Factors for mining recovery, royalties or metal streaming agreements could be applied.

The value of a particular realization, V^l_{econ}, is converted to a utility given the decision-makers risk preferences (Equation 1.20 or 1.21) for the objective function. The choice of the utility function and its associated parameters is subjective and would likely be a management policy decision. The risk position should consider the time frame of the decision alternative and the consequences of underperformance.

The perturbation of the design's geometric configuration occurs for a specified number of iterations, and the expected utility of the design is the average value across all L realizations. If the objective function value increases, the new geometry is retained; else, the perturbation is rejected. The process should consider a sufficient number of iterations such that the technical design converges to a stable solution. Beyond some threshold, the objective function value stabilizes, and additional iterations do not substantially improve the design. Figure 4.1 shows an example of the objective function value versus iterations for three technical designs using the one-dimensional synthetic example presented in Chapter 3. The objective function value stabilizes beyond approximately 600 iterations. In practice, this

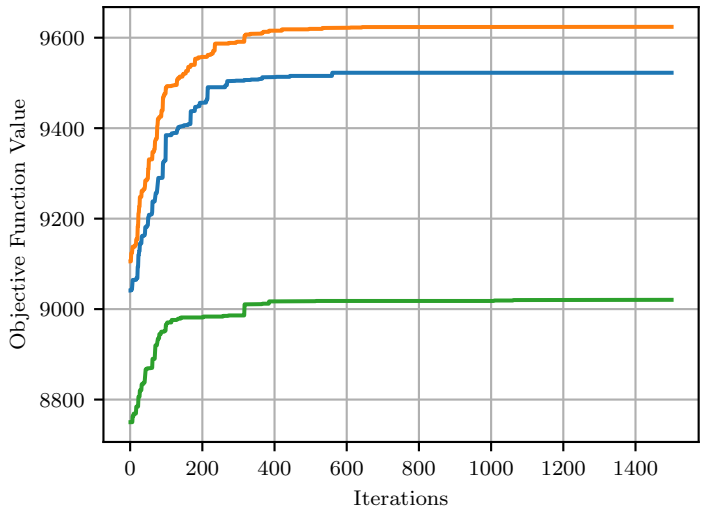

Figure 4.1: Number of iterations versus objective function value generated when optimizing three technical designs using the one-dimensional example in Chapter 3. The example uses a single structure spherical variogram model with a 32 unit range, a design selectivity of 4 units and fixed ore and waste values of 10 and -1 units, respectively.

number will depend on the technical design's selectivity, the geologic model's resolution, and the magnitude of the perturbations.

The wide range of mining methods and site-specific constraints makes generalizing stope optimization difficult. This greedy stochastic optimization algorithm works well for the simple minable shapes considered in this thesis. Alternative optimization algorithms may have to be considered if the scope of the engineering optimization increases, such as simulated annealing (Manchuk, 2007), mixed integer programming (Grieco & Dimitrakopoulos, 2018) or a hybrid dynamic-greedy algorithm (Nikbin, Ataee-pour, Shahriar, & Pourrahimian, 2020). Further refinement of initial stope vertices, vertex constraints and block model clipping (Manchuk, 2007) may also be warranted as the engineering scope increases. Consideration of the stope extraction sequence after optimization would provide a more realistic assessment of value.

The volume of the technical design is an essential consideration as uncertainty is volume dependent. The uncertainty in metal grades within a single 25x25x30 meter stope is different from the uncertainty within an entire panel that contains that stope. As volume increases, high and low values average, and uncertainty decreases. As uncertainty decreases around geologic boundaries or the variable driving the value function, less information is

required to make an optimal decision. The stage of project development determines the relevant volume of the transfer function. Early-stage projects likely consider large, possibly annual production volumes with widely spaced data. Later stage projects in production may consider smaller volume, more complex transfer functions such as a particular sub-level or pushback design at a monthly production volume. Greater uncertainty associated with smaller volumes will influence VOI and the choice of optimal data spacing.

4.3 Number of Realizations

When assessing uncertainty in a particular response, the appropriate number of realizations depends on the required precision. Greater precision requires a larger number of realizations. Pyrcz and Deutsch (2014) show that for a given tolerance and probability to be within that tolerance, the required number of realizations L can be calculated analytically. For example, to be within 5% of the 0.1 quantile, 90% of the time requires 100 realizations.

A VOI study differs from a traditional geostatistical study in that both true models T and realizations L must be defined. The uncertainty in the response depends on both T and L. The influence of T is two-fold. Firstly, the resampling of true models generates future data configurations. If T is too small, the true models may be biased by an unusually low or high realization due to randomness. Bias could be carried downstream into subsequent realizations. Secondly, the true model is input to the technical design and value function for subsequent VOI calculations. If T is too small, expected VOI calculations might be unstable, compounding with the previously mentioned potential bias. If L is too small, the assessment of uncertainty in the response variable will be imprecise. The technical design may not consider a reasonable space of uncertainty and may experience significant ore loss or dilution when compared against the true model.

The following example investigates the relationship between the number of true models and realizations. VOI is determined using the synthetic data in Section 3.1 and a range of T and L. Many values of $T = [1, 5, 10, 20, 30, 50, 100, 150, 200]$ and $L = [5, 10, 20, 30, 50, 100, 150, 200]$ are considered. All values of L are considered for each T. A single structure, spherical variogram model with a range of 32 units and no nugget, is used and a technical design scale of 4 units. The gross VOI for each combination of T and L is compared to a reference

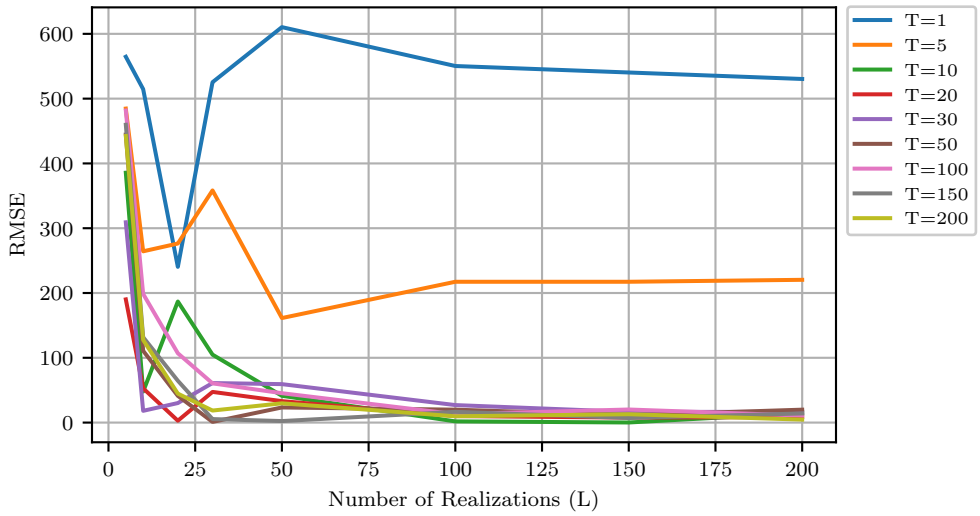

Figure 4.2: Root mean squared error (RMSE) for various combinations of T and L

expected gross VOI calculated with $G(0,\ T = 500)$, $G(c,\ L = 500)$. $T = 500$ and $L = 500$ is considered a reasonable reference case as both values exceed a practical maximum. Figure 4.2 shows the results expressed as root mean squared error (RMSE) in units of value relative to the reference expected value. L is shown on the x-axis and each coloured curve corresponds to a different value of T.

For all values of T the RMSE appears to stabilize beyond $L = 100$. Where $T = 1$ or $T = 5$, RMSE values are generally unstable for values of L less than 100. This instability is likely due to relatively few values entering the calculation, and the results may be sensitive to the chosen random number seed. For these smaller values of T the final RMSE is significantly higher than when considering $T \geq 10$ and $L \geq 100$. $T = 10$ and $L = 100$ are reasonable values for stable VOI calculations. The practitioner may choose some other T and L based on an acceptable level of error.

Ranking realizations could be an alternate approach for generating true models T. The idea is to generate a larger number of realizations, develop and calculate a ranking measure and then sort the realizations based on the measure. A ranking measure must correctly identify high and low realizations and correlate with the final production response (McLennan & Deutsch, 2005; Pyrcz & Deutsch, 2014). A subset of the larger number of realizations can then be selected, which target regularly spaced quantiles of the response measure, reducing the number of true models while still spanning the anticipated response uncertainty.

4.4 Computational Considerations

Computer time may be significant depending on the choices of T, L and C, the number of variables considered, the size of the model, the modelling workflow, the transfer function, and the optimization algorithm. Consider $k = 1, ..., K$ variables. Resampling creates $T * C * K$ new data sets. Resimulation generates $T * C * K * L$ realizations. L realizations for every $T * C * K$ data sets must be passed through an optimization algorithm to generate a technical design. Though the process generates a significant number of realizations, many are only required for intermediate steps and need not be stored long term. Keeping the T true realizations is critical, as all subsequent realizations are conditional to them. The practitioner can select the minimum number of models to achieve an acceptable level of error in the final result from Figure 4.2. If computer time is a significant bottleneck, ranking true models may be appropriate.

For any practical scale model, automation and parallelization of the workflow are necessary. For a given true model, each data configuration c is independent; thus, parallel execution of each branch of Figure 2.1 is possible. The ease of parallelization lends itself to applications of cloud computing. The practitioner should consider the file format of simulated realizations within the workflow. Some form of compressed binary file structure such as GSB (Barnett, 2014) can drastically increase read/write speed and reduce file size for large models. One drawback of a binary file structure is lack of human readability; however, this speed increase may be appreciable when considering tens of thousands of realizations.

Chapter 5

Managing Uncertain Value

The parameters required to determine VOI may be uncertain. Depending on the stage of the project, some of these parameters may be unknown. Mining methods, operational costs, and project economics could change before a project goes into production, modifying the value calculation. In some scenarios, it may not be possible to quantify the cost of uncertainty and determine VOI. Understanding the link between geologic, economic, and engineering uncertainty may allow for evaluation of the optimal sample spacing from accessible uncertainty measures. This chapter builds on the synthetic data set introduced in Chapter 3 by including a grade variable within the simulated rock types. Examples calculate geologic uncertainty measures to develop a link with value and explore uncertainty around economic parameters. The goal is a general understanding of how uncertainty reduces in different circumstances and a qualitative assessment of a reasonable drillhole spacing.

5.1 Synthetic Data

A synthetic data set is generated in the same manner as Chapter 3. The one-dimensional surface realizations are considered a boundary between rock type 0 and rock type 1. A lognormal-like distribution of gold grades is simulated unconditionally within each rock type. Rock type 1 represents a horizon of ore with $m_{ore} = 1$, $\sigma_{ore} = 2$, while rock type 2 represents waste with $m_{waste} = 0.1$, $\sigma_{waste} = 0.2$. The example uses a single structure spherical variogram model with a nugget of 0.2 and a range of 24 units for the ore rock type, a single structure spherical variogram model with a nugget of 0.2 and a range of 32 units for the waste rock type and a single structure spherical variogram model with no nugget and range of 32 units for the one-dimensional boundary realizations. Though a small synthetic example, the model replicates a hierarchical geomodelling workflow. Figure 5.1 shows an example of a single true grade model and rock type model. Unless otherwise stated examples use $T = 10$ true models and $L = 100$ realizations.

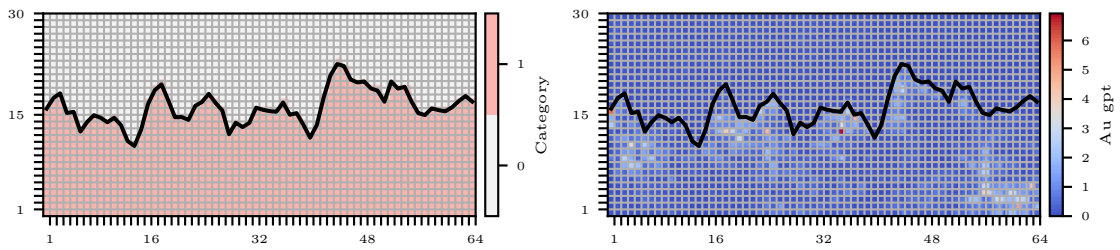

Figure 5.1: An example of one true model of gold grams per tonne (left) and rock type (right). The black line is the boundary realization.

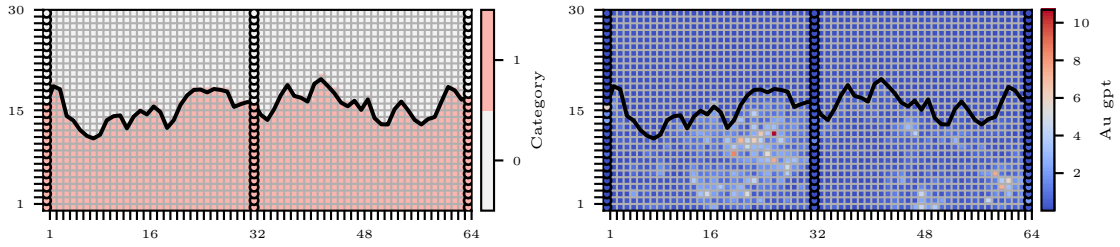

Figure 5.2: An example of a single realization of gold grams per tonne (left) and rock type (right) conditional to a 32 unit future data configuration resampled from the true model in Figure 5.1. The black line is the boundary realization.

$C = 6$ future data configurations are considered vertical drillholes that intersect and sample both the categorical and continuous models. Figure 5.2 shows an example of resampling the true model with a 32 unit drillhole spacing, and one resulting conditional boundary realization and gold realization. Before calculating measures of uncertainty, realizations are block averaged to a 2x2 unit grid.

5.1.1 VOI example

Calculation of the optimal data spacing and the maximum net VOI happens before calculating measures of uncertainty. Consider the value function parameters in Table 5.1 for use in the VOI workflow with the synthetic data set. There is no penalty for lost ore. $c = 1, ..., 6$ future data configurations are considered with drillhole spacings of [64,32,16,8,4,2] units. Each additional drillhole is a fixed length of 30 units with sample collection every one unit. The cost of drilling is \$25/unit length, and the design scale selectivity is four units. The data spacing that maximizes net VOI is 5.76 units (Figure 5.3). Measures of geologic uncertainty are calculated for each data spacing to determine the target level of uncertainty associated with the optimal spacing.

Table 5.1: Value function parameters. Costs are per tonne, values are in USD

Parameter	Symbol	Value
Au Price	p_{au}	\$1250/Oz.
Mining Cost	c_m	\$5
Processing Cost	c_p	\$10
Specific Gravity	SG	2.70 g/cm^3
Recovery Factor	f_{rec}	0.95
Conversion Factor	cf	31.1035

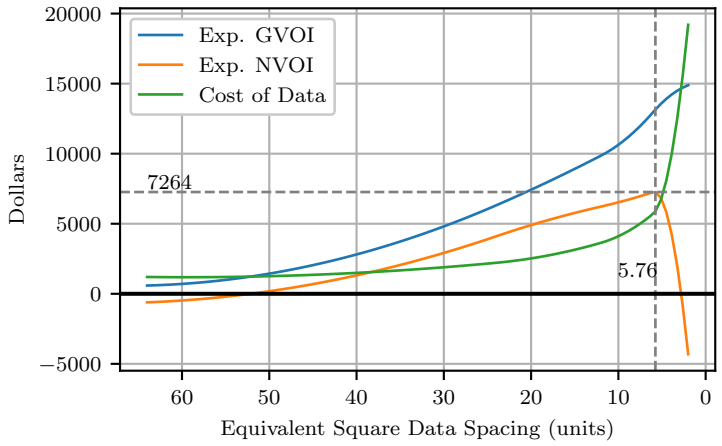

Figure 5.3: Cumulative VOI curves for the parameters in Table 5.1. The vertical dashed line highlights the optimal data spacing while the horizontal highlights the maximum net VOI.

5.2 Geologic Uncertainty

The set of simulated realizations provides access to measures of geologic uncertainty. The numerical VOI workflow identifies the data configuration that maximizes the net VOI and minimizes uncertainty costs. The maximum net VOI has a corresponding measure of geologic uncertainty that could be the optimal target uncertainty. Resolving uncertainty beyond this point is not cost-effective. Determining a target measure of uncertainty and optimal data spacing through VOI can link value and geology for future studies.

The probability distribution of L simulated values characterizes the uncertainty at a particular grid node $\mathbf{u}$. A set of probability distributions at all grid node locations provide a summary of the uncertainty. The average of the uncertainty measure at each grid node provides a single measure of uncertainty for each true model (Wilde, 2010). For a given data configuration, averaging the T single measures of uncertainty provides the expected measure of uncertainty for the data spacing. The following examples use the expected stan-

dard deviation, precision and probability of correct classification. For each $c = 1, ..., C$ data configurations, the corresponding block averaged $l = 1, ..., L$ realizations are post-processed to calculate the measure of uncertainty.

5.2.1 Standard Deviation

The standard deviation defined in Section 1.3 describes the spread of values about the mean. The conditional standard deviation at each grid node location is calculated as:

$$\hat{\sigma}_c(\mathbf{u}) = \sqrt{\frac{1}{L}\sum_{l=1}^{L}\left(z_c^l(\mathbf{u}) - m_{z_c}(\mathbf{u})\right)^2} \tag{5.1}$$

Where $m_{z_c}(\mathbf{u})$ is the mean of the local distribution:

$$m_{z_c}(\mathbf{u}) = \frac{1}{L}\sum_{l=1}^{L} z_c^l(\mathbf{u}) \tag{5.2}$$

The average standard deviation of all N grid node locations is taken as:

$$\overline{\sigma}_c = \frac{1}{N}\sum_{i=1}^{N} \hat{\sigma}_c(\mathbf{u}_i) \tag{5.3}$$

Figure 5.4 shows the average standard deviation for each data configuration for each true model. Each coloured line represents one of the $T = 10$ true models, and the black line is the average of all models. As more data is collected, the standard deviation decreases as the simulated values for a given grid node are more certain. The horizontal dashed line highlights the expected standard deviation that maximizes net VOI. This value represents the target standard deviation.

5.2.2 Precision

Precision defined in Section 1.3 describes the proportion of values that fall within some tolerance interval ti from the mean. A tolerance value $a = 15\%$ is used such that the tolerance interval is $ti = m_{z_c}(\mathbf{u}) * a$. Consider the indicator transform $i_c^{ti}(\mathbf{u})$:

$$i_c^{ti}(\mathbf{u}) = \begin{cases} 1, & \text{if } m_{z_c}(\mathbf{u}) - ti \leq z_c^l(\mathbf{u}) \leq m_{z_c}(\mathbf{u}) + ti \\ 0, & \text{otherwise} \end{cases} \tag{5.4}$$

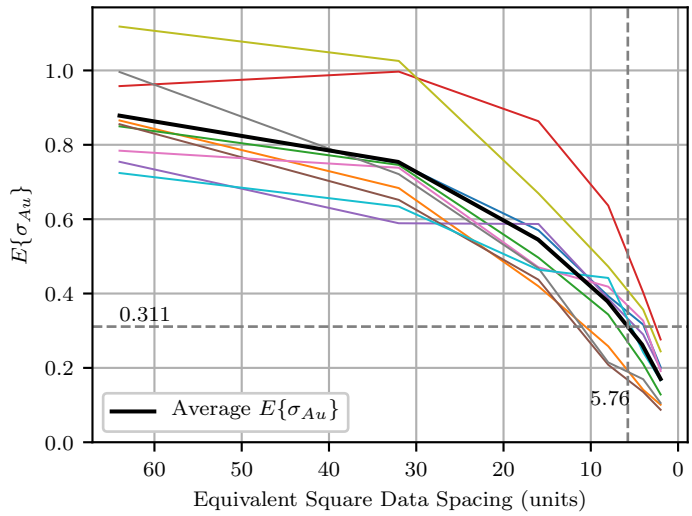

Figure 5.4: Expected standard deviation versus data spacing. The optimal sample spacing which corresponds to the maximum net VOI is highlighted by the vertical dashed line while the horizontal highlights the corresponding measure of uncertainty. Each coloured line represents one of the $T = 10$ true models and the black line is the average of all true models.

Precision is then the probability to be within the specified tolerance interval:

$$Prec_c^{ti}(\mathbf{u}) = \frac{1}{L}\sum_{l=1}^{L} i_c^{ti}(\mathbf{u}) \tag{5.5}$$

The average precision of all N grid nodes is then taken as:

$$\overline{Prec}_c^{ti} = \frac{1}{N}\sum_{i=1}^{N} Prec_c^{ti}(\mathbf{u}) \tag{5.6}$$

Figure 5.5 shows the probability of being within 15% of the mean for each data configuration for each true model. Each coloured line represents one of the $T = 10$ true models, and the black line is the average of all models. As more data is collected, the probability of being within 15% of the mean increases as the spread of simulated values at a given location decreases. The horizontal dashed line highlights the expected probability of being within 15% of the mean that maximizes net VOI. This value represents the target precision.

Interestingly, there are no obvious breaks in the expected uncertainty curve. The cost of information is the key in determining the optimal data spacing for this situation. The target precision is relatively low at 0.368 though this is related to the scale of the model. Achieving higher expected precision for a given data spacing would be possible by upscaling the realizations to a larger block scale.

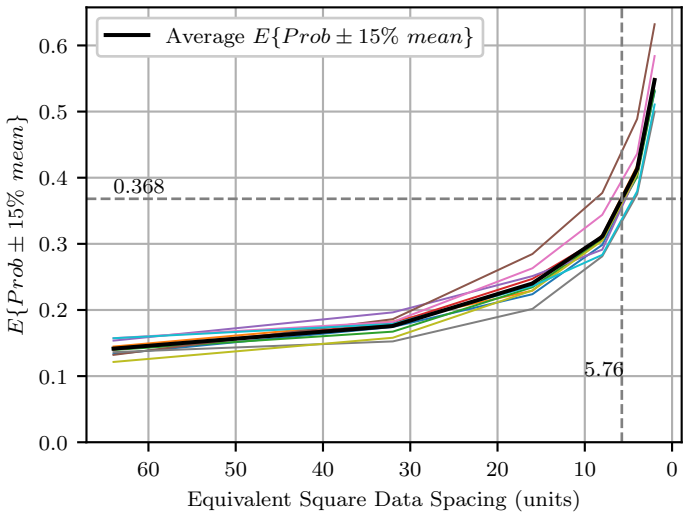

Figure 5.5: Expected probability to be ± 15% of the mean versus data spacing. The optimal sample spacing which corresponds to the maximum net VOI is highlighted by the vertical dashed line while the horizontal highlights the corresponding measure of uncertainty. Each coloured line represents one of the $T = 10$ true models and the black line is the average of all true models.

5.2.3 Probability of Correct Classification

The probability of correct classification defined in Section 1.3 is one minus the probability of misclassification. The probability of misclassification is equal to the sum of type I and type II errors. Determining the probability of type I and type II errors requires knowledge of the truth and a defined cutoff b to threshold the true values, $z_c^t(\mathbf{u})$, and the simulated values, $z_c^l(\mathbf{u})$. Type I errors or false positives occur when the simulated value exceeds the threshold and the true value does not. False negatives occur when the true value exceeds the threshold and the simulated value does not. Consider the indicator transforms $i_c^I(\mathbf{u})$ and $i_c^{II}(\mathbf{u})$:

$$i_c^I(\mathbf{u}) = \begin{cases} 1, & \text{if } z_c^l(\mathbf{u}) > b \text{ and } z_c^t(\mathbf{u}) < b \\ 0, & \text{otherwise} \end{cases} \tag{5.7}$$

$$i_c^{II}(\mathbf{u}) = \begin{cases} 1, & \text{if } z_c^l(\mathbf{u}) < b \text{ and } z_c^t(\mathbf{u}) > b \\ 0, & \text{otherwise} \end{cases} \tag{5.8}$$

Where the threshold b is the break even cutoff grade given the value function parameters:

$$b = \frac{cost_m + cost_p}{p_{au} * f_{rec} * \frac{1}{cf}} = 0.393 \text{ gpt Au} \tag{5.9}$$

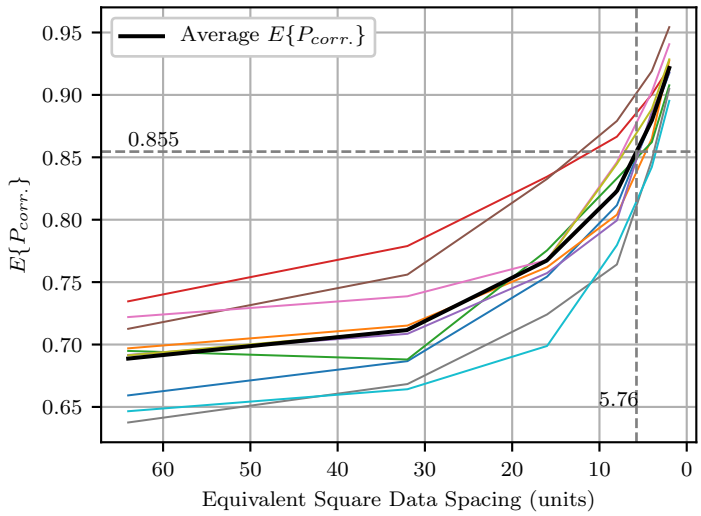

Figure 5.6: Expected probability of correct classification versus data spacing. The optimal sample spacing which corresponds to the maximum net VOI is highlighted by the vertical dashed line while the horizontal highlights the corresponding measure of uncertainty. Each coloured line represents one of the $T = 10$ true models and the black line is the average of all true models.

The probability of type I and type II errors are then:

$$P_c^I(\mathbf{u}) = \frac{1}{L}\sum_{l=1}^{L} i_c^I(\mathbf{u}) \tag{5.10}$$

$$P_c^{II}(\mathbf{u}) = \frac{1}{L}\sum_{l=1}^{L} i_c^{II}(\mathbf{u}) \tag{5.11}$$

The probability of correct classification is defined as:

$$P_c^{corr.}(\mathbf{u}) = 1 - \left(P_c^I(\mathbf{u}) + P_c^{II}(\mathbf{u})\right) \tag{5.12}$$

The average probability of correct classification for all N grid nodes is then taken as:

$$\overline{P}_c^{corr.} = \frac{1}{N}\sum_{i=1}^{N} P_c^{corr.}(\mathbf{u}) \tag{5.13}$$

Figure 5.6 shows the average probability of correct classification for each data configuration for each true model. Each coloured line represents one of the $T = 10$ true models, and the black line is the average of all models. As more data is collected, the probability of correct classification increases as the realizations more closely resemble the true model. The horizontal dashed line highlights the expected probability of correct classification that maximizes net VOI. This value represents the target probability of correct classification.

5.2.4 Link Between Geologic Uncertainty and Value

The relationship between geologic uncertainty and value is non-linear. A linear relationship would mean the optimal solution is always one of zero or an infinite amount of additional information. Understanding how the reduction of uncertainty relates to value may allow the practitioner to build a calibration curve for future applications. This link could remove the need for repetition of the full numerical VOI workflow.

Uncertainty and value are inversely related. As knowledge of the underlying geology improves, a technical design can better capture the detail. Better knowledge leads to increased value though at a particular point reducing uncertainty further has diminishing returns. Figure 5.7 shows the expected measures of geologic uncertainty from the previous section plotted against the gross VOI. Each coloured line represents one of the $T = 10$ true models, and the black line is the average of all models. The curves show increasing value for closer data spacing with no exact point of diminishing returns for the expected standard deviation and probability of correct classification. The expected precision curve appears to flatten beyond 0.4, roughly corresponding to the target measure of uncertainty obtained in the previous section. In scenarios where the point of diminishing returns is not apparent, considering the cost of data acquisition may provide a complete picture.

The gross VOI represents the cost of uncertainty or a lost opportunity cost due to geologic uncertainty. Realizing this value is not possible without sufficiently reducing the data spacing. It also represents the maximum cost the decision-maker should pay to achieve a particular level of geologic uncertainty. If a target level of uncertainty is known, as from the previous section, a data collection scheme can be developed to target the optimal level of uncertainty while honouring economic constraints.

5.2.5 Optimal Data Spacing and Geologic Uncertainty

If calculating the maximum net VOI is impossible or difficult, the optimal data spacing could be inferred, considering the learning curve concept introduced in Section 1.3. An appropriate level of uncertainty exists at the boundary between region one and region two, where the zone of resolving uncertainty transitions to the zone of high data availability or reduced learning rate. Plotting expected uncertainty against a linear scale, such as the

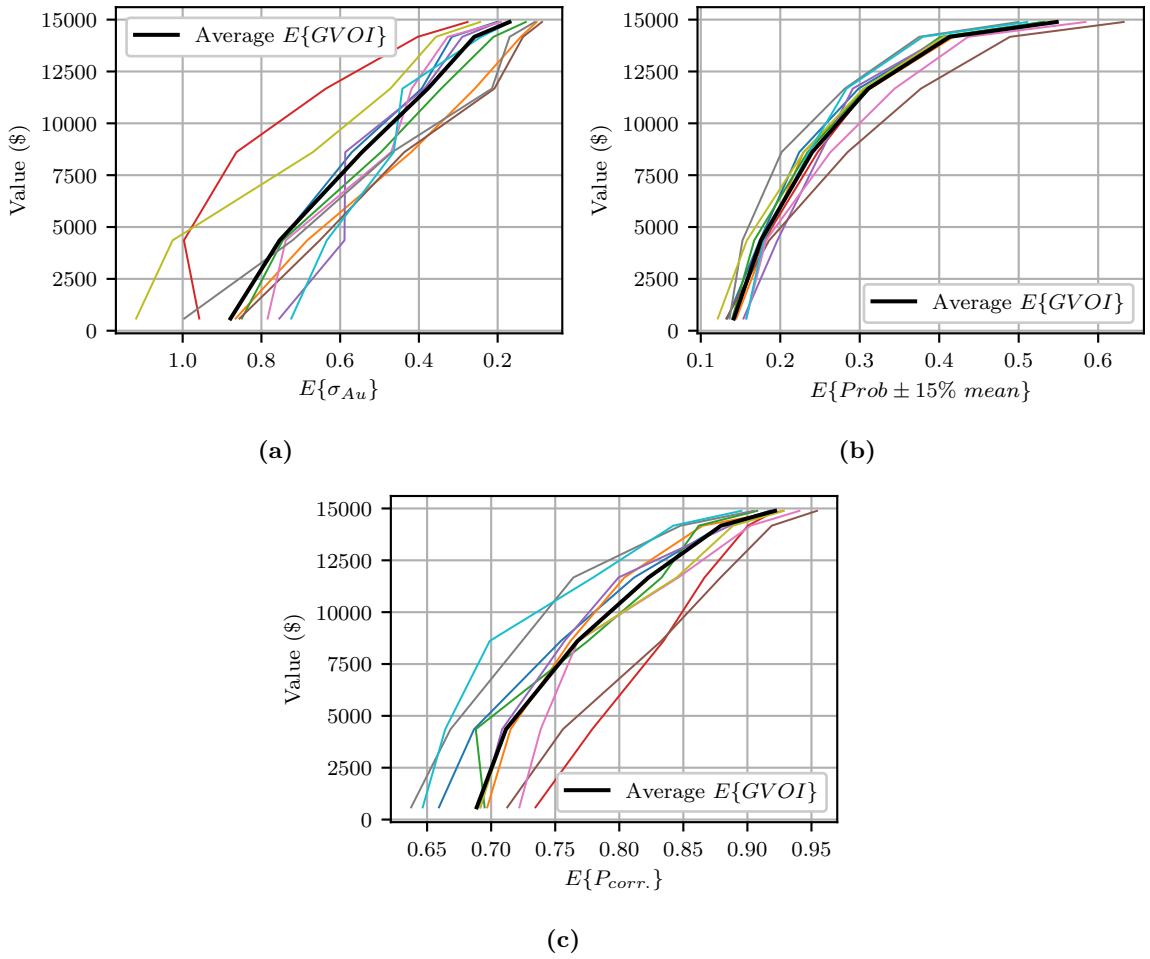

Figure 5.7: Expected gross VOI versus (a) expected standard deviation, (b) probability to be ± 15% of the mean and (c) expected probability of correct classification. Each coloured line represents one of the $T = 10$ true models and the black line is the average of all true models.

number of drillholes, may identify the point of diminishing returns (Barnett et al., 2018). No significant uncertainty resolution occurs beyond this point. Figure 5.8 shows the same expected standard deviation from Figure 5.4 however the x-axis is the number of additional drillholes (linear) rather than equivalent square data spacing (quadratic). The vertical dashed line reasonably identifies the boundary between zones 1 and 2 on the learning curve at eight drillholes. The corresponding expected standard deviation is 0.377 grams per tonne Au. This standard deviation corresponds to the point of diminishing returns or decreased learning rate. Much of the uncertainty resolution happens between 2 and 8 additional drillholes. With less than two drillholes, there is not enough information to significantly reduce the uncertainty. With greater than eight drillholes, the rate of uncertainty reduction decreases. There is another break at 16 drillholes where the expected uncertainty curve

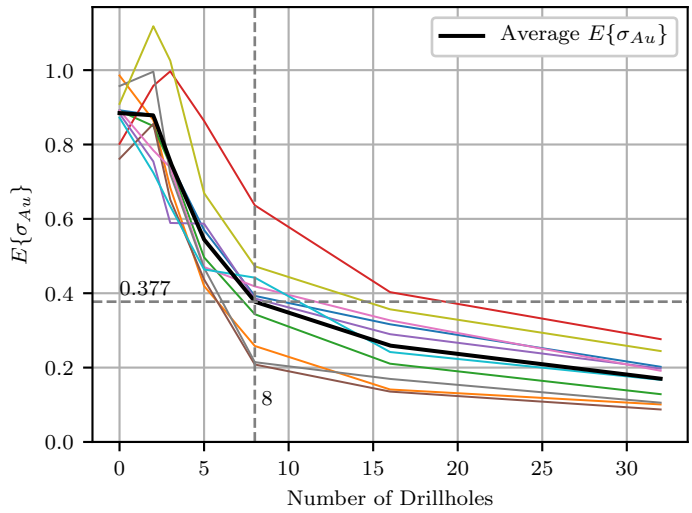

Figure 5.8: Expected standard deviation versus number of drillholes. The horizontal dashed line is the target uncertainty and represents a reasonable point of diminishing returns. Each coloured line represents one of the $T = 10$ true models and the black line is the average of all true models.

flattens again though the change in uncertainty between 8 and 16 drillholes is small relative to the amount of additional information required. The choice of 8 drillholes based on the expected uncertainty curve corresponds to a drillhole spacing of 8 units. This is wider than the 5.76 unit spacing (12 drillholes) identified through VOI calculation. Though the spacing is wider, the change in net VOI between these spacings is small at $\Delta NVOI = NVOI(5.76) - NVOI(8) = 7264 - 6873 = \$391$.

Though the expected uncertainty curve does not directly identify the true optimal data spacing, it provides a practical approximation with a more straightforward implementation. As seen in Figure 5.3, the net VOI for the equivalent square data spacing of 8 units is not significantly reduced from the true maximum. Inferring the point of diminishing returns from the expected uncertainty curve is subjective, and it could be argued that the point exists anywhere between 8 and 16 drillholes. Considering the cost of data may help the decision-maker decided on the number of data within this range. It is possible to infer a reasonable point of diminishing returns and determine the relationship between value and uncertainty without directly calculating VOI.

5.3 Economic Uncertainty

The selling price for the comodity is an essential contributor to the value function and directly influences the technical design optimization. Uncertainty around price influences VOI. High selling prices may justify additional information. Operational costs are also an essential factor in the value function. At the time of a VOI study, the mining method may be unknown. Costs such as mining, processing and general and administrative costs may have little confidence or be unknown. In certain situations, economic uncertainty may influence optimal data spacing; however, it primarily has a relative influence on the maximum net VOI.

5.3.1 Commodity Prices

The following example investigates the influence of the gold price on VOI. The numerical VOI workflow considers the distribution of average monthly gold prices from 2000-2020 (Figure 5.9). The synthetic data and value function parameters from Section 5.2 are used. Gold prices are retrieved from the World Gold Council (2020). The units are USD per ounce. For each T true model, a gold price is drawn randomly from the distribution for use in the value function. As the number of true models T controls the range of possible gold prices, the results may be sensitive to this number. The example considers the base case of $T = 10$ as well as 25 and 50. Figure 5.10 shows the results. Figure 5.3 shows the optimal data spacing and maximum net VOI for a fixed gold price of \$1250/oz.

Uncertainty in the gold price does not significantly change the choice of optimal data spacing though it does cause a relative change in the maximum net VOI. When considering ten true models (Figure 5.10 (a) and (b)), by chance, eight of the ten gold prices are higher than the fixed price of \$1250, leading to a gross VOI curve (blue) which does not flatten with decreasing data spacing. Though the optimal sample spacing is the same as the scenario with a fixed price, the maximum net VOI is greater. As the number of true models increases, more variability in the gold price occurs (Figure 5.10 (d) and (f)). This variability leads to a flattening of the gross VOI curve. With $T = 25$ (Figure 5.10 (c)) and $T = 50$ (Figure 5.10 (d)) there are a range of data spacings which have virtually the same net VOI. In both cases, the optimal data spacing is 6.38 units; however, the net VOI curve is relatively flat between 12 and 6 units. In this scenario, it seems reasonable to choose the widest data spacing that

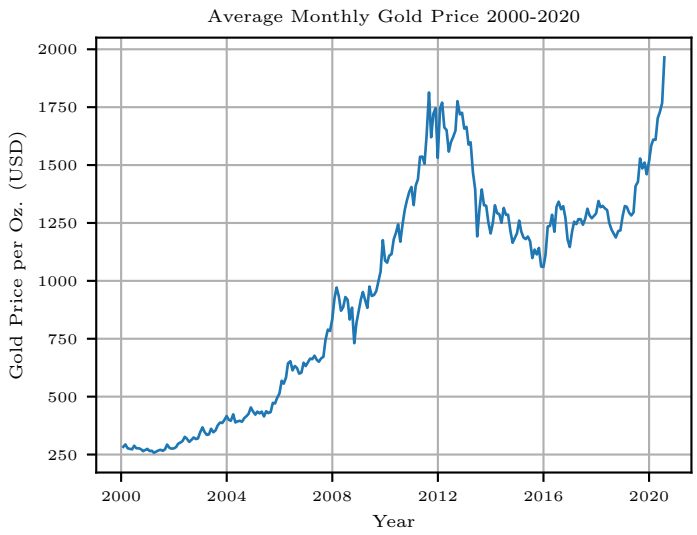

Figure 5.9: Average monthly gold price in USD from 2000-01-31 to 2020-07-31. Retrieved from the World Gold Council (2020).

gets close to the maximum net VOI.

5.3.2 Operational Costs

To investigate the influence of uncertain operational costs on VOI, the cost of mining and processing cost is varied for each true model. Each parameter is allowed to fluctuate ±30% of the fixed values of \$5 and \$10 for mining and processing, respectively. For each variable, a uniform random number is drawn from within the specified range. Like the previous section, as the number of true models T controls the range of possible costs, the results may be sensitive to this parameter. This example considers the base case of $T = 10$ as well as 25 and 50. Figure 5.11 shows the results. Uncertainty in operational costs has a relative impact on the maximum net VOI. As the number of true models increases, the cumulative gross VOI (blue) flattens slightly, leading to a small increase in the optimal data spacing. The magnitude of changes in the maximum net VOI due to uncertainty in operational costs is less than the price variability.

5.4 Summary

Understanding the relationship between uncertainty and value is essential for determining optimal data spacing. If VOI calculation is possible, one can determine a corresponding

target measure of geologic uncertainty. This measure of uncertainty can then be used as a link between value and more easily calculated geologic uncertainty measures for future studies. The expected uncertainty curve is sensitive to the choice of scale for the x-axis. When plotted on a quadratic scale such as the equivalent square data spacing, a breakpoint or point of diminishing returns may not be apparent. Plotting on a linear scale, such as the number of samples or number of drillholes, can better identify the point of decreased learning rate. The example in this chapter shows that the point of diminishing returns inferred from the expected uncertainty curve may not correspond with the spacing identified through VOI analysis. However, it is a practical approximation. The value corresponding to the optimal data spacing identified from geologic uncertainty is close to the true maximum net VOI. Uncertainty in the economic parameters entering the value and transfer function generally have a relative impact on the maximum net VOI. Considering a variable gold price and operational costs leads to a slight increase in optimal data spacing though it primarily causes the maximum net VOI to fluctuate. The variable gold price has the most significant impact on the maximum net VOI.

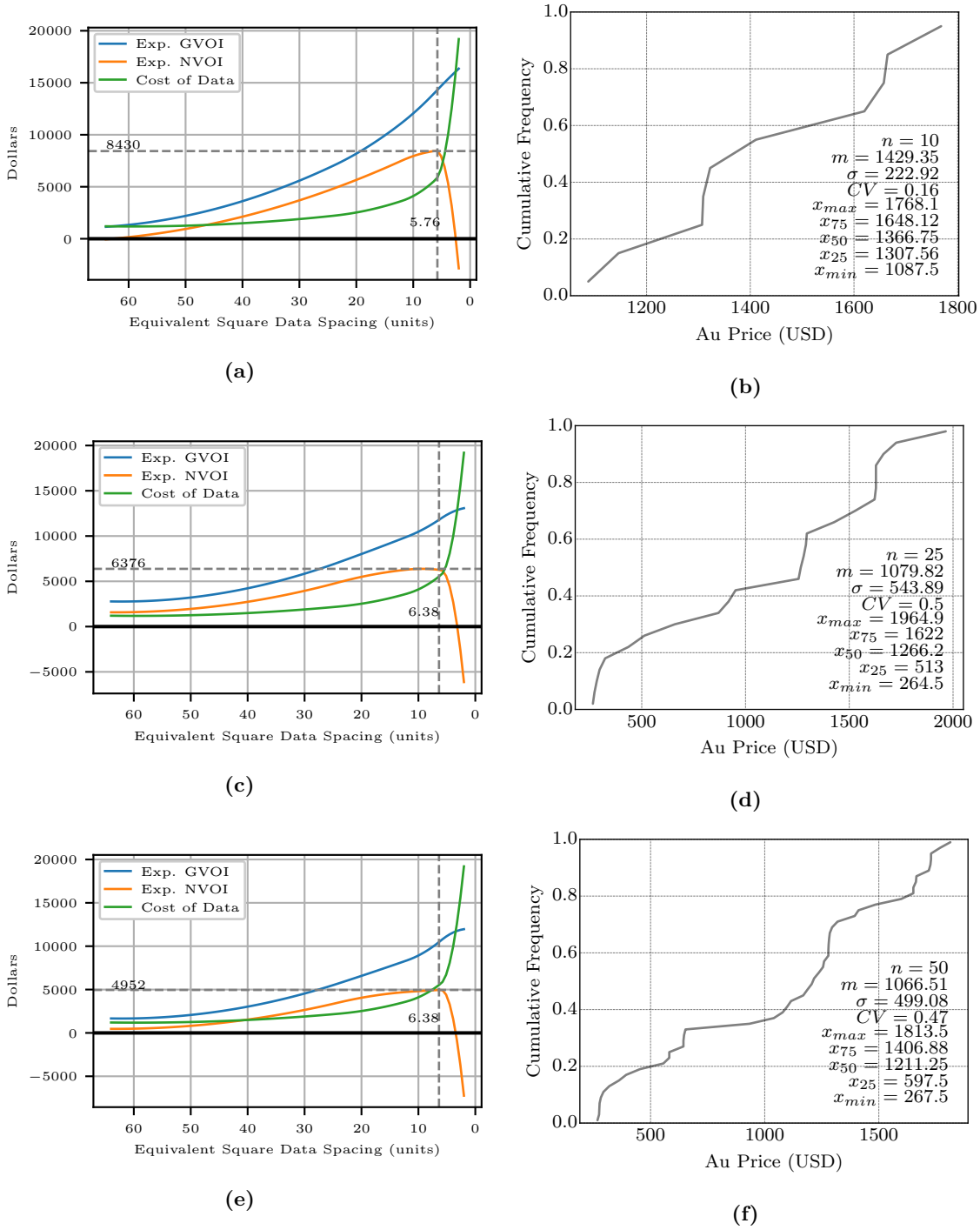

Figure 5.10: Cumulative VOI curves and distributions of gold prices for (a, b) $T = 10$, (c, d) $T = 25$ and (e, f) $T = 50$. The vertical dashed line highlights the optimal data spacing while the horizontal highlights the maximum net VOI.

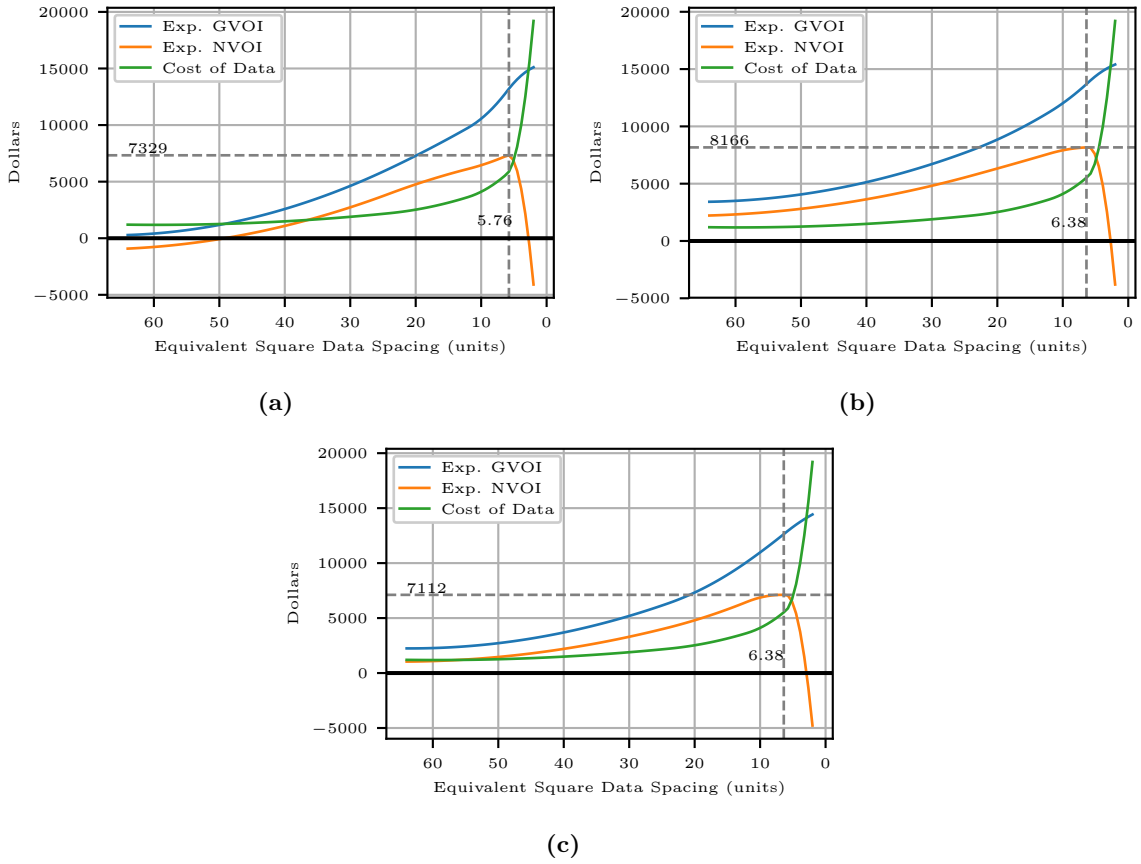

Figure 5.11: Cumulative VOI curves with variable operational costs for (a) $T = 10$, (b) $T = 25$ and (c) $T = 50$. The vertical dashed line highlights the optimal data spacing while the horizontal highlights the maximum net VOI.

Chapter 6

Case Study

The numerical VOI methodology is implemented on a gold deposit currently utilizing a sublevel open stoping mining method. The focus is on a previously mined-out area immediately below an exhausted open pit. The densely drilled study area provides access to a well conditioned, high-resolution true model and many possible data configurations. The resample and resimulate approach utilizes synthetic drillholes in underground fans from existing sublevels for increased control of data spacings. Results also include uncertainty in reported reserves for various data spacings.

The data for the case study is provided by Golden Star Resources (GSR) for research purposes. The Wassa Gold Mine is located in south-western Ghana within the Paleoproterozoic Ashanti greenstone belt. Gold mineralization is structurally controlled and characterized by generally steeply dipping networks of auriferous, laminated quartz-carbonate fault-fill veins. The vein system is north-south striking and dips between 50 and 80 degrees to the west.

6.1 Workflow Overview

This section summarizes the steps of the resample and resimulate VOI workflow. The proposed methodology requires two resampling and two resimulating steps. The first resampling and resimulating step is to generate categorical grade shell realizations. The second step resimulates Au within the grade shells to create a set of final realizations. The final realizations are passed through an optimization function to generate a stope design. The summary of the general steps is:

1. Exploratory Data Analysis, declustering and normal score transform of Au values

2. Calculate and model normal score variograms

3. Generate $T = 10$ true models using all existing drillholes with SGS
4. Generate $C = 12$ future synthetic data configurations with the UDE algorithm
5. Resample each true model with $C = 12$ data configurations
6. Resimulate $L = 100$ realizations of Au conditional to $C = 12$ future data configurations
7. Moving window average and threshold Au realizations to generate categorical grade shell realizations
8. Tag future data configurations by category
9. Resimulate $L = 100$ realizations of Au conditional to $C = 12$ future data configurations within grade shells
10. Pass each set of realizations through the SSO algorithm to generate a technical design
11. Calculate the value of the technical design with the true model
12. Calculate VOI

As rock type data is not directly available in the drillholes, a moving window average followed by a grade thresholding approach is adopted to generate grade shells. This approach allows for uncertainty in both the grade and volume of the mineralized envelope.

6.2 Data Set

The data set consists of 17,834 three-meter composites of gold immediately below and south of the B-Shoot open-pit (Figure 6.1). Data extents are shown in Table 6.1. Composites are x, y, z coordinate midpoints. The data is a mix of surface and underground diamond drillholes. The data is a subset of the 459,165 available composites across the property. No elements other than gold are available. Gold is approximately log-normally distributed. GSR had tagged the composite within high grade (HG) and low grade (LG) deterministic

Table 6.1: Study Area Dimensions

	Minimum	Maximum
X	39850 E	40075 E
Y	19800 N	20125 N
Z	615 m	732 m

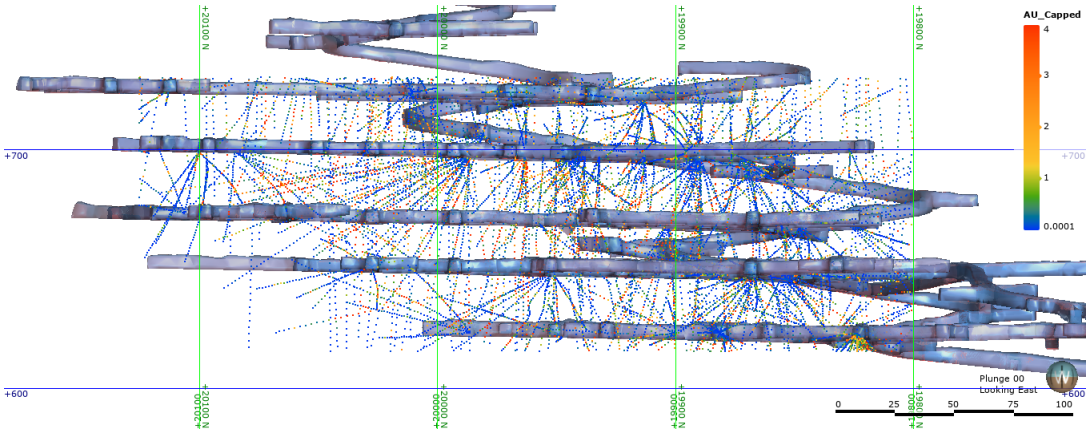

Figure 6.1: 3 meter capped Au composites within the study area looking east. Coordinate labels are in UTM meters, elevation is meters above sea level and the scale bar is meters.

grade shells. Figure 6.2 shows univariate gold statistics by category. The category "All Composites" includes all values within the grade shells and values outside either grade shell. Composites are capped at 30 grams per tonne, which was determined by GSR. Due to the highly irregular configuration of the drillholes, representative distributions are generated with nearest neighbour (NN) declustering before normal score transform. NN declustering is commonly applied when there are known constraints on the domain limits, such as within grade shells (Wilde, 2007). NN declustering can be robust relative to cell declustering in the presence of irregular data if the edge effects are managed appropriately. Despiking is performed though the number of samples at the detection limit is relatively small. 134 and 554 samples have values of 0.0001 and 0.001, respectively, representing 3.85% of the total samples.

6.3 Normal Score Variograms

Normal score variograms are calculated for both low-grade and high-grade categories and all composites grouped. The variogram model for all composites is used to generate the true, high-resolution models of Au. Subsequent workflow steps utilize the low and high-grade

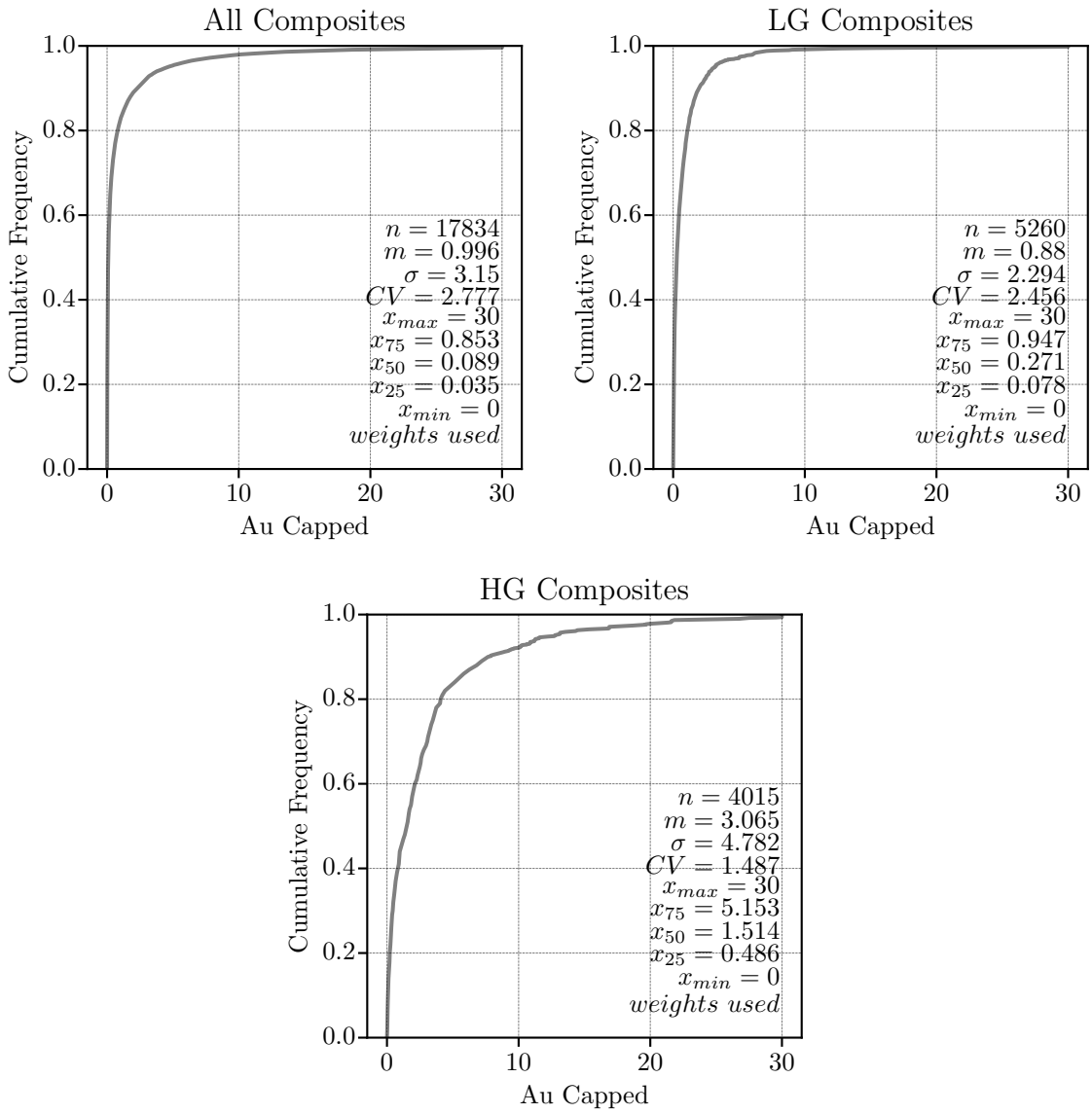

Figure 6.2: Empirical cumulative distribution functions of capped gold values and summary statistics for all, low grade and high grade composites based on GSR deterministic grade shells. All composites encompass HG, LG and data outside either grade shell.

variogram models after generation of categorical grade shell realizations.

The variogram model considering all composites is significantly more continuous than both the LG and HG variogram models. This is expected because the structure between the low and high values is captured in the combined variogram. All variogram model principal directions are north-south at 355 (-005) degrees and dipping gently to the south. Minor directions are down-dip of the vein structure dipping 65 degrees to the west.

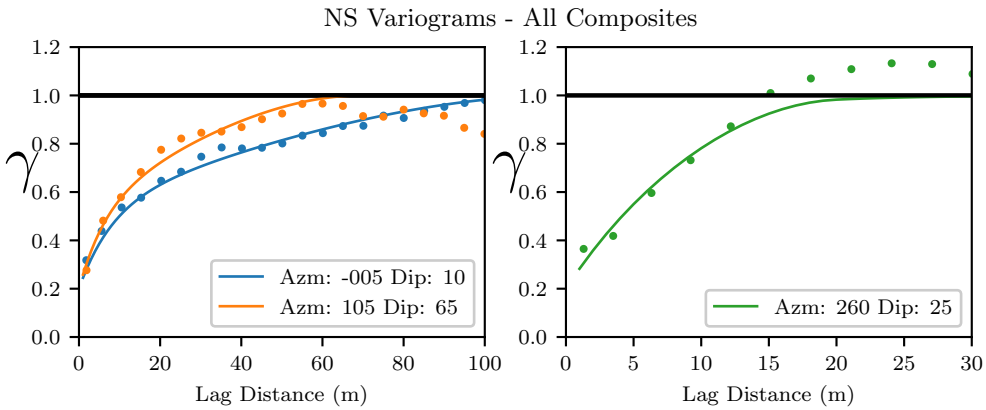

Figure 6.3: Directional variograms of the normal scores of Au for all composites

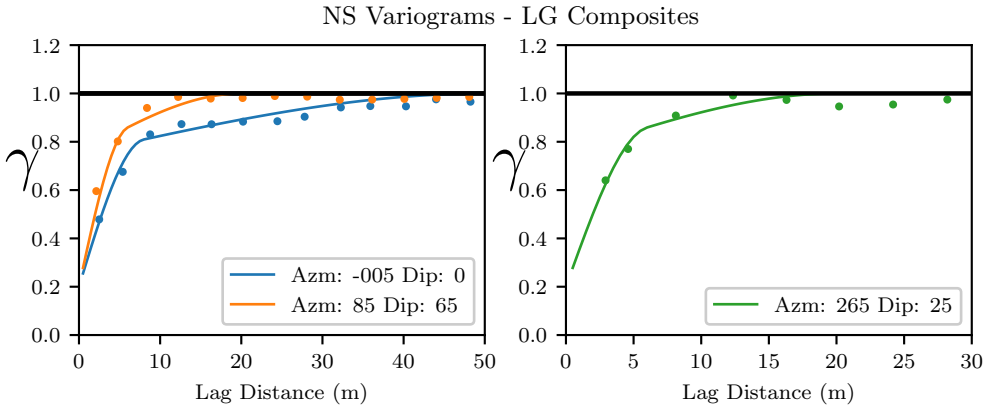

Figure 6.4: Directional variograms of the normal scores of Au for low grade composites

6.4 True Models

$T = 10$ true models are generated with all 17,834 composites and the corresponding variogram model using SGS. High-resolution true models are simulated at the same support of the data on a 1x1x1 meter grid. Plan view, east-west and north-south sections of the first true model are shown in Figures 6.6 , 6.7 and 6.8, respectively.

Good variogram and histogram reproduction are essential for the resampling of the true models. Figure 6.9 shows variogram and histogram reproduction for the true models. As the true models are well conditioned, there is little variability between the realizations.

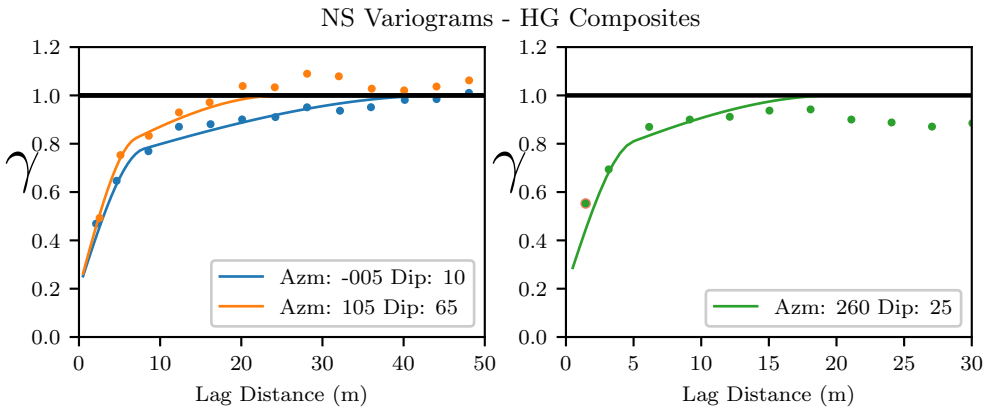

Figure 6.5: Directional variograms of the normal scores of Au for high grade composites

6.5 Future Data Configurations

Future data configurations consist of synthetic fans of drillholes collared in existing as-built sublevels. Generating synthetic drillholes allows for greater control over the resulting nominal drillhole spacing. Drillhole configurations are generated in a reverse fashion, as introduced in Section 4.1. Collars are generated on the 670 m and 700 m sublevels at approximately 5-meter spacing. Each collar location corresponds to a drillhole fan containing eight holes. Each drillhole is 150 m in length. The bottom drillhole in the fan dips at -25 degrees, with a 5-degree dip increment for each subsequent hole. The proposed spatial elimination algorithm sequentially removes drillhole collars and determines the corresponding average drillhole spacing within the domain.

$C = 11$ future data configurations are considered where $c = 0$ is the "current" data configuration. Figure 6.10 shows configuration $c = 1$. Table 6.2 shows the number of drillholes, drillhole groups and corresponding drillhole spacing (DHS) for each configuration. Drillhole spacing is reported as the average equivalent square drillhole spacing calculated with a fixed volume approach as in J. L. Deutsch et al. (2015). The choice of clipping limit and fixed volume for the DHS model are subjective and influence the final result. The DHS model is clipped to within 25 m of the nearest sample to prevent extrapolation into sparsely sampled areas in the eastern portion of the domain. The fixed search volume corresponds to the ranges of the variogram model for all composites with dimensions of 100x60x20 m.

The cost drilling is taken from the Golden Star Resources (2019) technical report and

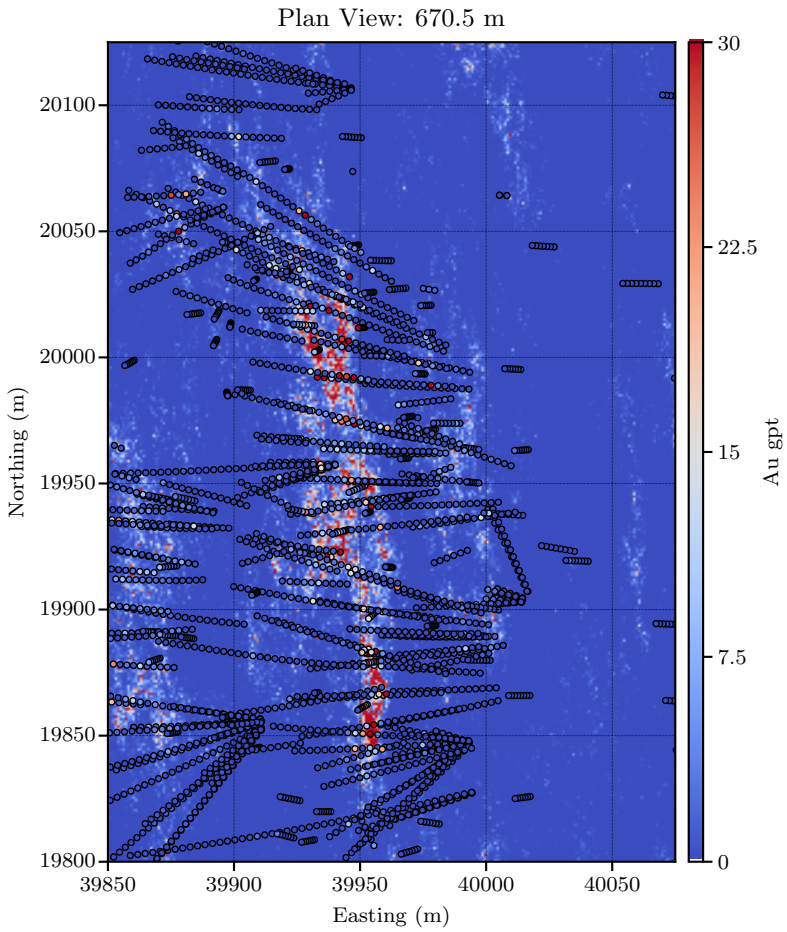

Figure 6.6: Plan view section of the first true model with drillhole composites.

summarized in Table 6.3. The cost of acquisition, $V^{cost}(c)$, for each configuration is the number of drillholes $*150\ m * \$124.52$.

6.6 Resample and Resimulate

6.6.1 Step One

The first resampling step samples the true models. Each model is resampled by all 12 data configurations generating $T * C = 120$ new Au datasets. The distributions of Au resampled from the first true model are compared against the distribution of real drillhole composites in Figure 6.11. As the resampled drillholes have different configurations than the real data, they cannot reproduce this distribution exactly. As more data is collected, the resampled distribution approaches the true reference distribution. The distribution of

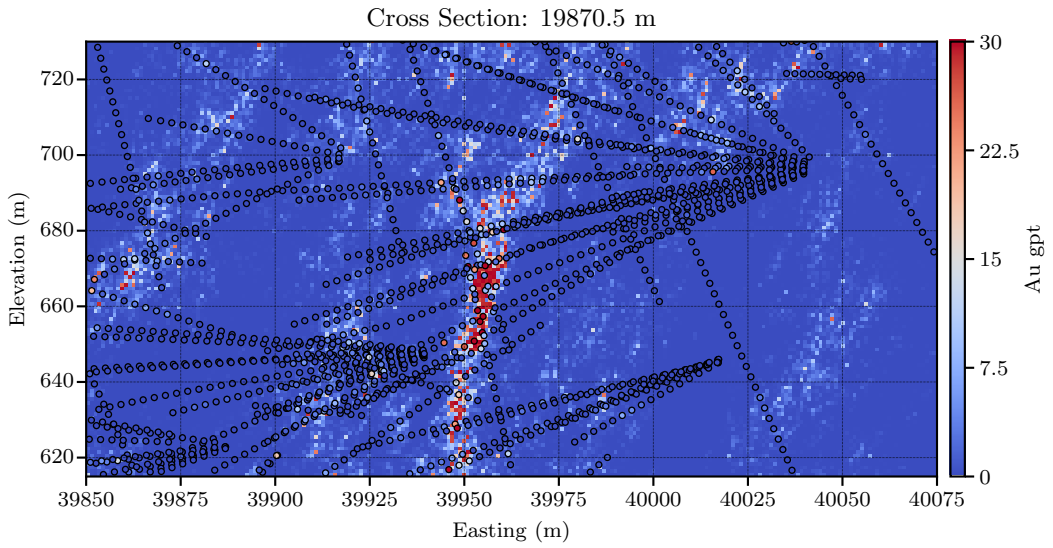

Figure 6.7: East-west section of the first true model with drillhole composites.

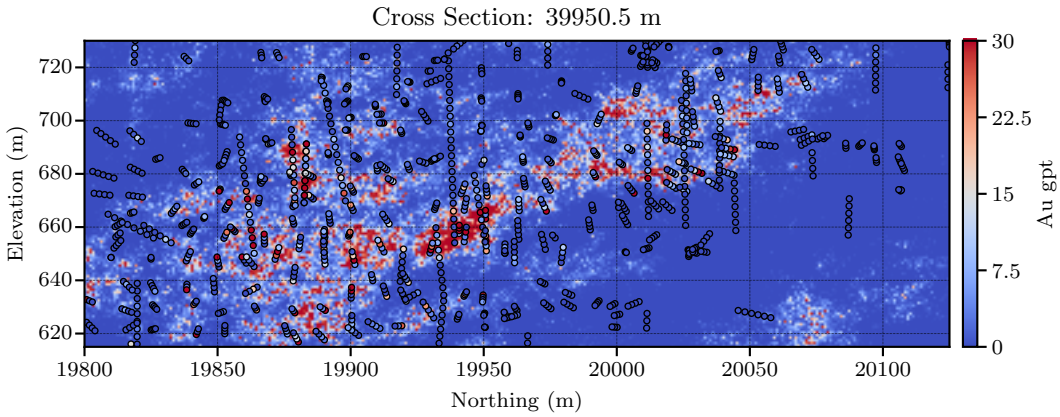

Figure 6.8: North-south section of the first true model with drillhole composites.

Au in configuration $c = 9$ corresponds closely to the real distribution. Configuration 9 has a DHS of 9.01m, which is close to the DHS of the reference drillholes. Table 6.4 shows the mean and standard deviation of each resampled configuration for true model $t = 1$.

The first resimulating step generates realizations of Au conditional to the samples drawn from the true models. Simulation occurs on a 2.5x2.5x2.5 m grid, generating $L = 100$ realizations for each data set. This process generates $T * C * L = 12000$ total realizations of Au. The simulation considers all resampled data and the variogram model of all composites. For illustration, Figure 6.12 shows the histogram reproduction for true model $t = 1$ and data configuration $c = 10$.

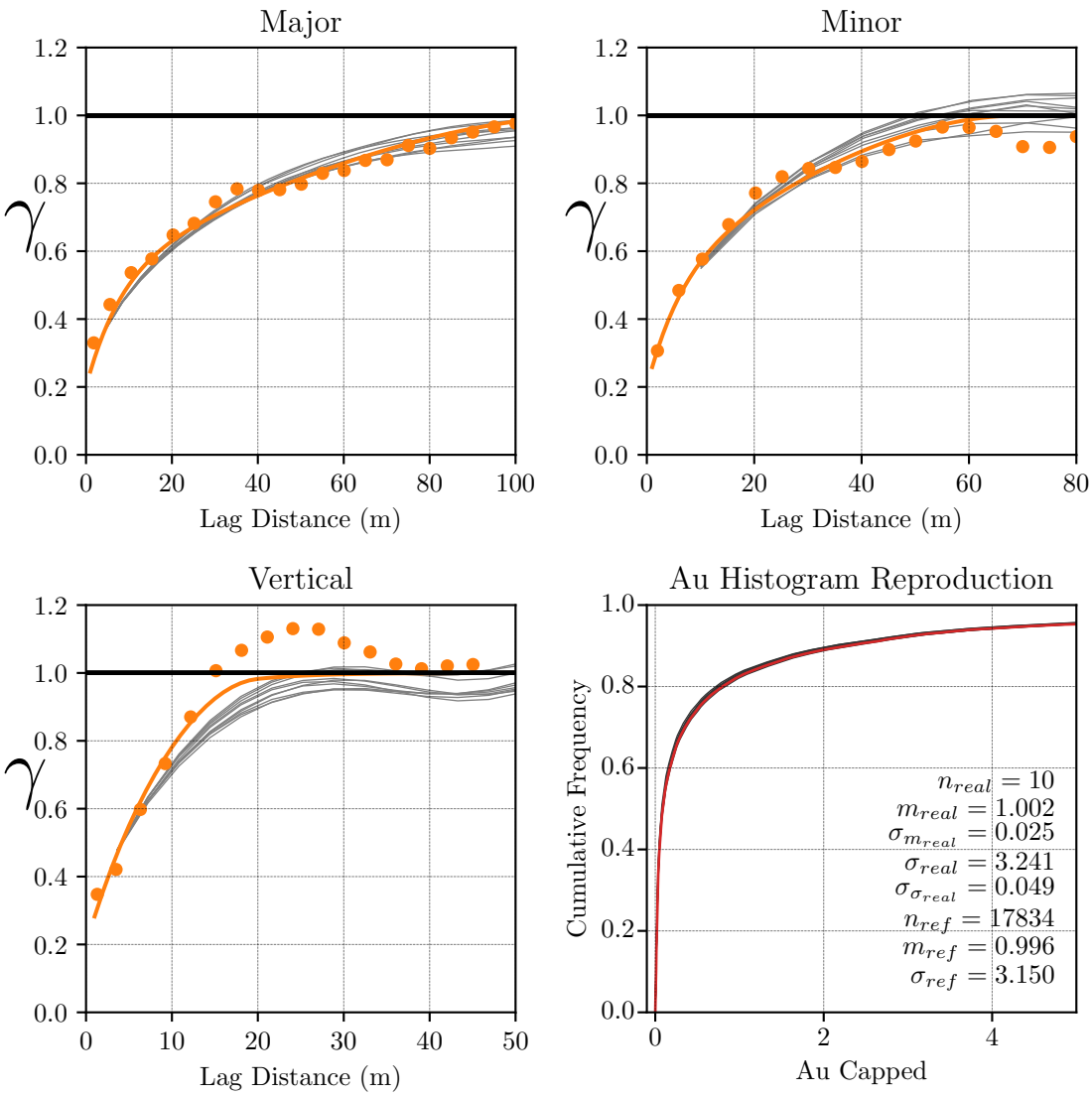

Figure 6.9: Variogram and histogram reproduction for $T = 10$ true models.

6.6.2 Moving Window Average

The realizations of Au are averaged using a moving window with a Gaussian weighting kernel to generate categorical grade shell realizations. The moving window smooths the continuous realizations, which are then thresholded to create categorical variables. A certain degree of smoothing is required, so the grade shells vary gradually over space and do not exactly honour the simulated data. The moving window is 50x50x25 m with an azimuth of 260 degrees and a dip of -65 degrees. Figure 6.13 shows a plan view example of a grade shell model. Category 0 is outside either grade shell, category 1 is LG, and category 2 is HG. LG and HG thresholds are chosen such that the resulting grade shell volumes are close to

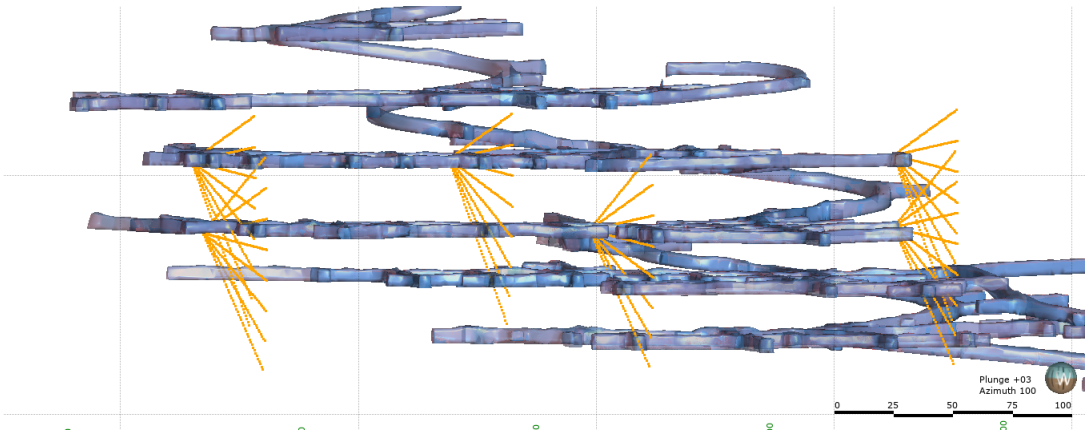

Figure 6.10: Configuration $c = 1$ which corresponds to an average equivalent square drillhole spacing of 30.51 m. Drillhole fans are collared on the 670 m and 700 m sublevels. View is looking east and the scale bar is meters.

Table 6.2: Data configurations and with the number of drillholes, the number of drillhole groups and the average equivalent square drillhole spacing (DHS) within the domain.

C	**Drillholes**	**Groups**	**DHS (m)**
0	32	4	38.59
1	48	6	30.51
2	56	7	24.06
3	72	9	20.97
4	96	12	17.53
5	112	14	14.64
6	144	18	13.00
7	176	22	11.08
8	200	25	9.97
9	232	29	9.01
10	328	41	7.06
11	568	71	4.99

the deterministic grade shell model provided by GSR. Thresholds of 0.42 and 2.0 grams per tonne Au are used for LG and HG, respectively. Figure 6.14 shows the distribution of grade shell volumes by data configuration for true model $t = 1$. Each curve represents $L = 100$

Table 6.3: Costs per meter of data acquisition

Cost	**Cost per Meter**
Drilling	$103.33
Assay	$11.36
Geological Logging	$9.62
Consumables	$0.21
Total	$124.52

Table 6.4: Declustered mean and standard deviation for resampled data configurations.

C	**Mean Au gpt**	**Stdev Au gpt**
0	0.840	3.073
1	0.946	3.323
2	0.913	3.247
3	0.911	3.223
4	0.880	3.191
5	0.913	3.285
6	0.924	3.260
7	0.887	3.179
8	0.939	3.316
9	0.981	3.393
10	1.018	3.406
11	1.033	3.425

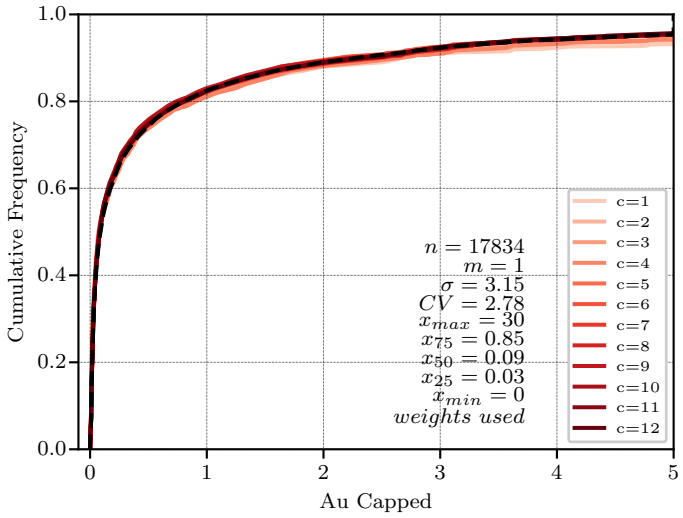

Figure 6.11: Cumulative declustered histograms of resampled datasets for the first true model. The dashed black line (and stat block) is the distribution of real drillhole composites.

grade shell volumes. The dashed gray line represents the deterministic volume from the GSR model, and the dashed black line is the average of all realizations.

6.6.3 Step Two

The second resampling step tags the samples drawn from the first resampling step by the grade shell realizations. This process creates $T * C * L = 12000$ new data sets with a categorical grade shell variable, each of which captures variability in the geology. There is a unique data set for each subsequent realization in the second resimulation step.

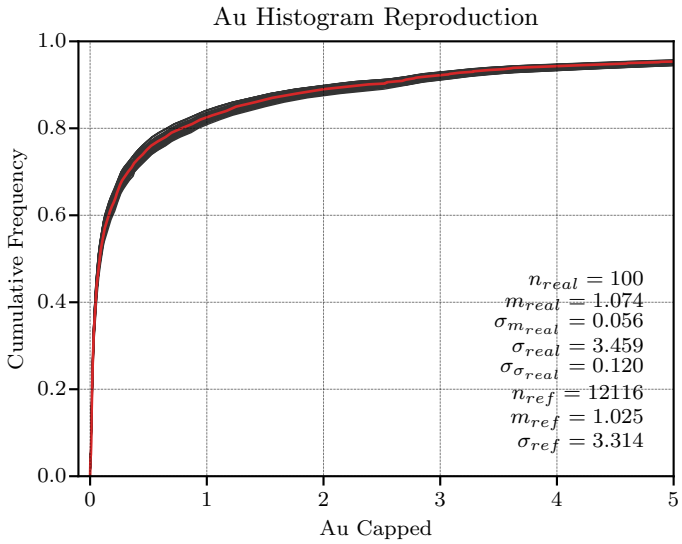

Figure 6.12: Au histogram reproduction for configuration $c = 10$ drawn from true model $t = 1$.

The second resimulation step simulates Au by category, considering the grade shells generated through the moving window average. Each realization uses the tagged drillhole data from the second resampling step. This process creates $T * C * L = 12000$ final realizations for stope optimization.

6.7 Stope Optimization

A transfer function is required to calculate a response from the input model of geology. This workflow's transfer function is a series of stope geometries that form a mining panel spanning the 645 m, 670 m and 700 m sublevels. The transfer function input is the set of final realizations from the second resimulation step and value function, and the output is value in dollars. The transfer function or stope geometry is optimized through the application of the SSO algorithm based on differential evolution (DE). DE is a heuristic evolutionary optimization algorithm based on mutation and recombination processes present in natural biological evolution (Rainer & Price, 1997). The stope optimization process requires defining a value function and parameters, a set of technical engineering constraints and an objective function. The objective function value is minimized while respecting the technical constraints.

Stope optimization is simplified in this case study. Each stope has eight vertices with fixed

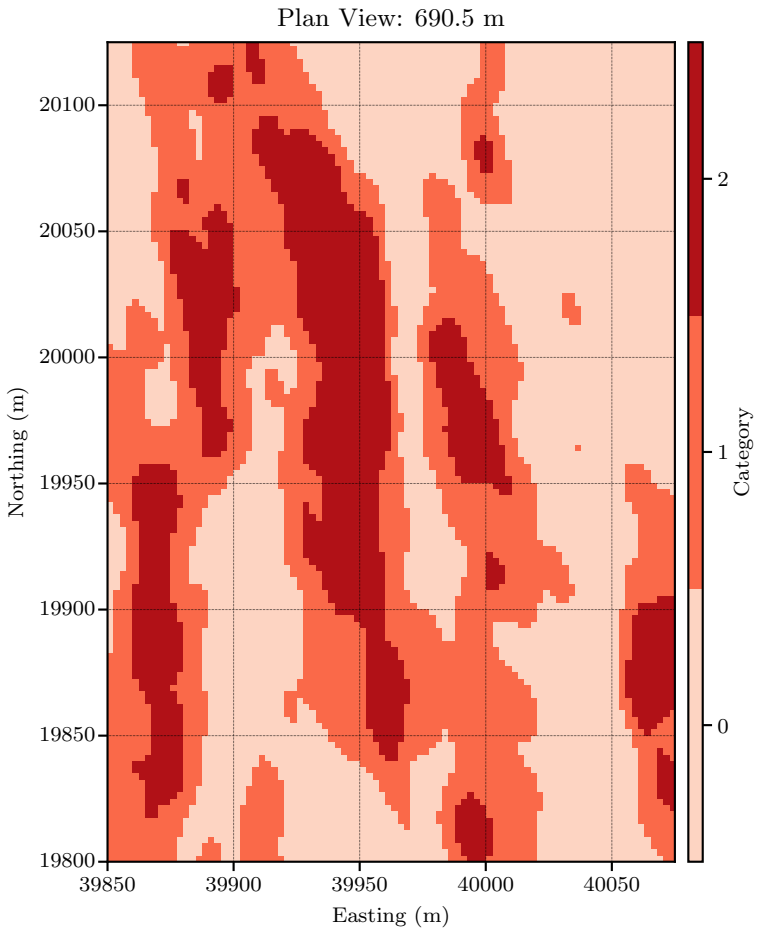

Figure 6.13: Plan view section though a grade shell model. Category 0 is outside, 1 is LG and 2 is HG.

elevation. The stope's length is fixed at 25 m along the ore body's strike at 355 degrees. Initial stope vertices are generated along strike, parallel to existing sublevel infrastructure, at a 50 m width. Each vertex is free to move perpendicular to the strike giving each initial stope geometry 8 degrees of freedom for optimization. The stope geometry in this work is a reasonable initial volume which honours the technical constraints and may not be the true optimum.

6.7.1 Value Function

Value function parameters are taken from the Golden Star Resources (2019) technical report and summarized in Table 6.5.

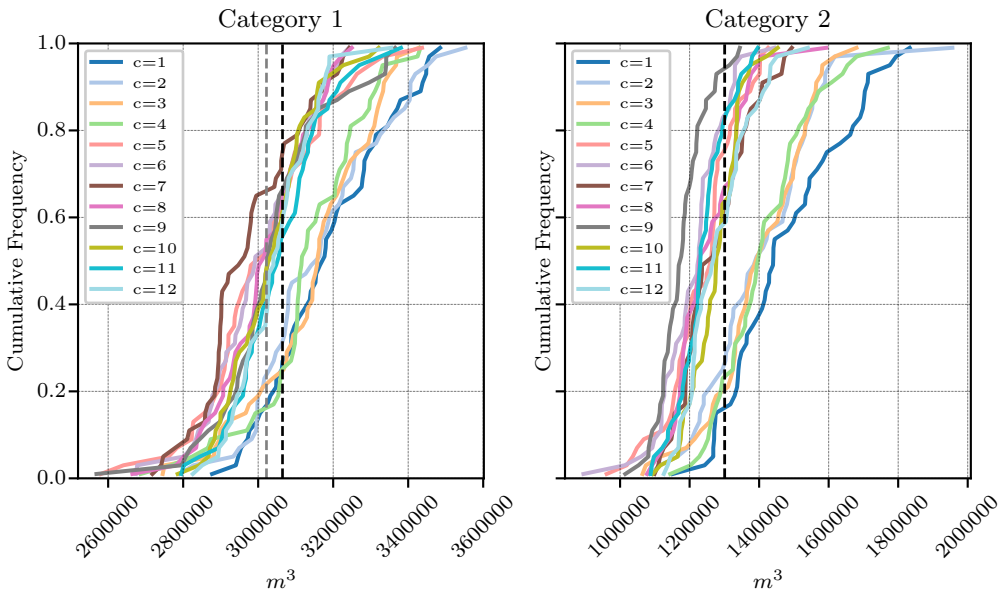

Figure 6.14: LG (left) and HG (right) grade shell volumes for each data configuration for true model $t = 1$. The dashed gray and black lines overlap for category 2.

Table 6.5: Value function parameters. Costs are per tonne, values are in USD.

Description	Parameter	Value
Specific Gravity	SG	2.8 g/cm^3
Block Volume	v_{blk}	15.625m^3
Au Price	p_{Au}	\$1250/Oz.
Conversion Factor	cf	31.1035
Mining Cost	c_m	\$43
Processing Cost	c_p	\$25
G&A Cost	c_{ga}	\$12
Plant Recovery	f_{rec}	0.94
Mining Recovery	f_{mine}	0.95
Dilution Factor	f_{dil}	1.10
Royalty Factor	f_{roy}	0.95
Stream Factor	f_{str}	0.916

The value of a particular stope geometry is the sum of the net value of each block within the geometry. Net value of each block is calculated using the parameters in Table 6.5. Diluted grades are calculated considering 10% dilution at zero grade (consistent with GSR documentation):

$$z^l_{c_{(dil)}}(\mathbf{u}) = \frac{z^l_c(\mathbf{u}) * v_{blk}}{v_{blk} * f_{dil}} \tag{6.1}$$

Recovered grams of gold are calculated as:

$$z^l_{c_{(rec)}}(\mathbf{u}) = z^l_{c_{(dil)}}(\mathbf{u}) * v_{blk} * SG * f_{rec} * f_{mine} \tag{6.2}$$

Gross value per block is then calculated as:

$$V^l_{c_{(gross)}}(\mathbf{u}) = z^l_{c_{(rec)}}(\mathbf{u})/cf * p_{Au} * f_{roy} * f_{str} \tag{6.3}$$

The cost of mining each block is:

$$Cost^l_c(\mathbf{u}) = v_{blk} * f_{dil} * SG * \Big(c_m + c_p + c_{ga}\Big) \tag{6.4}$$

The net value of each block is then:

$$V^l_{c_{(net)}}(\mathbf{u}) = V^l_{c_{(gross)}}(\mathbf{u}) - Cost^l_c(\mathbf{u}) \tag{6.5}$$

The economic value of the stope is the sum of the net values of the N blocks within the design:

$$V^l_{econ} = \sum_{i=1}^{N} V^l_{c_{(net)}}(\mathbf{u}_i) \tag{6.6}$$

The value of the stope geometry for each of the $l = 1, ..., L$ realizations is then passed to the objective function.

6.7.2 Objective Function

An objective function which characterizes the optimization objective while incorporating appropriate constraints is required. The objective function value is the expected value of the stope geometry across all $L = 100$ realizations. A neutral position on risk is adopted such that the expected utility is equal to the expected value. The objective function is expressed as:

$$O(D(scale,\ G(c,\ L = 100))) = \frac{1}{L}\sum_{l=1}^{L} V^l_{econ} \tag{6.7}$$

Stope technical constraints are summarized in Table 6.6. If violation of the constraints occurs on a particular iteration, vertices are adjusted until the constraints are satisfied.

Table 6.7: Differential evolution parameters.

Description	Parameter	Value
Population Size	NP	10
Dimensions	D	8
Crossover Probability	$crossp$	0.9
Mutation Constant	mut	[0.5,1]
Random Restart Iterations	K	50
Random Restart Threshold	g	10^{-6}
Algorithm Iterations	its	1000

Table 6.6: Stope optimization technical constraints.

Parameter	Value
Stope Length	25 m
Minimum Width	10 m
Maximum Width	30 m
Maximum Span	39.05 m

6.7.3 Differential Evolution

A DE/rand/1 mutation scheme is adopted for stope optimization. The notation specifies that the population vector to be mutated is randomly chosen (rand), and the mutation consists of one (1) weighted difference vector (Storn, 1996). Other mutation schemes exist and are presented by Storn (1996) and Price et al. (2006). A random restart mechanism is adopted from Mohamed (2014) to prevent convergence to a local minimum. If each population vector's fitness values change less than a specified tolerance g, over a specified number of iterations K, the entire population, but the current best vector is randomly reinitialized.

In this implementation, the dimensionality is the number of degrees of freedom in the stope design or $D = 8$. The initial population of stope vertex positions is generated by randomly sampling a position $\pm$ 25 m of the initial vertex, perpendicular to strike. A population size of $NP = 10$ is used with a crossover probability of 0.9 and a mutation constant randomly drawn $\in$ $[0.5, 1.0]$. Randomly selecting the mutation constant is referred to as dithering and may speed algorithm convergence in some scenarios (Price et al., 2006). Differential evolution parameters are summarized in Table 6.7. An example of the objective function value versus algorithm iteration using the parameters in Table 6.7 is shown in Figure 6.15.

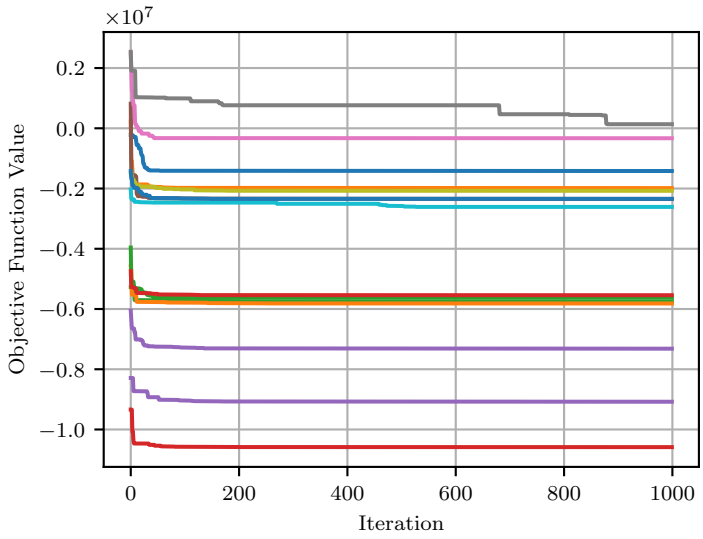

Figure 6.15: Objective function value versus iterations. The sign of the value is negative the algorithm converges towards a minimum value. Each line represents the objective function value for a single stope geometry.

Eighteen individual stope shapes are optimized to form a panel spanning the 645 m and 670 m sublevels. Figure 6.16 shows optimized stope shapes for the 670 m sublevels for four different data configurations plotted over the true model. The top left plot corresponds to data configuration $c = 1$, top right is configuration $c = 4$, bottom left is configuration $c = 8$ and bottom right is configuration $c = 12$. The corresponding equivalent square data spacings are 38.59, 20.97, 11.08 and 4.99 m, respectively. In all scenarios, the stope geometries conform to the strike of the mineralization. As more information is collected, the stopes better capture the high-grade mineralization, which is particularly true for the northern end of the sublevel.

6.8 Value of Information

VOI is calculated by considering the true model and the optimized panel geometry comprised of 18 stopes with the value function. The value with current information in Equation 6.8 is calculated with the panel geometry optimized on the geologic model $G(c = 0,\ L = 100)$. The value with future information in Equation 6.9 is calculated with the panel geometries optimized on the set of geologic models $\{G(c,\ L = 100),\ c = 1, ..., 11\}$. N

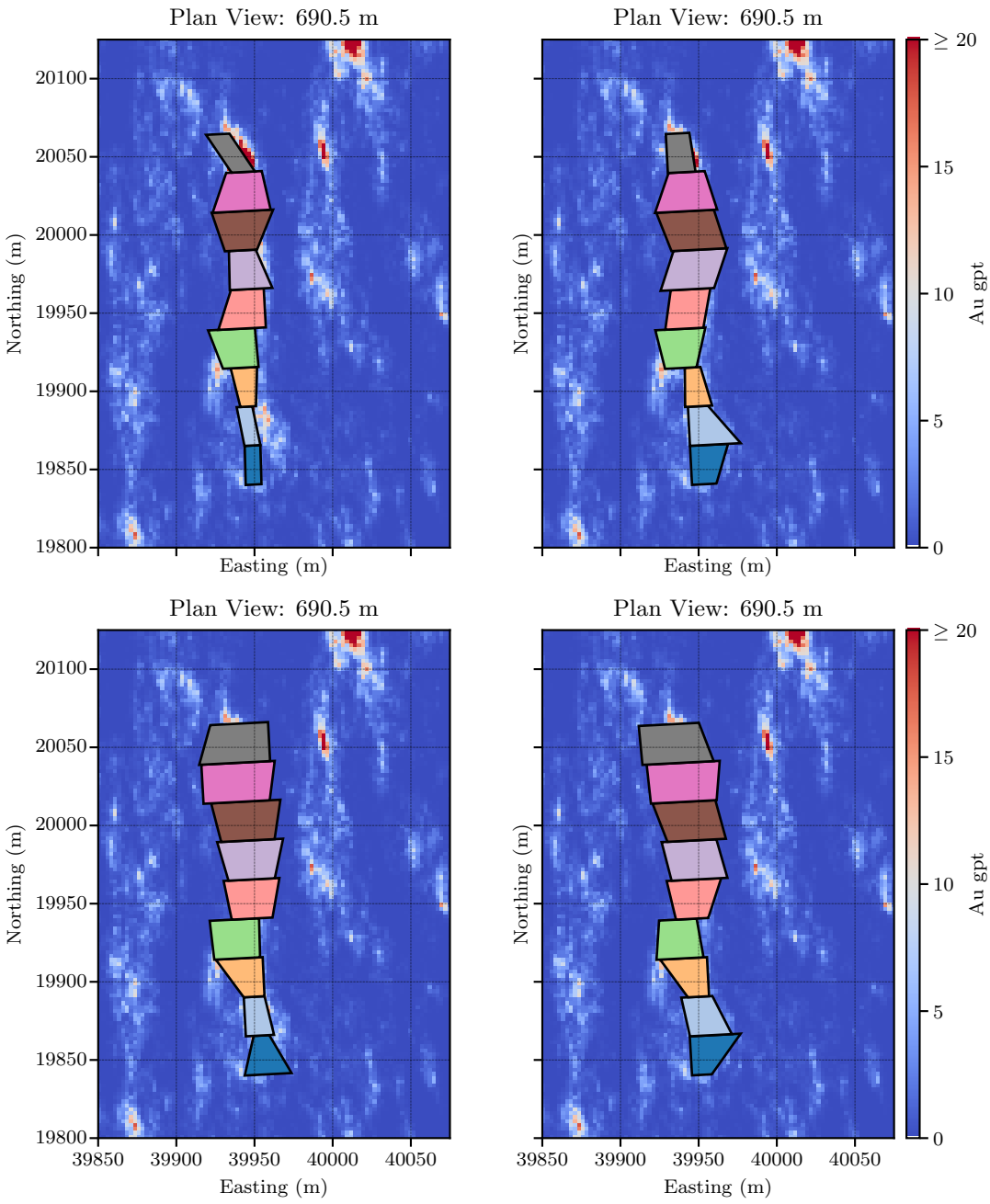

Figure 6.16: Optimized stope geometries for the 670 m sublevel for data configurations $c = 1$ (top left), $c = 4$ (top right), $c = 8$ (bottom left) and $c = 12$ (bottom right) plotted over the true model $t = 1$.

is the number of blocks within stope design $j = 1, ..., 18$.

$$V^t(0) = \sum_{j=1}^{18} \sum_{i=1}^{N} V^t_{0_{(net)}}(\mathbf{u}_{i,j}), \quad t = 1, ..., T \tag{6.8}$$

$$V^t(c) = \sum_{j=1}^{18} \sum_{i=1}^{N} V^t_{c_{(net)}}(\mathbf{u}_{i,j}), \quad c = 1, ..., C; \quad t = 1, ..., T \tag{6.9}$$

The gross value of information is calculated as the difference between the value with future information and the value with current information:

$$GVOI^t(c) = V^t(c) - V^t(0), \quad c = 1, ..., C; \quad t = 1, ..., T \tag{6.10}$$

The net value of information is calculated as the difference between the gross VOI and the cost of acquiring data configuration c:

$$NVOI^t(c) = GVOI^t(c) - V^{cost}(c), \quad c = 1, ..., C; \quad t = 1, ..., T \tag{6.11}$$

The expected $GVOI$ and $NVOI$ are taken as the average across all T true models:

$$E\{GVOI(c)\} = \frac{1}{T} \sum_{t=1}^{T} GVOI^t(c), \quad c = 1, ..., C \tag{6.12}$$

$$E\{NVOI(c)\} = \frac{1}{T} \sum_{t=1}^{T} NVOI^t(c), \quad c = 1, ..., C \tag{6.13}$$

Figure 6.17 shows the cumulative VOI curves. The vertical dashed line highlights the optimal drillhole spacing of 12.4 m, while the horizontal dashed line highlights the maximum net VOI of $\$20.87 \times 10^6$. The thin blue and orange lines show the cumulative $GVOI$ and $NVOI$ for each of the $T = 10$ true models, while the thick blue and orange lines are the $E\{GVOI\}$ and $E\{NVOI\}$, respectively.

6.9 Geologic Uncertainty

As introduced in Chapter 5, the drillhole spacing that maximizes net VOI can be used to determine a target level of geologic uncertainty. Figure 6.18 shows the expected standard deviation of gold plotted against the equivalent square drillhole spacing (quadratic) and the number of additional drillholes (linear). When plotted on a linear scale, the point of diminishing returns becomes more evident. The optimal drillhole spacing of 12.4 m corresponds to 165 additional drillholes. The greatest resolution of geologic uncertainty occurs between 32 and 165 drillholes. Beyond this point, additional information has diminishing returns as the rate of uncertainty reduction decreases significantly.

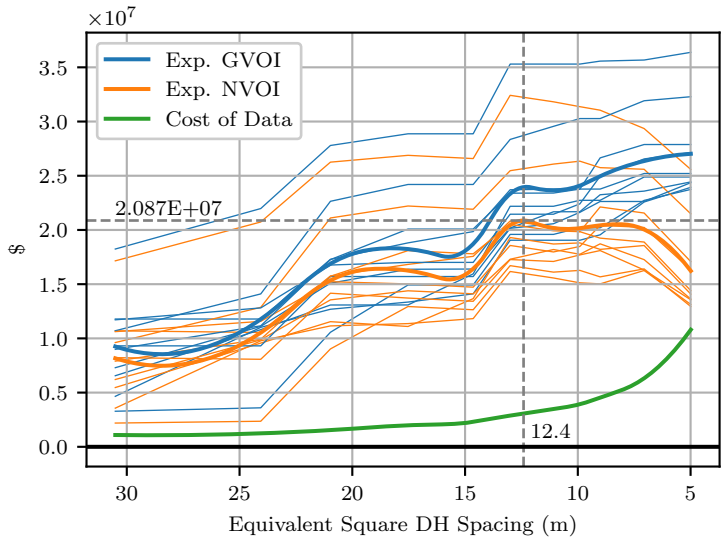

Figure 6.17: Cumulative expected VOI curves. The optimal drillhole spacing of 12.4 m is highlighted by the vertical dashed line. Thin blue and orange lines represent the gross and net VOI curves for each of the $T = 10$ true models.

6.10 Reserve Uncertainty

Understanding how reserves change with increasing information is an important concept related to the value of information. Reserve reporting with anticipated future data configurations can be implemented with a resample and resimulate strategy. Reserves reporting can be either optimistic or pessimistic. As more information is collected, these reserve numbers begin to converge. Optimistic reserves or undiluted perfect information (UPI) reserves are calculated by optimizing a stope design in a one-for-one fashion. That is, a stope is optimized for each of the L realizations and metrics are calculated against that realization. The UPI reserve is optimistic as it assumes perfect knowledge of geology. There are as many UPI reserve estimates as there are realizations. Pessimistic reserves or no additional data (NAD) reserves are calculated by optimizing a stope design in a one-for-many fashion. That is, a stope design is optimized across all L realizations, and then metrics are calculated against each realization. The NAD reserve is considered pessimistic as with widely spaced data, the vein structure may not overlap between realizations. There are as many NAD reserve estimates as there are realizations.

The starting point for reserve uncertainty is a set of $L = 100$ realizations constrained to all available real drillholes. UPI and NAD reserves are calculated for this set of realizations.

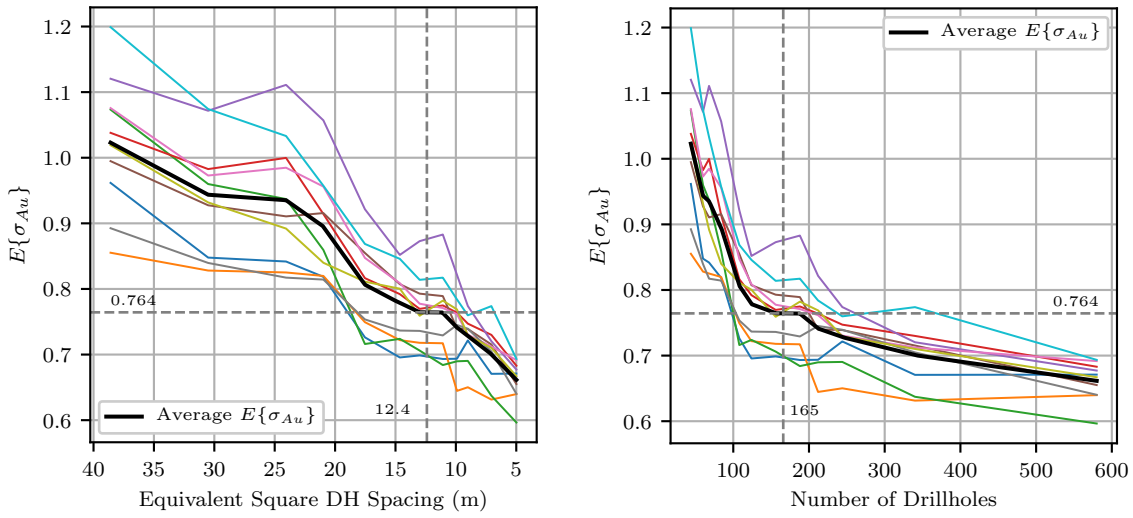

Figure 6.18: Average expected standard deviation of Au against (a) equivalent square drillhole spacing and (b) number of additional drillholes. The optimal drillhole spacing of 12.4 m corresponds to 165 additional drillholes. Each coloured line represents one of the $T = 10$ true models and the black line is the average of all true models.

Reserve metrics are panel tonnes, grade and recovered gold ounces. All available drillholes are decimated or rolled back into $C = 10$ data sets with equivalent square drillhole spacings ranging from 30.2 m to 8.01 m. For reserve reporting, no synthetic drillholes are considered. For each of the $C = 10$ data configurations, a set of $L = 100$ realizations are generated, repeating the UPI and NAD stope optimization process. This process generates a distribution of uncertainty in the UPI and NAD reserves for each drillhole spacing. Figures 6.19, 6.20 and 6.21 shows panel tonnes, grade and recovered ounces for UPI and NAD reserves, respectively. Panel tonnes for the NAD reserve are a single value as there is only one technical design that results in a single value. A particular stope is only chosen for development if its net value is greater than zero. With wider spaced data configurations, fewer stopes exceed this threshold resulting in smaller expected tonnages. At approximately 13 m drillhole spacing, the UPI and NAD tonnages converge, and the standard deviation does not reduce significantly beyond this point. As only net positive stopes are developed, the panel's expected grade does not change significantly as more information is collected; however, the standard deviation of gold reduces. Again, for spacings closer than 13 m, uncertainty in the expected panel grade stabilizes. Similarly, the expected recovered gold ounces and standard deviation stabilizes beyond 13 m drillhole spacing. These reserve metrics correspond well

with the 12.4 m drillhole spacing that maximizes net VOI.

NAD reserves may also be viewed relative to UPI reserves by considering an incomplete information factor (IIF). The IIF is the relative difference between the current knowledge and the perfect knowledge of geology. A factor close to 1 indicates complete information as the optimistic and pessimistic case are close. For each data configuration and each $L = 100$ realizations, the NAD value is datumed relative to the corresponding UPI value. Figure 6.22 shows the distribution of IIF values (blue dots) and the expected IIF (orange line) for the range of drillhole spacings. For panel tonnes and recovered gold ounces, as more information is collected, the uncertainty in the factor decreases and approaches 1. The IIF is roughly 1 for all data configurations for the grade as only net positive stopes are chosen for development. Beyond 13 m drillhole spacing, the IIF converges to 1, and the uncertainty is relatively constant.

6.11 Assumptions and Limitations

General limitations of the resample and resimulate approach are introduced in Section 2.5. One assumption made in this case study is that the variogram model is the same for all data configurations. In this case study, variogram calculation considers sufficient data such that estimates are deemed an accurate representation of the true variogram; however, this may not be true for all scenarios. One limitation of this study is the simplicity of the stope optimization process. Though the enforcement of technical considerations ensures the geometries are reasonable from an engineering perspective, they are not true optimums. No partial blocks are considered in the value function though optimization takes place on a reasonably fine grid. No consideration has been given to the sequencing of the stope geometries, and they are treated as a complete panel. Only net positive stopes are included within the panel though no economic consideration has been given to mine plan modifications related to leaving unmined material behind. No consideration has been given to the timing of the collection of data with respect to stope sequencing. It is assumed that all drill collar locations on either sublevel are available at all times, and the act of collecting information does not interfere with or delay the mine plan.

6.12 Summary

The numerical VOI workflow could be adapted to a variety of mining scenarios. Future data configurations are simulated such that they accurately represent the true reference distribution. This resampling process provides access to data configurations at virtually any data spacing. The resimulation process provides access to a posterior uncertainty distribution for value calculations. VOI is then calculated as the difference in value with and without future information. In this case study, the net VOI is relatively flat for spacings closer than the optimal 12.4 m. The choice of optimal spacing is sensitive to the cost of information. A decrease in the cost of information could lead to closer optimal data spacing. Additional drillhole configurations could be considered to more precisely determine the optimal. Considering a greater number of true models may further refine the expected VOI curves. The target standard deviation determined through the VOI analysis corresponds reasonably well with the point of decreased learning rate seen when plotting the expected uncertainty curve with a linear x-axis. One could argue that the point of diminishing returns occurs just beyond 200 drillholes, though Figure 6.17 shows that achieving this data spacing is a marginal gain in value. Reserve reporting considering a range of data spacings corresponds well to the VOI results. Pessimistic and optimistic reserve calculations converge at the optimal data spacing, and uncertainty in tonnes, grade and contained metal do not reduce significantly for closer spacings. This is summarized well by the incomplete information factor, which converges to 1.0 at the optimal data spacing.

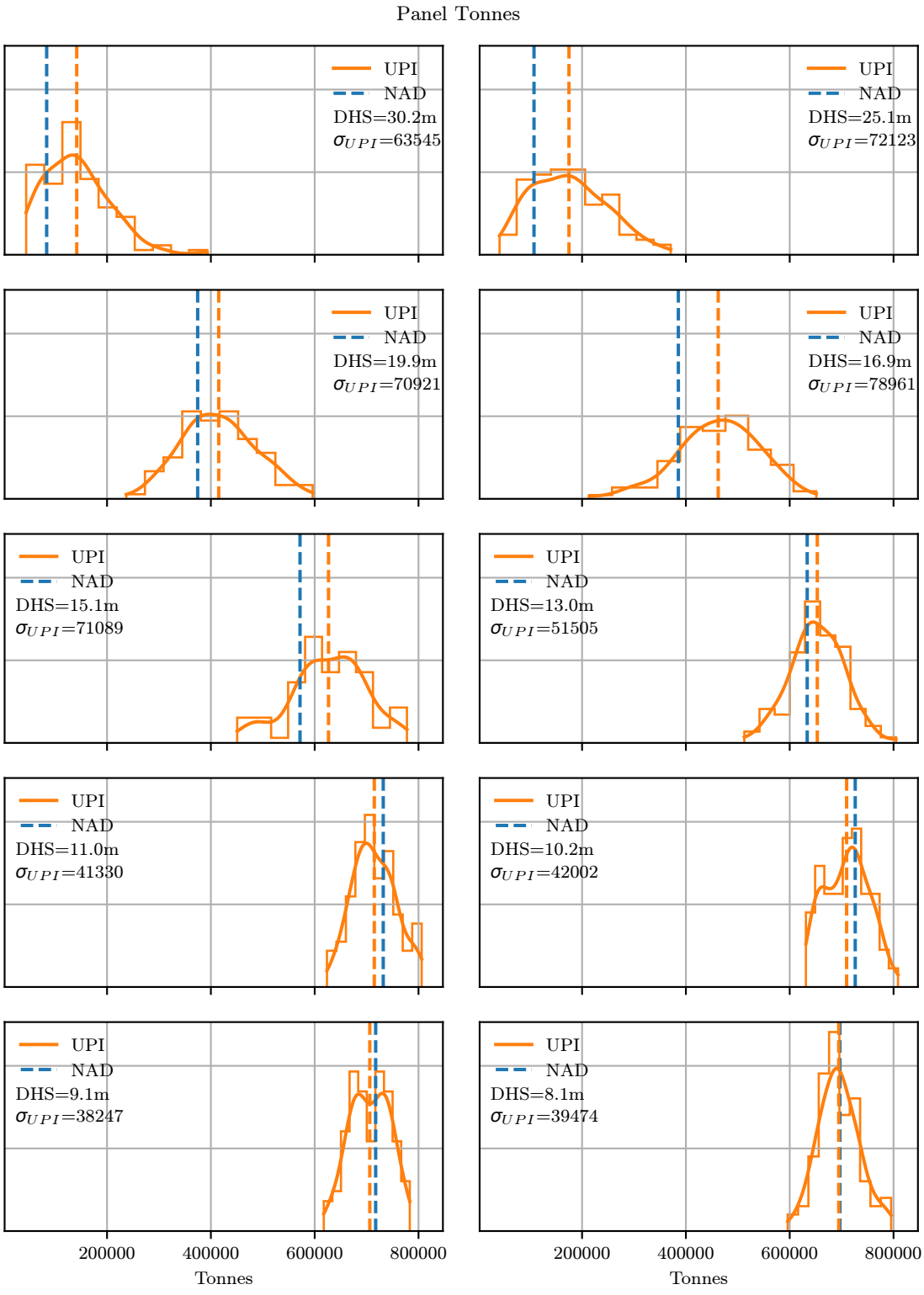

Figure 6.19: Uncertainty in panel tonnes by drillhole spacing. The dashed lines are the expected values of the respective distributions. All plots share both x and y axes. UPI = undiluted perfect information, NAD = no additional data.

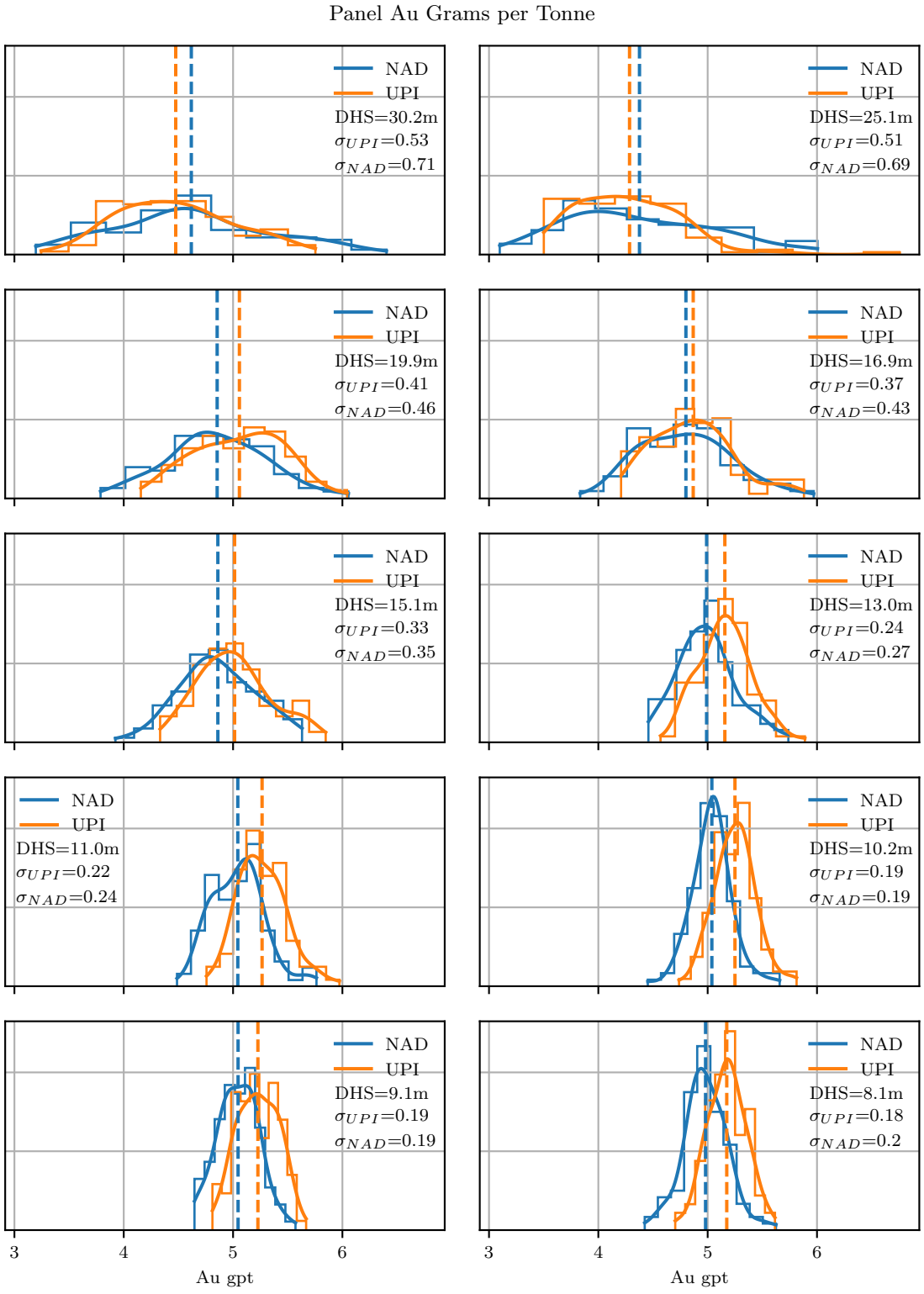

Figure 6.20: Uncertainty in panel Au grade by drillhole spacing. The dashed lines are the expected values of the respective distributions. All plots share both x and y axes. UPI = undiluted perfect information, NAD = no additional data.

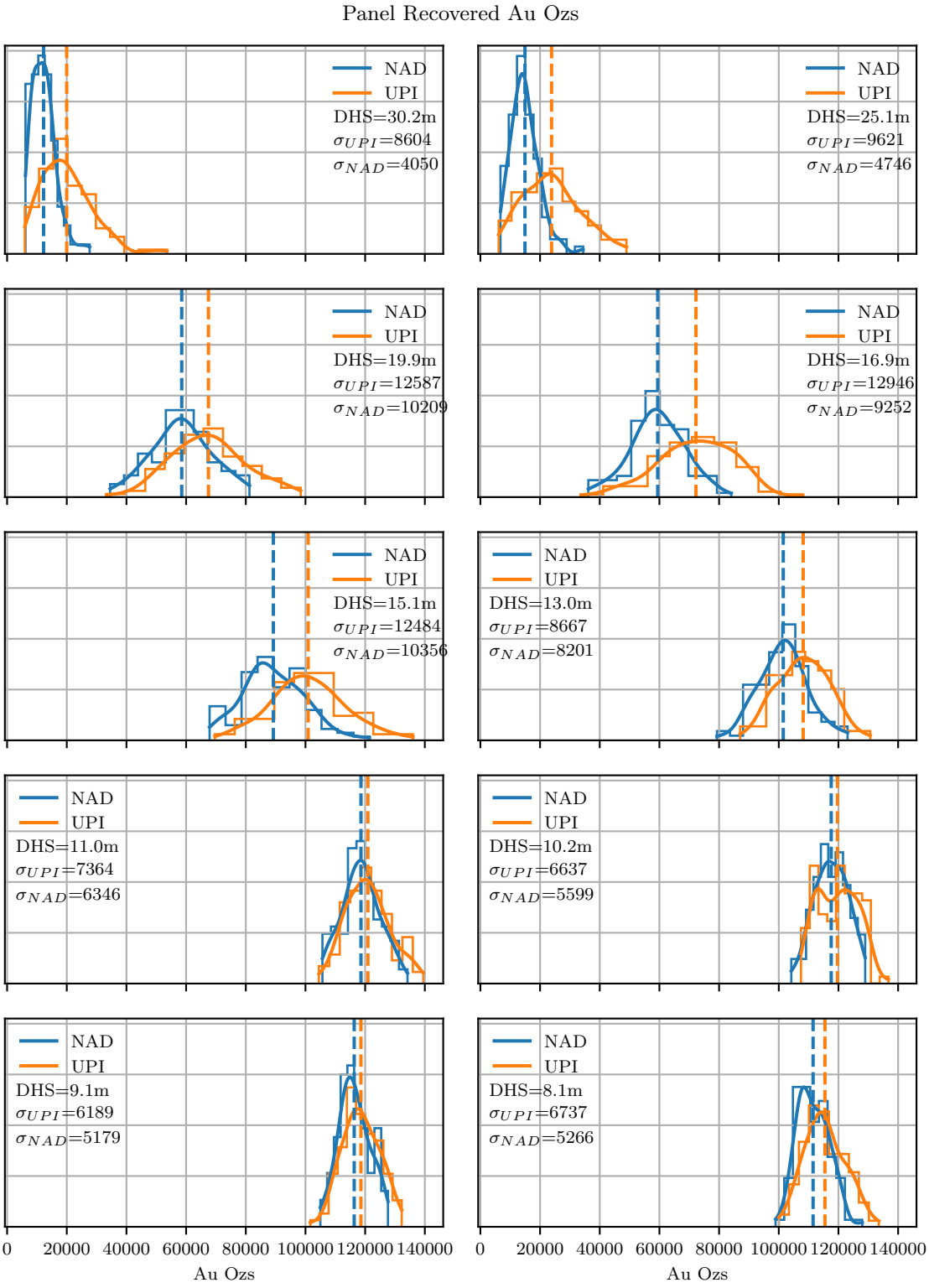

Figure 6.21: Uncertainty in panel recovered Au ounces by drillhole spacing. The dashed lines are the expected values of the respective distributions. All plots share both x and y axes. UPI = undiluted perfect information, NAD = no additional data.

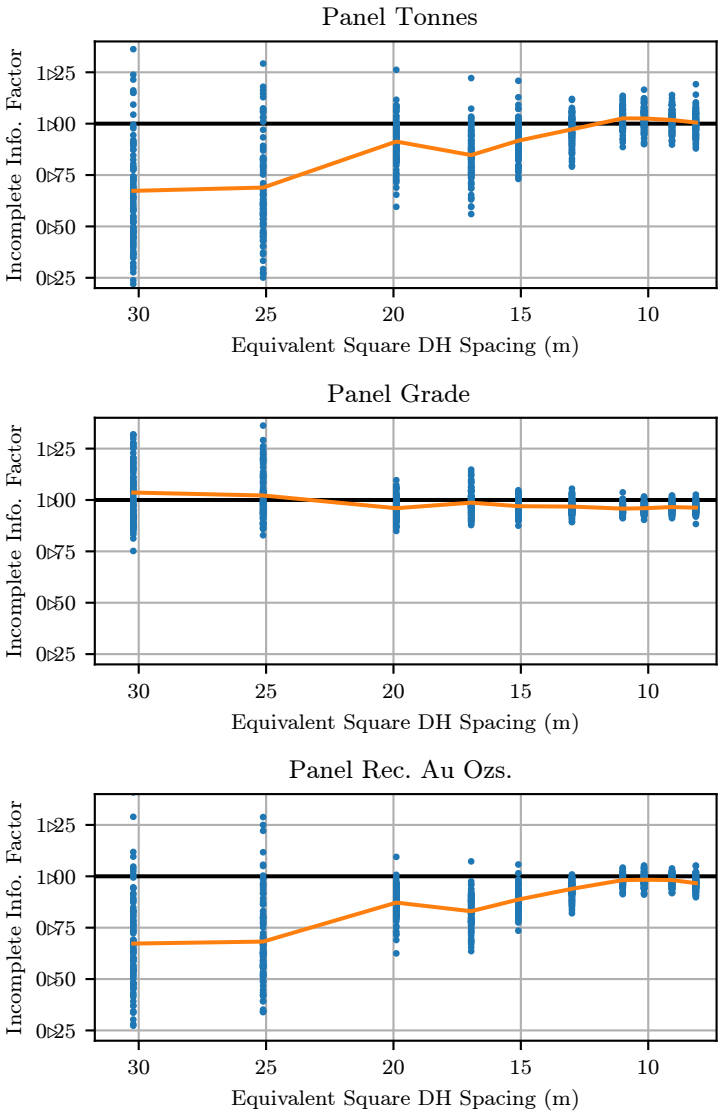

Figure 6.22: Incomplete information factor for tonnes (top), Au grade (middle) and recovered Au ounces (bottom) by drillhole spacing. The orange line is the average of the realizations.

Chapter 7

Conclusions and Future Work

Collecting the correct amount of information is an essential objective for any mining project operator. Understanding how geologic uncertainty changes with information is a critical component of this problem. Geologic heterogeneity is present at multiple scales and is typically resolved in a non-linear way. Collecting too little information leads to no meaningful uncertainty reduction. Collecting too much information has diminishing returns. VOI is a tool that allows a decision-maker to optimize the collection of information given their site-specific and operational constraints. VOI can identify over or under drilling, either saving costs or increasing value. Though directly influenced by data spacing, this is not the only parameter that controls VOI. The interaction of geologic continuity, technical engineering design parameters, operational cost structures, economic factors, decision-maker risk preferences, and information cost results in a non-linear VOI response. The numerical approach to quantifying VOI is developed and documented in a mining context and then implemented with a practical example.

7.1 Topics Covered and Contributions

The application of VOI analysis is not commonplace in the mining industry. Decisions concerning information collection and the amount of information may be subjective and based on practitioner experience. A contribution of this thesis is the documentation of the numerical VOI framework for mining scenarios. Mining projects are unique in the sense that transfer functions are commonly a complex response to geologic, engineering and economic parameters. This framework allows a decision-maker to remove potential subjectivity from the decision of information collection. Chapter 2 presents the numerical resample and resimulate VOI framework and discusses potential confounding factors and limitations. The resampling of simulated realizations provides access to future data configurations. Passing the realizations through a transfer function establishes value. As with any simulation-based geostatistical technique, enough data is required for inference of the histogram and

variogram to achieve reasonable results.

The principal factors which govern VOI and discussion regarding their interaction are documented in Chapter 3. Both the nugget effect and the variogram range influence the proportion of maximum attainable value generated. The scale of selectivity in the engineering design also influences the proportion of maximum value. As selectivity becomes finer, the geologic detail resolved by future information can be captured, generating increased value. The engineering design scale relative to the sample spacing and domain size influences the point of diminishing returns. The relationship between geologic and engineering scales and optimal data spacing is shown to be non-linear. Operational cost structures such as ore value and penalties for dilution also influence the choice of optimal sample spacing. It is shown that if the decision-maker has a risk preference other than risk-neutral, information is inherently more valuable as there is an opportunity to learn about the downside risk or upside potential.

The practical implementation details of the proposed framework and presented in Chapter 4. The collection of future information is discussed, and the Uniform Drillhole Elimination (UDE) algorithm is proposed for partitioning drillhole data into spatially reasonable groups. The algorithm is a practical tool to sequentially eliminate drillholes while maintaining uniformity within the remaining holes. The goal is to sequence the drillholes in a way that would mimic a natural infill drill campaign. An additional contribution of this chapter is the documentation of the number of true models and realizations required for stable VOI results. Results show that 10 true models and 100 realizations are appropriate.

The relationship between geologic uncertainty and data spacing can be used to provide guidance on the optimal data spacing. This concept is presented in Chapter 5. It is shown that a data spacing selected using only measures of geologic uncertainty corresponds closely to the optimal data spacing identified by VOI analysis. Uncertainty in economic parameters is shown to have a relative impact on VOI. The choice of optimal data spacing does not change though the total value generated fluctuates as the gross and net VOI curves are scaled up or down.

Chapter 6 is a case study implementing the proposed methodology and techniques on an operational underground gold mine in West Africa. A full geostatistical model is built

to characterize the truth. The UDE algorithm defines 12 drillhole configurations ranging from 40 to 5 m equivalent square drillhole spacing. The true models are resampled, and 100 realizations are generated for each data configuration. The SSO algorithm generates individual stope shapes that form a mining panel. Assessing the value of information for all future data configurations identifies an optimal data spacing of 12.4 m. A contribution of this chapter is the documentation of uncertainty in reported reserves versus data spacing. Reserves are calculated under the assumption of perfect geologic knowledge and compared to reserves tabulated with current knowledge over a range of data spacings. An Incomplete Information Factor (IIF) is developed to illustrate the relative difference between perfect and current knowledge. Uncertainty in reported reserves (tonnes, gold grade and recovered gold ounces) are shown to stabilize at approximately 13 m data spacing which corresponds well with the optimal spacing identified by VOI.

The main contribution of this thesis is to document the numerical VOI framework and present the factors that influence how information creates value. This framework goes beyond the traditional measures of geologic uncertainty versus data spacing, as value is a function of numerous parameters. This framework can be used to support and remove subjectivity from the decision-making process regarding information collection. The methodology developed can be applied to real mineral deposits to optimize data spacing.

7.2 Limitations

A general limitation of the proposed framework is a frozen conceptual model. Technical design parameters are chosen for a mining method based on knowledge of the deposit. There is no flexibility within the framework to adapt a new conceptual geologic model if warranted by future information. This implies a certain level of geologic knowledge must be obtained prior to implementing the VOI framework.

Implementing the numerical VOI workflow can be difficult and computationally expensive. $T * L * C$ realizations must be generated for each variable. This number could be significant, depending on the number of future data configurations. Storage of realizations may present an issue depending on the number of grid nodes considered. Interim realizations do not need to be kept, but the true models must be retained. For any practical scale model,

automation and parallelization of the workflow are necessary.

A limitation of the current workflow is that there is no consideration for the mining sequence. It is assumed that all drillhole collar locations are available at any time, and the collection of information does not interfere with or delay extraction. A more realistic framework would account for the mine plan and include penalties for potentially delaying ore extraction. Collar locations respect physical constraints such as topography and existing infrastructure, though additional detail regarding permissible drill pads and rig movement could be included. When generating future drillholes, it is assumed that the holes do not deviate, and there are no twinned or wedged holes.

A more realistic framework would also consider sequential information gathering schemes. It is currently assumed that all future information is gathered in a single event, consists of a single data type, and represents perfect information. Naturally, different amounts or types of information are required at different stages of development. Incorporating a phased approach to VOI with detailed mine planning accounting for time value may provide more realistic results.

A limitation of the proposed workflow is the generally simplified value and transfer functions. All costs associated with a mining operation are variable over both time and space. The value function in this work does not directly account for the time value of money or variable costs. For value calculations it is assumed the entire technical design is exacted at once. Penalties, if applied to the value function, are assumed constant. Establishing accurate penalties for ore loss and dilution may be difficult in practice and are inherently specific to the operation. A more complex value function incorporating recovery curves and other non-linearities could be considered.

The technical designs generated throughout this work are not necessarily optimal. Though they respect reasonable technical constraints from an engineering perspective. A rigorous optimization process that includes detailed geometry refinement and consideration of partial blocks may provide more accurate results. The cost of acquiring data is assumed constant over time and for all quantities. In practice, applying a cost discount for acquiring information simultaneously, such as having multiple drill rigs turning at once, is appropriate. There may be additional costs associated with delaying development or production due to

limited information.

7.3 Future Work

The value of information in a mining context presents a unique challenge in that the solution space is immense. The number of possible mine plans or stope geometries is virtually infinite, which necessitates a numerical approach. A key component of future research is to circumvent the full numerical workflow and stochastic optimization. A valuable area for future research is the development of an analytical VOI methodology for complex and realistic problems. Analytical approaches currently exist though are generally restricted to simple problems and rely on strong Gaussian assumptions. An analytical solution would bypass the computationally expensive numerical workflow though it is not clear how this approach extends to real mining problems.

Another area of future research is the development of accurate approximations of value. A current challenge of the numerical approach is the definition of a transfer function to convert a geological model into a value response. Approximating value requires evaluating multiple scenarios numerically and constructing a response surface model to make future predictions. This approach represents challenges in generating a sufficient number of responses and selecting model characteristics applicable to different types of deposits.

References

Abzalov, M. (2016). *Applied mining geology*. Springer International Publishing.

Athens, N. D., & Caers, J. K. (2019). A monte carlo-based framework for assessing the value of information and development risk in geothermal exploration. *Applied Energy*, *256*, 113932. Retrieved from http://www.sciencedirect.com/science/article/pii/S0306261919316198 doi: https://doi.org/10.1016/j.apenergy.2019.113932

Barnes, R. (1986). Cost of risk and the value of information in mine planning. In R. Ramani (Ed.), *Application of computers and operations research in the mineral industry* (pp. 459–469). Soc of Mining Engineers of AIME.

Barnett, R. M. (2014). *A compressed binary format for large geostatistical models* (CCG Annual Report 16). Edmonton AB: University of Alberta. Retrieved from http://www.ccgalberta.com

Barnett, R. M., Lyster, S., Pinto, F. A., MacCormack, K., & Deutsch, C. V. (2018, 09). Principles of data spacing and uncertainty in geomodeling. *Bulletin of Canadian Petroleum Geology*, *66*(3), 575-594.

Benndorf, J. (2020). Optimization methods to translate online sensor data into mining intelligence. In *Closed loop management in mineral resource extraction: Turning online geo-data into mining intelligence* (pp. 83–101). Cham: Springer International Publishing. Retrieved from https://doi.org/10.1007/978-3-030-40900-5_5 doi: 10.1007/978-3-030-40900-5_5

Bernoulli, D. (1954). Exposition of a new theory on the measurement of risk. *Econometrica*, *22*(1), 23–36. Retrieved from http://www.jstor.org/stable/1909829

Bhattacharjya, D., Eidsvik, J., & Mukerji, T. (2010). The value of information in spatial decision making. *Mathematical Geosciences*, *42*(2), 141–163. doi: 10.1007/s11004-009-9256-y

Bickel, E. J., Gibson, R. L., McVay, D. A., Pickering, S., & Waggoner, J. (2006). Quantifying the reliability of and value of 3d land seismic. *Proceedings of the 2006 SPE Annual Technical Conference and Exhibition, Society of Petroleum Engineers*, *SPE 102340*, 832-841.

Bratvold, R. B., & Begg, S. (2009). *Making good decisions*. Society of Petroleum Engineers.

Bratvold, R. B., Bickel, E. J., & Lohne, H. P. (2009, Aug). Value of information in the oil and gas industry: Past, present, and future. *Society of Petroleum Engineers*, *12*(4), 630–638. doi: https://doi.org/10.2118/110378-PA

Caers, J. (2011). *Modeling Uncertainty in the Earth Sciences.* John Wiley and Sons Ltd. Retrieved from `https://onlinelibrary.wiley.com/doi/book/10.1002/9781119995920` doi: 10.1002/9781119995920

Coopersmith, E. M., Burkholder, M. K., & Schulze, J. H. (2006). Value-of-information lookbacks–was the information you gathered really worth getting? *Proceedings of the 2006 SPE Annual Technical Conference and Exhibition, Society of Petroleum Engineers*, *SPE 101540*, 1–7.

Cuba-Espinoza, M. A. (2014). *Simulated Learning Model for Mineable Reserves Evaluation in Surface Mining Projects* (CCG Thesis). Edmonton AB: University of Alberta.

Deutsch, C. V., & Beardow, A. P. (1999). Optimal drillhole spacing and uncertainty in prediction of oil sands bitumen and fines content. *CIM Annual Meeting, Calgary, Alberta.*

Deutsch, C. V., & Journel, A. G. (1998). *Gslib - geostatistical software library and user's guide.* New York - Oxford: Oxford University Press.

Deutsch, J. L., Barnett, R. M., & Deutsch, C. V. (2015). *Latest Kriging Program* (CCG Annual Report 17). Edmonton AB: University of Alberta. Retrieved from `http://www.ccgalberta.com`

Dohm, C. (2005). Quantifiable mineral resource classification: A logical approach. In O. Leuangthong & C. V. Deutsch (Eds.), *Geostatistics banff 2004* (pp. 333–342). Dordrecht: Springer Netherlands. Retrieved from `https://doi.org/10.1007/978-1-4020-3610-1_34` doi: 10.1007/978-1-4020-3610-1_34

Eidsvik, J., Bhattacharjya, D., & Mukerji, T. (2008, 07). Value of information of seismic amplitude and CSEM resistivityValue of information of AVO and CSEM. *Geophysics*, *73*(4), R59-R69. Retrieved from `https://doi.org/10.1190/1.2938084` doi: 10.1190/1.2938084

Eidsvik, J., Dutta, G., Mukerji, T., & Bhattacharjya, D. (2017, May 01). Simulation–regression approximations for value of information analysis of geophysical data. *Mathematical Geosciences*, *49*(4), 467–491. Retrieved from `https://doi.org/10.1007/s11004-017-9679-9` doi: 10.1007/s11004-017-9679-9

Eidsvik, J., & Ellefmo, S. L. (2013, Oct 01). The value of information in mineral exploration within a multi-gaussian framework. *Mathematical Geosciences*, *45*(7), 777–798. Retrieved from https://doi.org/10.1007/s11004-013-9457-2 doi: 10.1007/s11004-013-9457-2

Eidsvik, J., Mukerji, T., & Bhattacharjya, D. (2015). *Value of Information in the Earth Sciences*. Cambridge: Cambridge University Press. Retrieved from http://ebooks.cambridge.org/ref/id/CBO9781139628785 doi: 10.1017/cbo9781139628785

Englund, E. J., & Heravi, N. (1993). Conditional simulation: Practical application for sampling design optimization. In A. Soares (Ed.), *Geostatistics tróia '92: Volume 1* (pp. 613–624). Dordrecht: Springer Netherlands. Retrieved from https://doi.org/10.1007/978-94-011-1739-5_48 doi: 10.1007/978-94-011-1739-5_48

Froyland, G., Menabde, M., Stone, P., & Hodson, D. (2018). The value of additional drilling to open pit mining projects. In R. Dimitrakopoulos (Ed.), *Advances in applied strategic mine planning* (pp. 119–138). Cham: Springer International Publishing. Retrieved from https://doi.org/10.1007/978-3-319-69320-0_10 doi: 10.1007/978-3-319-69320-0_10

Golden Star Resources. (2019). *NI 43-101 Technical Report on Resources and Reserves, Golden Star Resources, Wassa Gold Mine, Ghana* (Tech. Rep.).

Grayson, C. (1960). *Decisions under uncertainty: Drilling decisions by oil and gas operators*. Harvard Business School, Division of Research.

Grieco, N., & Dimitrakopoulos, R. (2018). Grade uncertainty in stope design—improving the optimisation process. In R. Dimitrakopoulos (Ed.), *Advances in applied strategic mine planning* (pp. 573–589). Cham: Springer International Publishing. Retrieved from https://doi.org/10.1007/978-3-319-69320-0_33 doi: 10.1007/978-3-319-69320-0_33

Howard, R. A. (1966a). Decision analysis: Applied decision theory. In D. B. Hertz & J. Melese (Eds.), *Proceedings of the fourth international conference on operational research* (pp. 55–71). Wiley-Interscience.

Howard, R. A. (1966b). Information value theory. *IEEE TRANS ACTIONS ON SYSTEMS SCIENCE AND CYBERNETICS*, *SSC-2*(No. 1), 22-26.

Howard, R. A. (1968). The foundations of decision analysis. *IEEE TRANS ACTIONS ON SYSTEMS SCIENCE AND CYBERNETICS*, *SSC-4*(No. 3), 211-219.

Howard, R. A. (1980). An assessment of decision analysis. *Operations Research*, *28*(1), 4-27. Retrieved from https://doi.org/10.1287/opre.28.1.4 doi: 10.1287/opre.28.1.4

Howard, R. A., & Abbas, A. E. (2015). *Foundations of decision analysis, global edition*. Pearson Education Limited.

Howard, R. A., & Matheson, J. E. (1983). *Readings on the principles and applications of decision analysis: General collection*. Strategic Decisions Group.

Hustrulid, W., Kuchta, M., & Martin, R. (2013). *Open pit mine planning and design, two volume set & cd-rom pack*. CRC Press.

Journel, A., & Kyriakidis, P. (2004). *Evaluation of mineral reserves: A simulation approach*. Oxford University Press.

Keeney, R. L., & Raiffa, H. (1993). *Decisions with multiple objectives: Preferences and value trade-offs*. Cambridge University Press. doi: 10.1017/CBO9781139174084

Kochenderfer, M. J. (2015). *Decision Making Under Uncertainty: Theory and Application*. The MIT Press.

Laxminarayan, R., & Macauley, M. K. (2012). *The value of information*. Springer Science+Business Media. doi: https://doi-org/10.1007/978-94-007-4839-2

Lu, D., Ye, M., Neuman, S. P., & Xue, L. (2012). Multimodel bayesian analysis of data-worth applied to unsaturated fractured tuffs. *Advances in Water Resources*, *35*, 69 - 82. Retrieved from http://www.sciencedirect.com/science/article/pii/S0309170811001990 doi: https://doi.org/10.1016/j.advwatres.2011.10.007

Machuca-Mory, D. F., & Deutsch, C. V. (2006). *A Program for the Robust Calculation of Drillhole Spacing in Three Dimensions* (CCG Report 08). Edmonton AB: University of Alberta.

Manchuk, J. (2007). *Stope Design and Sequencing* (CCG Thesis). Edmonton AB: University of Alberta.

McLennan, J. A., & Deutsch, C. V. (2005). Ranking geostatistical realizations by measures of connectivity. *Society of Petroleum Engineers*. doi: 10.2118/98168-MS

Mohamed, A. W. (2014). Rdel: Restart differential evolution algorithm with local search mutation for global numerical optimization. *Egyptian Informatics Journal*, *15*(3), 175 - 188. Retrieved from http://www.sciencedirect.com/science/article/pii/S1110866514000279 doi: https://doi.org/10.1016/j.eij.2014.07.001

Neufeld, C. T. (2005). *Guide to Sampling* (Centre for Computational Geostatistics (CCG)

Guidebook Series Vol. 2). Edmonton AB: University of Alberta. Retrieved from http://www.ccgalberta.com

Nikbin, V., Ataee-pour, M., Shahriar, K., & Pourrahimian, Y. (2020). A 3d approximate hybrid algorithm for stope boundary optimization. *Computers and Operations Research*, *115*, 104475. Retrieved from http://www.sciencedirect.com/science/article/pii/S0305054818301357 doi: https://doi.org/10.1016/j.cor.2018.05.012

Parnell, G. S., Bresnick, T. A., Tani, S. N., & Johnson, E. R. (2013). *Handbook of decision analysis*. John Wiley and Sons Ltd. Retrieved from https://onlinelibrary.wiley.com/doi/abs/10.1002/9781118515853 doi: 10.1002/9781118515853.ch1

Phillips, J., Newman, A. M., & Walls, M. R. (2009). Utilizing a value of information framework to improve ore collection and classification procedures. *The Engineering Economist*, *54*(1), 50-74. Retrieved from https://doi.org/10.1080/00137910802711883 doi: 10.1080/00137910802711883

Pinto, F. A. C. (2015). *Advances in Data Spacing and Uncertainty* (CCG Thesis). Edmonton AB: University of Alberta.

Pitard, F. (1993). *Pierre gy's sampling theory and sampling practice, second edition: Heterogeneity, sampling correctness, and statistical process control*. Taylor & Francis.

Polasky, S., & Solow, A. R. (2001, Jul 01). The value of information in reserve site selection. *Biodiversity & Conservation*, *10*(7), 1051–1058. Retrieved from https://doi.org/10.1023/A:1016618206124 doi: 10.1023/A:1016618206124

Price, K., Storn, R., & Lampinen, J. (2006). *Differential evolution: A practical approach to global optimization*. Springer Berlin Heidelberg.

Pyrcz, M., & Deutsch, C. (2014). *Geostatistical reservoir modeling*. OUP USA.

Raiffa, H., & Schlaifer, R. (1961). *Applied statistical decision theory*. Wiley.

Rainer, S., & Price, K. (1997). Differential evolution – a simple and efficient heuristic for global optimization over continuous spaces. *Journal of Global Optimization*(11), 341-359. doi: 10.1023/A:1008202821328

Rojas, O., & Cáceres, A. (2011). The use of conditional simulation for drill hole spacing evaluation and decision-making in telégrafo project, northern chile. *The AusIMM Eighth International Mining Geology Conference Proceedings 2011*, 443-451.

Rossi, M., & Deutsch, C. (2013). *Mineral resource estimation*. Springer Science & Business Media. Retrieved from https://books.google.ca/books?id=gzK_BAAAQBAJ

Scheidt, C., Li, L., & Caers, J. (2018). *Quantifying uncertainty in subsurface systems*. Wiley.

Schlaifer, R. (1959). *Probability and statistics for business decisions*. New York - Toronto - London: McGraw-Hill Book Company.

Silva, V. M., & Deutsch, C. V. (2019). *Guide to Simulation in the Presence of Sampling Error* (Centre for Computational Geostatistics (CCG) Guidebook Series Vol. 24). Edmonton AB: University of Alberta. Retrieved from `http://www.ccgalberta.com`

Silva, D. S. F. & Boisvert, J. B. (2014). *Two New Tools: Directional Survey to GSLIB XYZ Format and Drill Hole Spacing* (CCG Annual Report 16). Edmonton AB: University of Alberta. Retrieved from `http://www.ccgalberta.com`

Stegall, D., Gomes, J., Oliveira, R., Ribeiro, N., Queiroz, R., Carvalho, M., & Souza, C. (2005). How to estimate the value of information (voi) of a 4d seismic survey in one offshore giant field. *Proceedings of the 2005 SPE Annual Technical Conference and Exhibition, Society of Petroleum Engineers*, *SPE 95876*, 3–5.

Storn, R. (1996). On the usage of differential evolution for function optimization. In *Proceedings of north american fuzzy information processing* (p. 519-523).

Strebelle, S. (2002, Jan 01). Conditional simulation of complex geological structures using multiple-point statistics. *Mathematical Geology*, *34*(1), 1–21. Retrieved from `https://doi.org/10.1023/A:1014009426274` doi: 10.1023/A:1014009426274

Trainor-Guitton, W. J., Caers, J. K., & Mukerji, T. (2011, Nov 01). A methodology for establishing a data reliability measure for value of spatial information problems. *Mathematical Geosciences*, *43*(8), 929–949. Retrieved from `https://doi.org/10.1007/s11004-011-9367-0` doi: 10.1007/s11004-011-9367-0

Trainor-Guitton, W. J., Mukerji, T., & Knight, R. (2013, May 01). A methodology for quantifying the value of spatial information for dynamic earth problems. *Stochastic Environmental Research and Risk Assessment*, *27*(4), 969–983. Retrieved from `https://doi.org/10.1007/s00477-012-0619-4` doi: 10.1007/s00477-012-0619-4

Trainor-Guitton, W. J., Ramirez, A., Yang, X., Mansoor, K., Sun, Y., & Carroll, S. (2013). Value of information methodology for assessing the ability of electrical resistivity to detect co2/brine leakage into a shallow aquifer. *International Journal of Greenhouse Gas Control*, *18*, 101 - 113. Retrieved from `http://www.sciencedirect.com/science/article/pii/S1750583613002661` doi: https://doi.org/10.1016/j.ijggc.2013.06.018

Ulrych, T. J., Sacchi, M. D., & Woodbury, A. (2001, 01). A Bayes tour of inversion: A tutorial. *Geophysics*, *66*(1), 55-69. Retrieved from https://doi.org/10.1190/1.1444923 doi: 10.1190/1.1444923

Von Neumann, J., & Morgenstern, O. (1944). *Theory of games and economic behavior 1st ed.* Princeton University Press.

Waggoner, J. R. (2002). Quantifying economic impact of 4d seismic projects. *Proceedings of the 2002 SPE Annual Technical Conference and Exhibition, Society of Petroleum Engineers*, *SPE 77969*, 111–115.

Wilde, B. J. (2007). *Wide array declustering for representative distributions (The Ultimate DECLUS Program)* (CCG Annual Report 9). Edmonton AB: University of Alberta. Retrieved from http://www.ccgalberta.com

Wilde, B. J. (2010). *Data Spacing and Uncertainty* (CCG Thesis). Edmonton AB: University of Alberta.

Witter, J. B., Trainor-Guitton, W. J., & Siler, D. L. (2019). Uncertainty and risk evaluation during the exploration stage of geothermal development: A review. *Geothermics*, *78*, 233 - 242. Retrieved from http://www.sciencedirect.com/science/article/pii/S0375650518303183 doi: https://doi.org/10.1016/j.geothermics.2018.12.011

World Gold Council. (2020). *Gold prices.* Retrieved 2020-08-18, from https://www.gold.org/goldhub/data/gold-prices

Yüksel, C., Minnecker, C., Shishvan, M. S., Benndorf, J., & Buxton, M. (2019, Oct 01). Value of information introduced by a resource model updating framework. *Mathematical Geosciences*, *51*(7), 925–943. Retrieved from https://doi.org/10.1007/s11004-018-9770-x doi: 10.1007/s11004-018-9770-x